Titre: Title:	Understanding 2D Transport in Microfluidic Systems
Auteur: Author:	Etienne Boulais
Date:	2023
Type:	Mémoire ou thèse / Dissertation or Thesis
Référence: Citation:	Boulais, E. (2023). Understanding 2D Transport in Microfluidic Systems [Thèse de doctorat, Polytechnique Montréal]. PolyPublie. https://publications.polymtl.ca/56769/

POLYTECHNIQUE MONTRÉAL
affiliée à l'Université de Montréal

Understanding 2D Transport in Microfluidic Systems

ETIENNE BOULAIS
Département de génie physique

Thèse présentée en vue de l'obtention du diplôme de *Philosophiæ Doctor*
Génie physique

Novembre 2023

POLYTECHNIQUE MONTRÉAL
affiliée à l'Université de Montréal

Cette thèse intitulée :

Understanding 2D Transport in Microfluidic Systems

présentée par **Etienne BOULAIS**
en vue de l'obtention du diplôme de *Philosophiæ Doctor*
a été dûment acceptée par le jury d'examen constitué de :

Jean PROVOST, président
Thomas GERVAIS, membre et directeur de recherche
Bruno BLAIS, membre
Martin Z. BAZANT, membre externe

DEDICATION

If you understand, you're probably wrong
- Jacques Lacan

ACKNOWLEDGEMENTS

Pushing this project to the end has not been easy, and I couldn't have done it had I not been surrounded by extraordinary people, who helped shape these past couple of years.

I would first like to thank my project advisor Thomas for giving this project to work on, for helping me go to conferences and meet other experts in the field and for supporting me in my career plans. I would also like to thank Thomas for giving me the opportunity to teach in his classes, both as a teaching assistant and as a lecturer over the years. This kickstarted a passion for teaching which brought me a lot, and I am grateful for you giving me these first opportunities.

I would also like to thank my friends from the grad student office, especially Sandryne, Oscar, Lucas, Marie, Myriam, Julien, Fred. Being around you guys has made these years bearable, and it has been a godsend to have like-minded people to rant, laugh, discuss with over the years. As the years go by, friends get lost and disappear, but you have stayed around, and are among the people left around me who I feel truly close to. I have also loved discovering a lifelong passion for karaoke with you.

Among these friends from the office, I would like to particularly thank Pierre-Alexandre. When we first met, we seemed to be completely incompatible and diametrically opposed in our ways of being. Throughout the year, however, you have become one of the few friends who I think understands me truly. You have become one of my best friends and I feel like I have learned a lot from working with you. This project is a massive success thanks in great part to the excellent experimental work you have done, and I feel it wouldn't be a fraction of what it is without the great collaboration we have had. I hope you find satisfaction and fulfilment in the work you are doing now, and that you keep doing great things.

I would like to give a very warm thank you to all of the student who I had the privilege of teaching to during all of these years. Thank you for trusting me, and coming to the different classes I taught. It has been a tremendously humbling experience to see you start your physics journey in the thermodynamics class, still fresh out of CEGEP and confused by this new wall of physics, then see you the year after in classical mechanics, within a year grown and become solid physics students, to seeing you create incredible projects from scratch in the project class the year after. I have learned just as much, if not more, from your questions, remarks, and work in all of these classes. In the tougher moments when I was frustrated with science, research, and physics, coming to the class and spending an hour convincing you that this is a field worth pursuing helped me remind myself of why I chose this path in the first

place. I have an immense love for this department, and this is due to the incredible potential and energy that I see in you guys. I wouldn't have stayed in this department for a third of my life if it hadn't been so.

Finally, I would like to thank my parents for believing in me and supporting me all of these years. Thank you for fostering a love of science in me at a young age, and for encouraging me in all my projects, even when the weirder ones. I wouldn't be here without your continued support.

RÉSUMÉ

Les technologies microfluidiques, manipulant des microlitres de fluide dans des systèmes millimétriques, peuvent faciliter les expériences en chimie et dans les sciences de la vie. Ces systèmes permettent une grande parallélisation, une réduction du temps des expériences, une consommation de réactifs minime et une réduction des coûts. À l'échelle microfluidique, les phénomènes de transport ont un comportement qualitatif très différent du comportement macroscopique, ce qui nécéssite des modèles théoriques spécialisés.

Les systèmes microfluidiques consistant en des réseaux de microcanaux sont très bien compris. Des modèles complets pour l'écoulement et la diffusion dans les microcanaux sont disponibles, et une fois que le comportement d'un canal individuel est analysé, ces éléments peuvent être arrangés en réseaux complexes. Ces réseaux sont ensuite étudiés en utilisant la théorie des circuits linéaires, à la manière des circuits électriques. Ces outils de modélisations, combinés avec les avancées dans les technologies de fabrication, ont permis le développement de systèmes incroyablement sophistiqués, poussant le paradigme à sa limite.

Cependant, depuis la deuxième moitié des années 2000, de nouvelles technologies microfluidiques apparaissent, suivant un nouveau paradigme de microfluidique 2D. Dans ces systèmes, l'écoulement évolue dans un espace 2D, la diffusion et la convection ne sont plus découplées, et la logique séquentielle des circuits est remplacée par une logique de champs où chaque élément interagit avec tous les autres en même temps. Ces technologies requièrent de nouveaux outils théoriques permettant de guider leur design et leur opération.

Cette thèse présente un cadre théorique complet pour analyser l'écoulement et la diffusion dans ces systèmes microfluidiques 2D. Les modèles présentés sont inspirés de résultats classiques d'autres domaines de la mécanique des fluide, qui sont ici assemblés dans une méthode unifiée accessible aux scientifiques et ingénieurs travaillant en microfluidique. Ces modèles ont d'abord été développés pour analyser les sondes microfluidiques, mais ont ensuite été généralisés à un éventail de technologies microfluidiques 2D.

Nous présentons d'abord une revue de résultats classiques de la théorie du transport, avec un accent sur les outils reliés aux potentiels complexes et aux transformations conformes. Nous montrons ensuite comment ces résultats peuvent être appliqués pour obtenir des profils de vitesse et de concentration complets dans les sondes microfluidiques. Les mêmes résultats sont ensuite étendus à la plus grande famille des dispositifs microfluidiques 2D. Nous terminons avec deux exemples de technologies dont l'invention a été guidée par les outils présentés, puis une discussion des avenues futures.

ABSTRACT

Microfluidic technologies, technologies manipulating microliters of fluid on millimiter chips, hold the promise of automating routine experiments in chemistry and life sciences by drastically increasing throughput and reducing costs. At this scale, fluid mechanical phenomena behave in a qualitatively different manner than what our macroscale intuition predicts, which calls for specialized models to help in understanding, analyzing, and designing efficient new technologies.

Microfluidic systems conceived as networks of microchannels have been thoroughly studied. Complete models for flow and diffusion in microchannels are readily available, and once the behavior of a single strip of channel is understood, elements can be arranged in complex networks and analyzed using the theory of linear circuits, analogous to how electric circuits are modeled. These modeling tools, combined with advances in soft lithography, have enabled engineers to develop state-of-the-art technologies that push the network paradigm to its limit.

However, since the second half of the 2000s, a growing number of new microfluidic systems have emerged that break away from this "networks of microchannels" paradigm. More and more systems are being developed following a new paradigm of flow-field, or 2D microfluidics. In these new systems, flow is free to evolve in 2D space, diffusion and convection are no longer fully decoupled, and the sequential logic of linear circuits is replaced by a field logic where every element interacts with every other at once. These new field-based technologies demand the production of new theoretical tools that can be used to guide their design and operation.

In this dissertation, we present a complete theoretical framework for analyzing flow and diffusion in such 2D microfluidic systems. The models we present are inspired by classic results in other fields of fluid mechanics, and are collected into a unified toolbox accessible to scientists and engineers working in microfluidics. The models were first developed to analyze microfluidic probes, but were then extended to apply to a wide range of microfluidic technologies.

We begin with a review of classical results in transport theory and fluid mechanics, in particular tools related to complex potential and conformal transforms. We then show how these results can be applied to obtain complete flow and concentration maps in microfluidic probes and adjacent systems. We then generalize the results to obtain a framework applicable to the entire range of field-based microfluidics. We finish with two examples of new technologies that were invented using this theoretical framework, as well as discussion on where to take the work next.

TABLE OF CONTENTS

LIST OF FIGURES

CHAPTER 1 INTRODUCTION

1.1 Microfluidic systems

Microfluidic systems appeared in the tail end of the 1970s, when technological leaps in microfabrication, driven by the field of microelectronics, gave engineers tools to precisely manufacture silicon devices. Interest grew on how to use these microfabrication techniques not just to create electronic circuits, but also to miniaturize mechanical systems [1]. As an offshoot of this newly growing field of MEMS (Micro-Electromechanical Systems), engineers began working on miniaturizing fluid manipulation technologies, giving birth to the first microfluidic systems. The design paradigm for these early systems was quite straightforward: micrometer-sized networks of channels would be etched on silicon, and used to manipulate nanoliter-scale volumes of fluid. Miniaturization of such fluidic experiments promises lower reagent consumption, lower costs of operations, as well as much higher throughput for a number of routine experiments in domains such as analytical chemistry and life sciences [2].

Side by side with this new technology came a need for solid analytical tools that could help scientists design and operate these systems. At the milimeter to micrometer scale that microfluidic systems operate in, fluids behave in a manner that is qualitatively very different to the one we are used to in our macroscopic world. Namely, inertial effects are often negligible, and mixing is limited by diffusion rates, which are often extremely slow. Fortunately, these effects of scale could be exploited to develop a complete description of flow and transport in microfluidic systems. At low Reynolds number, flow profiles for channels of almost any conceivable cross-sections were developed and applied, following existing work on Poiseuille flow [3]. Diffusion, approximately decoupled from convection, could be studied using quasi-1D models, allowing for a complete description of mixing in microchannels [4]. Finally, once transport in a single channel element was completely understood, these channel elements could be assembled in complex networks using a theory analogous to the theory of linear electric circuits [5]. This paradigm, pushed to its logical limit, enabled the design of extremely elaborate microfluidic systems. For example, complex, temporally varying microenvironments were generated for bacteria populations [6], and in the limit, highly parallel arrays of valves enabled the fabrication of microfluidic analogs to random access memory (RAM) [7].

However, from the early 2000s, a growing number of technologies start appearing which fall outside of the simple "networks of microchannels" paradigm. Probe-type systems are used to precisely mark biological surfaces [8], large chambers are used to create adjustable

spatial concentration gradients [9], complex arrangements of droplets parallelize chemical reactions [10], complex matrices of obstacles are used to trap cells in chambers [11], just to name a few. In these new systems, many of the hypothesis on which the theory of channel-based microfluidics was built are no longer respected. Flow is no longer unidirectional but rather free to evolve in any direction in the 2D plane. Likewise, diffusion can no longer be analyzed in a quasi-1D manner as had been done before, but rather forms complex footprints in the plane, whose shape and behavior is intrinsically linked with the flow profile. Most of these early sytems are designed using scaling arguments [12], simple point-source models [13], or bulky finite element simulations [14]. These approaches all offer a quantitative description of the transport phenomena in play, but the description they offer is incomplete and often limited in its range of applicability. There is thus a real need for a complete theoretical framework, analogous to the one used in linear networks of microchannels, that could be used to analyze these new flow-field based microfluidic systems.

1.2 Definition of the problem

The problem we are tackling is this: We want to conceive flexible models for transport in 2D microfluidic systems. These models should be general and applicable to a range of different technologies, and enable us to precisely predict flow pattern and diffusion profiles in these systems. A schematic figure illustrating the difference between channel based and 2D microfluidics is shown in figure 1.1

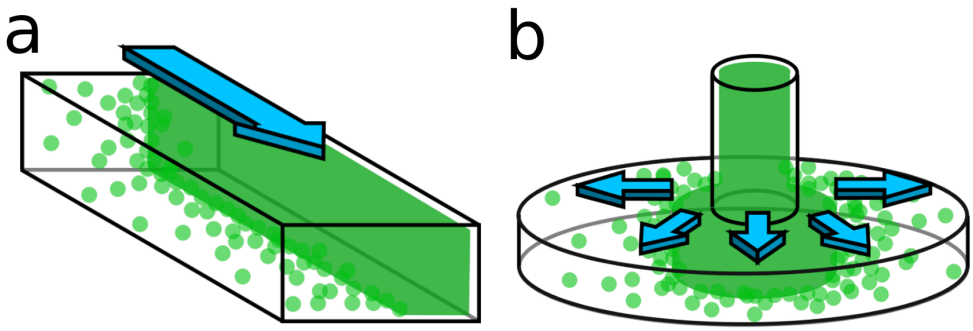

Figure 1.1 Comparison of the channel-based and 2D microfluidics paradigms. a) The microchannel, base unit of the channel network paradigm, in which flow is unidirectional and decoupled from diffusion, b) Point source in a 2D microfluidic system, where flow is free to evolve in all directions and is closely coupled to the diffusion pattern

Fortunately for us, most of the theoretical machinery for analyzing flow and diffusion in low Reynolds, two dimensional flow fields already exists, but is scattered across different areas

of fluid mechanics and applied mathematics. The objective is thus to gather this knowledge and form a cohesive toolbox that is immediately applicable to microfluidics.

Once the models are conceived, they should then be used to guide the design of real-life microfluidic technologies. Just like the channel paradigm could, when pushed to its logical limit, yield such impressive systems as microfluidic RAM, new theoretical tools for 2D systems can open up the door to previously unthinkable technologies.

As a secondary point (which we tackle in chapter 5), the models should be accessible and usable to engineers and scientists working on microfluidic technologies. They should be as easy to use as possible. In this way, they can be of use not just to fluid mechanics experts, but also to graduate students with a typical engineering mathematical background. The project thus involves not only thorough bibliographic research and application of mathematical tools to engineering, but also has an important communication and outreach aspect to it. After all, scientific research only finds its purpose if other people use it.

1.3 Research objectives

The main objective of this work is to **develop a complete theoretical framework for understanding transport in 2D microfluidic systems**. This objective can be broken down into a number of sub-objectives.

1. **Formulate an analytical model describing convection and diffusion in 2D microfluidic systems**

   This objective involves gathering mathematical tools from various areas of fluid mechanics and assembling them in a coherent analytical model for 2D microfluidic systems. This model should provide a complete description of flow and concentration profile within microfluidic systems, and be flexible enough to be applied to a large range of devices.

2. **Verify the predictions of the model against experimental results**

   The predictions made by the theoretical models should be thoroughly compared with experimental results in order to validate their applicability and their exactness.

3. **Use the newly developed theory to guide the design of new microfluidic technologies**

   Using the theoretical toolbox thus developed, we should be able to imagine, design and analyze new technologies that couldn't have existed before. This guiding of the design of new technologies is, in a sense, the test of a model's strength.

4. **Make the theory accessible to a wider audience of engineers working in microfluidics**

   Beyond using the framework thus developed in the lab, there should be a directed effort towards disseminating the tools I worked on in this dissertation and making them accessible to a wider audience of scientists and engineers in microfluidics.

Objective 1 is tackled in chapters 3 and 4. Objective 2 was done throughout the work that is presented in chapters 3, 6, and 7. Objective 3 is tackled in Chapters 6 and 7, where I present new microfluidic technologies that were fabricated and operated using the theoretical models that I developped in this work. Finally, objective 4 has been accomplished through scientific presentations and workshops given throughout my PhD, a exhaustive list of which is given in the list of contribution, and is distilled in a tutorial review we published in Lab on a Chip in 2023, the body of which is presented in chapter 5.

1.4 Contribution

I have strived, throughout this work, to always properly attribute work that wasn't mine. Science is after all a collaborative effort, and no project exists in a vacuum. The initial outline of the project, as well as some preliminary theoretical results, were done by Thomas Gervais. Experimental work that enabled my theory to be materialized in the real world was done by talented experimentalists in the group, most notably Pierre-Alexandre Goyette and Oscar Boyadjian. The bulk of my contribution to this project was in assembling and applying the theoretical tools that I will present in the next sections, as well as situating them in a wider scientific context.

1.5 Structure of the dissertation

The object of this study is the analysis of transport phenomena in 2D microfluidic systems. We begin the document with a review of mathematical tools from a number of areas of fluid mechanics, focusing on flow and diffusion in 2D geometry. In order to avoid needlessly duplicating information, the literature review focuses primarily on mathematical tools, and a survey of the microfluidic technologies under study is included in chapter 5.

In chapter 3, I give an outline of the initial problem, formulated in the context of microfluidic probes. I show how we can use the tools of conformal mapping to obtain flow and concentration profile for a number of probe-related systems. I also compare the theoretical models to experimental results and show examples of applications. This section gathers re-

sults that were published in a Nature Communications article in 2019 [15], co-authored by Pierre-Alexandre Goyette and myself.

Chapter 4 is a theoretical article published in Physics of Fluids in 2020 [16], where I go into more details about the solution procedure described in our original Nature Communications article. I show explicit theoretical solutions for a number of different flow and diffusion regimes, provide "recipes" for generating new, more complex solutions, and show how the same tools can be applied not only to microfluidic systems but to other areas of fluid mechanics as well, namely the analysis of flow in disordered media and groundwater mechanics.

Chapter 5 consists of a tutorial review published in Lab on a Chip in the Winter of 2023 [17], where I show how a large number of microfluidic systems fall under the 2D microfluidics umbrella, and proceed to outline a general methodology for answering quantitative questions about flow and diffusion in such devices.

Chapters 6 and 7 show how the theoretical machinery introduced in the previous two sections can be utilized in order to guide the design of tangible new technologies, showing two examples of published systems that were designed using these theoretical tools, then fabricated and operated by experimentalists in the group [18] [19].

I finish in Chapter 8 with discussion of the limitations of the method, as well as ideas and recommendations for future directions of research.

CHAPTER 2 LITERATURE REVIEW

This dissertation is about applying analytical tools to the understanding of microfluidic technologies. A literature review for this project should include two aspects: a review of the mathematical tools used to analyze flow and diffusion in the relevant geometries, and a review of the microfluidic technologies that these tools apply to. Review of the microfluidic technologies that operate using flow fields rather than channel geometries is already done in the published articles, so in order to not duplicate information, we will present in this literature review an overview of the mathematical tools that have been used to model flow and diffusion in planar geometries. These mathematical tools will form the backbone of the theoretical work we present afterwards. Survey of specific open-space microfluidic technologies is done in chapter 3, and a broader review of 2D microfluidics at large is done in the first section of the review article presented in chapter 5.

2.1 Flow

Flow of water (or other relevant solvents such as ethanol) in microfluidic systems is determined by the incompressible Navier-Stokes equation [20], which dictates the behavior of newtonian liquids in normal situations. No procedure exists for solving the Navier-Stokes equation in the general case, and instead any field of fluid mechanics usually proceeds by exploiting symmetries in the problem, or looking specific geometries and regimes of flow.

In the case of microfluidic systems, an assumption that is usually made is that Reynolds numbers are very low [21], usually in the range of 10^{-3} or smaller. This means that the nonlinear term in the Navier-Stokes equation usually disappears, and the equation describing the flow becomes the Stokes equation, combined with the appropriate continuity equation. In the absence of body force, for a newtonian liquid, this yields

$$\mu\nabla^2\vec{u} - \nabla p = 0 \tag{2.1}$$

$$\vec{\nabla}\cdot\vec{u} = 0 \tag{2.2}$$

Where μ is the viscosity, $\vec{u}$ the 3D velocity field, and p the scalar pressure field. Behavior of the Stokes equation departs significantly from our everyday experience with fluid mechanical phenomena [22]. The absence of inertial effect and disappearance of the time derivative means that flow responds instantaneously to a modification in boundary conditions. The lack of

inertial effects also means that flow at this scale is time-reversible. Phenomena described by Stokes flow are dominated by viscous forces, which are usually negligible at macroscopic scales.

The system of equation can become problematic in certain infinite geometries. For instance, no uniformly valid solution exists for flow around an infinitely long cylinder. This is the famous "Whitehead's paradox" [23] which, according to the apocryphal story, led Alfred North Whitehead to quit fluid mechanics and pursue philosophy. Fortunately, in simple closed domains such as those we usually treat in microfluidics, this equation is well-behaved and usually straightforward to solve.

2.1.1 Microchannels

The equations for Stokes flow in microchannels can be further simplified by the fact that flow is unidirectional. The resulting system of equations describes the well-known Poiseuille flow, formalized by Jean Leonard Marie Poiseuille in his studies of blood flow in arteries [24]. Nowadays Poiseuille flow is included in most introductory textbooks on fluid mechanics, and flow profiles have been obtained for almost any conceivable channel cross-sections [3]. The problem of Poiseuille flow is described by Poisson's equation, and as such has strong analogies with problems in other areas of physics, including electrostatics, torsion of elastic beams, stochastic processes, and many others [25].

Hagen-Poiseuille law dictates that the flow rate Q is proportional to the pressure gradient Δp, with the constant of proportionality R_{hyd} called hydraulic resistance. Hydraulic resistance, which scales with the fourth power of the radius [5] becomes very important in microfluidic channels, where channel radii are of the order of the millimiter or micrometer.

Direct analogy can be made between the Hagen-Poiseuille law and Ohm's Law $\Delta V = R\ I$. This allows us to model networks of microchannels using the tools of elementary circuit theory. This electric-fluidic analogy can be pushed further, with analogs to other typical circuit elements added to the toolbox (actionable valves for transistors, reservoirs for capacitors, burst valves for diodes, etc).

The analogy with circuit theory formed the backbone of the modeling of microfluidic systems up until the 2000s. This logically went hand-in-hand with the direction of the field at the time. Microfluidics as a field of research was spawned in the wake of incredible strides in silicon etching techniques in the 1970s [26] [27], and from its inception held the promise of replicating the advances of microelectronics (which went from room-sized computers to smart watches in a manner of a couple decades) for fluid-mechanical operations. This conceptual edifice

reached its peak in the early 2000s, where the circuit logic of the theory was combined with advanced soft lithography techniques to create impressive systems, comparable in complexity to early microcomputers [7] [6].

2.1.2 The Hele-Shaw cell

While Poiseuille's law is very useful for analyzing unidirectional flow, a number of microfluidic systems operate with flow and diffusion that are free to evolve in 2D space. In order to study such a system, our starting point must be a geometry that better reflects this 2D aspect. In this work, we will be instead studying flow in the Hele-Shaw cell [28]. Introduced in an 1898 letter to Nature, the Hele-Shaw cell consists of a domain confined between two parallel plates separated by a gap that is much smaller than the characteristic length of the flow in the other directions. This geometry is very appropriate to model microfluidic chambers and channels, which are often much wider than they are deep (because of the way they are fabricated, either through Silicon etching, CNC milling or layer-by-layer 3D printing, all of which favor this sort of geometry). Provided that the gap is thin enough and that inertial effects are negligible, flow in the Hele-Shaw cell is given by [20]

$$\mathbf{u} \approx -\frac{1}{2\mu} z\,(d-z) \left(\frac{\partial p}{\partial x}\hat{\mathbf{x}} + \frac{\partial p}{\partial y}\hat{\mathbf{y}} \right) \tag{2.3}$$

Where μ is the viscosity, d is the gap between the plates, p is the pressure field and $\mathbf{u}$ is the velocity field.

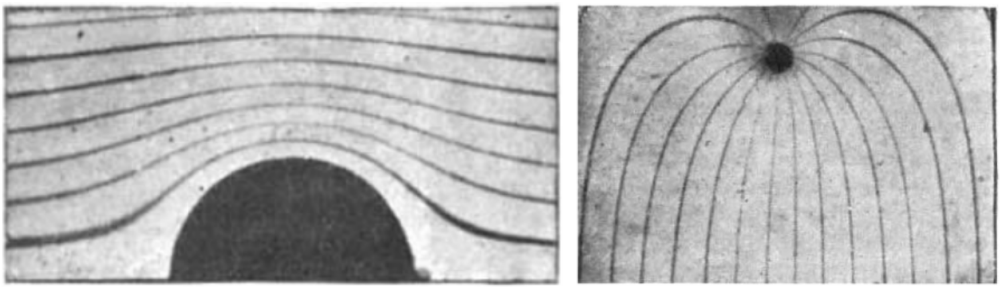

Figure 2.1 Flow in the Hele-Shaw cell. Streaks of ink are injected in the flow to highlight streamlines, which behave exactly like 2D electric field lines. From [28]

Flow in the Hele-Shaw cell is thus the gradient of a 2D potential function (which is proportional to $p\,(x,y)$) modulated by a parabolic profile in the z direction. The simple behavior of flow in the z direction allows us to treat the problem as a 2-dimensional one. We can then define a velocity potential $\phi\,(x,y)$ in such a way that, in the xy plane, $\nabla\phi = \mathbf{u}$. Combining

this with equation 2.3 as well as the continuity equation $\nabla \cdot \mathbf{u} = 0$ gives us the equation for the velocity potential

$$\nabla^2 \phi = 0 \tag{2.4}$$

Which is just the Laplace equation in 2 dimensions. What equation 2.4 implies, which was observed by Hele-Shaw in his article, is that the streamlines in the Hele-Shaw cell will behave exactly analogously to electric field lines in a 2D electric field. Equation 2.3 breaks down in a thin bounary layer in the vicinity of obstacles with no-slip boundary conditions, but potential flow formulation will generally remain valid in the rest of the domain.

The Hele-Shaw cell has been an object of extensive study because of the unstable behavior of viscous interfaces within it. The work of Saffman and Taylor in the 1960s showed that a fluid pushed through a Hele-Shaw cell containing a more viscous fluid generated an unstable interface, with the generation of long finger-like structures [29] [30]. This "viscous fingering" behavior has been studied thoroughly [31] [32], and has found applications in fields related to growth phenomena [33], flow in fractured rocks [34], and hydrocarbon extraction [35].

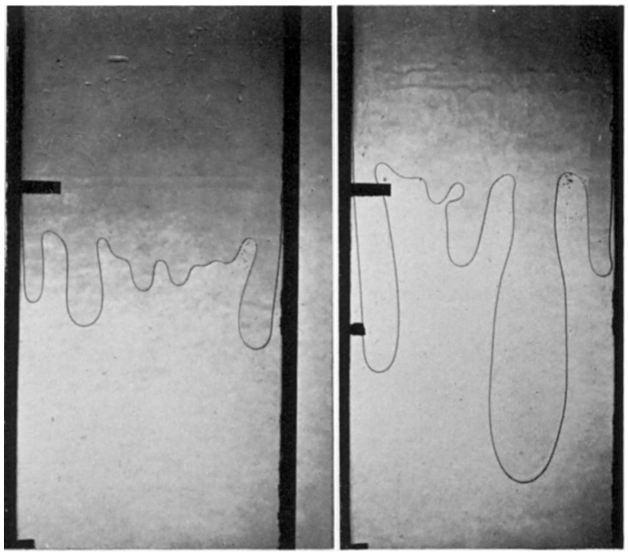

Figure 2.2 Unstable interface in the Hele-Shaw cell. From [29]

The present work is mostly concerned with single-phase flow, and we will not treat unstable interfaces. Problems of multiphase flows in Hele-Shaw cells do still appear in some microfluidic applications, in particular in droplet microfluidics [36], in some rheological experiments [21], in micromodels for porous soils [37], as well as in self-coalescence modules [38]. Some of these applications are briefly described in chapter 5, sections 5.4.5 and 5.10.

2.1.3 Darcy flow

There is a very strong mathematical analogy between flow in the Hele-Shaw cell and flow in 2-dimensional porous media. This can be seen in the constitutive equation 2.4, which is analogous to the equation for Darcy flow in 2 dimensions, and through the extensive analogies between viscous fingering in Hele-Shaw cells and the same phenomenon in porous media [39].

In his extensive review of the water resource projects for the city of Dijon [40], Darcy recognized that flow discharge in underground water sources was proportional to a pressure gradient. This was later formalized into Darcy's law, which forms the starting point for most study of groundwater mechanics (see for example [41]). Like flow in the Hele-Shaw cell, flow in 2D porous media can be expressed as the gradient of a potential function, which means that, up to a renaming of variables, most of the results in this work, are also applicable to Darcy flows. This also means that we can reuse a lot of results that have already been discovered in the context of groundwater research and apply them to the resolution of flow problems in microfluidic systems.

The strong analogy between flow in the Hele-Shaw cell and flow in porous media also means that most of the results we present are extensible to paper microfluidics [42], and microfluidic flow through porous media like hydrogels [43] or cell tissues (for example in staining or perfusion experiments). A good part of the work presented here deals with convection-diffusion phenomena. In most groundwater applications, the diffusion of heat or of a dilute tracer in the water through random motion is usually vanishingly small and is neglected. However, at the scale of paper microfluidics and microfluidic flow through hydrogels, having a framework that considers both convection and diffusion in porous media might be significant.

2.1.4 Complex potential

Description of our flow problem through the 2D Laplace equation enables us to use complex flow formulation. By expressing our position vector as the complex number $z = x + i\ y$, the velocity potential can be written as a complex function of a single variable $\Phi(z)$.

$$\Phi(z) = \phi + i\ \psi \tag{2.5}$$

The real part ϕ of this complex potential corresponds to the level set of the potential, while the imaginary part represents the stream function ψ. Complex potential formulation for hydrodynamics is explicited in detail in classic textbooks such as Lamb [44], or in Strack [45] for the analog case of 2D Darcy flow.

Complex potential formulation has been used extensively to study fluid mechanical problems at a range of scales. We note for instance its use in the study of airfoil design [46], vortex dynamics [47], ship hull design [48], in the study of turbulent mixing behind hills or buildings [49], etc. In groundwater mechanics, complex potential formulation has been used to study thermal feedback in groundwater heat pumps [50] [51], tracking the saltwater-freshwater interface in coastal aquifers [52], or transit properties of particles in fractured rocks [53]. Examples of this application of complex potential theory to flow problems are illustrated in figure 2.3.

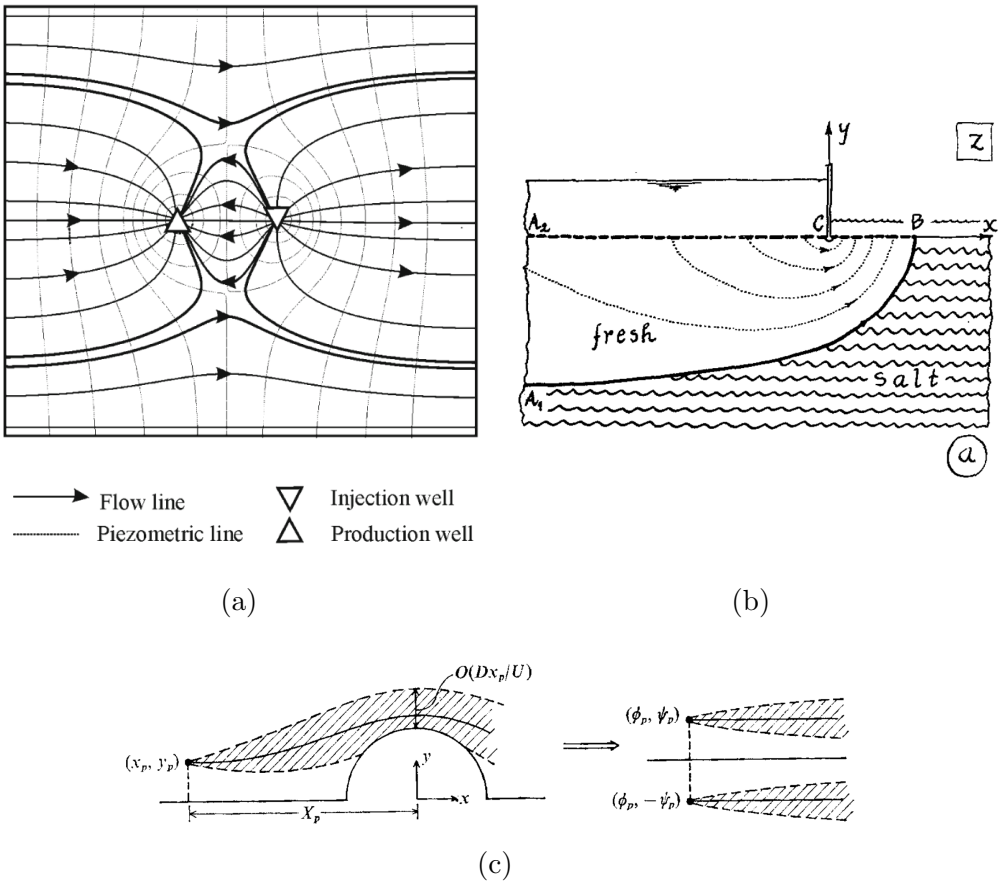

Figure 2.3 Examples of application of complex flow theory to problems at different scales. (a) Thermal feedback in groundwater heat pumps, from [51], (b) Interface problems in coastal aquifers, from [52], (c) turbulent dispersion behind semicircular hills, from [49]

2.1.5 Flow singularities

One advantage of potential flow theory is that equation 2.4 is linear, which allows flow to be determined using superposition of basic elements. In particular, flow can be obtained by

adding together flow singularities and simple background flow terms. In most applications in fluid mechanics, flow singularities are usually situated outside of the domain of interest, as they represent non-physical source or sink terms. An example of this would be potential flow past a cylinder, which can be represented as the superposition of a dipole source and a straight flow (see Lamb, sections 68, 69 [44]). In such a domain, the dipole source is inside of the cylinder and thus not directly present in the flow.

In many groundwater applications, though, the singularities are present directly in the flow. These flow singularities in Darcy flow can represent wells which inject or extract water from aquifers, which are often quasi-planar. These well systems are very analogous to the microfluidic systems we will be studying, as we will highlight in further sections. Applications of groundwater systems constituted as superposition of point sources and sinks include study of rainwater drainage in soils [54], porosity calculation in carbonate aquifers [55], soil decontamination processes [56], hydrocarbon extraction [35], upconing in coastal aquifers [57], etc. Examples of such systems are illustrated in figure 2.4.

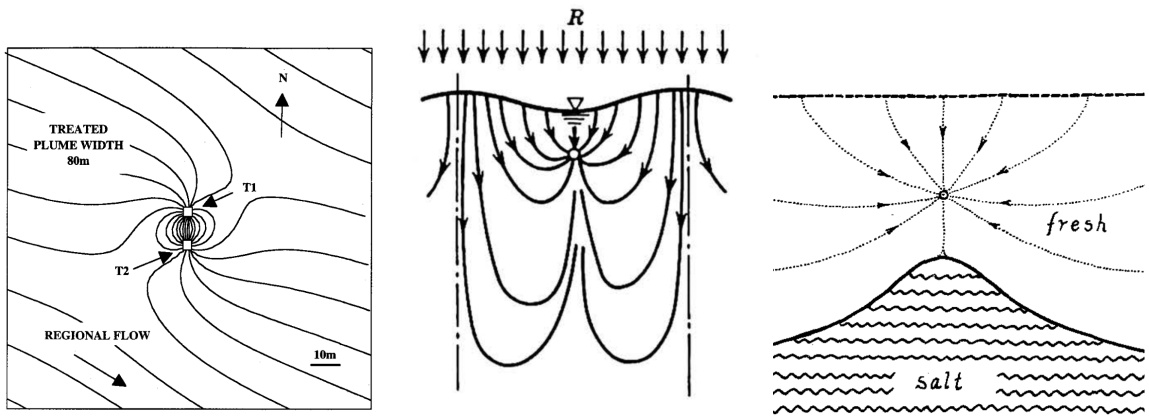

(a) (b) (c)

Figure 2.4 Groundwater systems built as superposition of flow singularities. (a) Decontamination of soils using source-sink well pairs, from [56]. (b) Drainage of rainwater through arrays of sinks, from [54]. (c) Upconing near drains in coastal aquifers, from [52].

Flow singularities are significant in this work, as we will study systems that are built by injecting and aspirating fluid in Hele-Shaw cells. In these "multipolar microfluidic" systems, the singularities are directly present in the domain, in the form of point-like apertures from which we impose constant mass flux. An overview of multipolar microfluidic technologies is presented in chapter 3.

2.1.6 Conformal mapping

The main advantage of complex number formulation for flow theory is that it directly enables the use of conformal mapping. Conformal maps are a family of transformations of the complex plane onto itself which locally preserve angles. For a function of a complex number $f(x+iy) = u(x,y) + iv(x,y)$, the condition of local angle preservation is formalized in the Cauchy-Rieman conditions [58].

$$\frac{\partial u}{\partial x} = \frac{\partial v}{\partial y} \qquad \frac{\partial v}{\partial x} = -\frac{\partial u}{\partial y} \tag{2.6}$$

Two key results follow directly from these conditions. The first is that the set of conformal maps of the complex plane to itself corresponds exactly to the set of analytic functions of a single complex variable. The second result is that maps that are conformal will preserve solutions to the Laplace equation [59]. This means that a conformal map applied to a harmonic function will yield a function that is also harmonic. This has historically made conformal mapping a tool of choice for studying 2D problems described by Laplace's equation, including problems of electrostatics [60], optics [61], heat transfer [62], growth processes [63], and elastic deformations [64]. In the context of hydrodynamics, conformal mapping has also been a tool of choice. Problems of flow in Hele-Shaw cell and 2D Darcy flow are described by the Laplace equation, and as such the techniques of conformal maps are directly applicable. Most of the work cited in sections 2.1.4 and 2.1.5 uses conformal mapping to analyze flow problems in complex geometries.

Applications of conformal mapping rely on the Riemann mapping theorem, which states that any simply connected domain can be conformally mapped to the unit circle. In practice, this means that there exists a map from any simply connected domain to any other simply connected domain. This equivalence has been used to find properties of complex electric circuit elements [66] [67], heat transfer coefficients for beams of different cross-sections [62] [68], properties of complex-shaped waveguides [69], as well as in the study of the propagation of cracks in brittle medium [70]. In all of these situations, a physical problem is first solved in a simple geometry (often a square, a circle, or a semi-infinite strip), and the solution is then mapped to the more complex domain to obtain quantitative results. In the general case, the map may not have a representation as a combination of simple functions, but extensive numerical methods have been developed to find such maps. One category of map that comes up often in engineering applications is Schwarz-Christoffel maps, which are maps from the upper half-plane to the interior of polygons. Schwarz-Christoffel maps for simple 2 or 3-sided polygons are given in terms of exponential and logarithm functions, while maps to

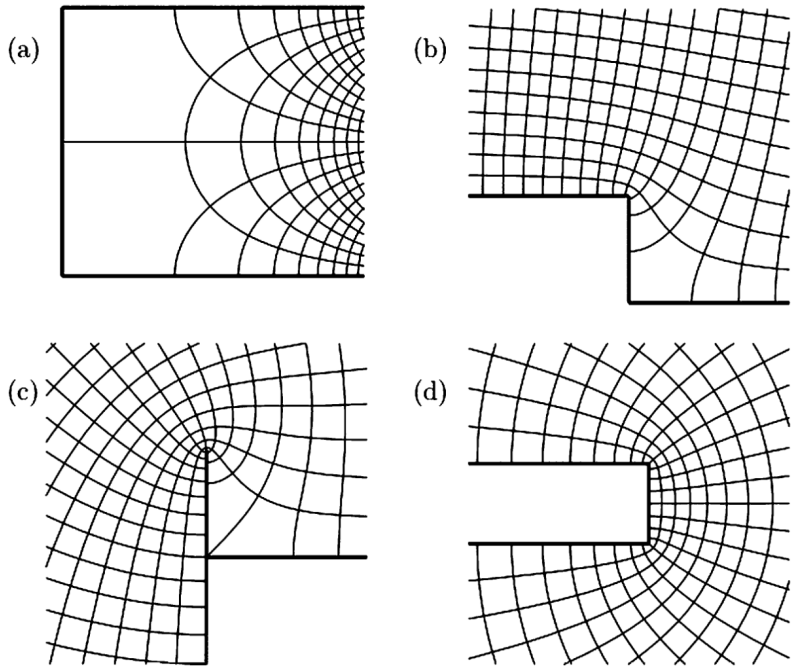

Figure 2.5 Conformal maps of the upper half-plane to different polygonal domains. From [65]

the interior of rectangles and squares are given in terms of elliptic functions [59]. Maps for arbitrary polygons usually do not have analytical expressions, but numerical methods for computing Schwarz-Christoffel maps are widely available [65]. Extensions of the Riemann mapping theorem to doubly connected domains exist [59], but in general multiply connected domains are much more difficult to treat. There has been significant work applied to the extension of the principles of conformal mapping to multiply connected domains [71] [72].

In the present work, conformal mapping will be one of the tools of choice we use for developing a theory of flow and diffusion in microfluidic systems. We will mainly treat systems that exist in the semi-infinite plane, although systems in bounded geometries are studied in section 4.9 and chapter 7.

2.2 Diffusion

Microfluidic systems often involve not just flow but also diffusion, be it from reagents, dyes, or drugs diluted in the liquid, or from liquids at different temperature put in contact with each other. Complete understanding of these technologies involves knowing the mixing properties of these diffusing species, and tracking how they are convected through the devices. In this section we give an overview of the mathematical tools used for modelling convection and

diffusion of these diluted species in our systems.

For the present work, we focus solely on dilute solutions, so that the concentration of a dilute species does not significantly affect the properties of the flow. This will allow us to decouple the two problems: we first solve for flow in the device, and then solve for convection-diffusion of the dilute species.

2.2.1 Brownian motion and Fickian diffusion

The simplest diffusive phenomena are described by Fickian diffusion, where the diffusive substance is modeled as an ensemble of independent random walkers, which leads to a mass flux proportional to the local concentration gradient [73].

The first recorded description of brownian motion dates back to the Roman epicurean Lucretius, who described the random movement of dust particles in the air [74]. Modern observations can be traced back to Jan Igenhousz's study of charcoal particles on a liquid film [75] and of course Robert Brown's microscope observation of the jittering of pollen. In the 1880s, lord Rayleigh also described sound waves in solid materials as discrete entities randomly bouncing around the interior of the domain [76].

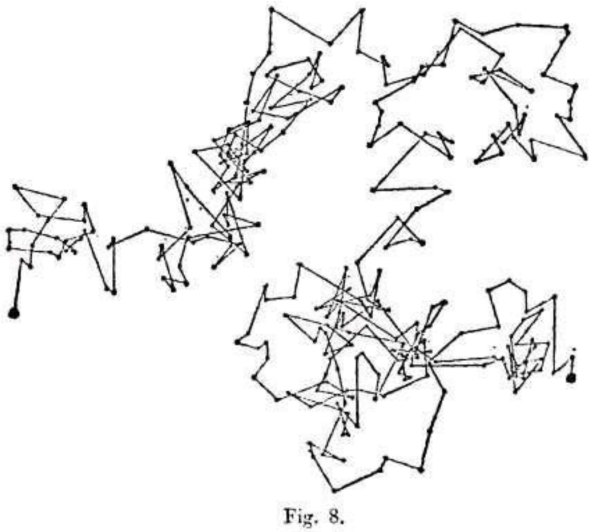

Figure 2.6 Experimental images of brownian motion from Jean Perrin. From [77]

In the same years, considerable development was being made in the mathematical modeling of heat and diffusion. Fourier published his famous studies of heat conduction in 1822 [78], where he recognized heat flux to be proportional to the temperature gradient, and formulated the heat equation, describing transient conduction phenomena. In 1855, Adolf Fick formulated an

analog law for mass transport in dilute systems [79], recognizing mass flux to be proportional to concentration gradient and explicitly making the analogy with Fourier's law for heat.

In the early 1900s, explicit links were made between the random walk phenomena first observed by Igenhousz and Brown and the theory of linear diffusion as described by Fourier and Fick. Bachelier's PhD thesis on the fluctuation of stock price is regarded as one of the first mathematical description of brownian motion [80]. The work did not have immediate impact, despite being recognized today as pioneering both the study of diffusion phenomena and the application of mathematical analysis to economics. In 1905, statistician Karl Pearson sent a letter to nature describing the problem of the random walk [81], and asking for help in elucidating the mathematics of the problem. The answer to Pearson's problem, cementing the link between random walk processes and Fickian diffusion, was provided by Einstein [82], in work whose experimental validation was done 2 years later by Perrin [83], earning Perrin the Nobel prize in physics. Experimental images from Perrin, as they appeared in his book "the atoms" [77], are shown in figure 2.6.

Fickian diffusion is the starting point for studying diffusion in microfluidic systems. Fick's law prescribes mass flow proportional to the concentration gradient

$$\mathbf{J} = -D\nabla c \tag{2.7}$$

Where the factor of proportionality is called the diffusion coefficient, and can be obtained from the characteristic step length l and time τ of the random walk (which can themselves be found from the physical characteristics of the system using Einstein's equation [5]).

$$D = \frac{l^2}{\tau} \tag{2.8}$$

In the absence of convection or reaction, the diffusion equation is thus

$$\frac{\partial c}{\partial t} = D\nabla^2 c \tag{2.9}$$

Which reduces to the Laplace equation for the steady-state case. Because of the form of the equation, the units in which the concentration c is expressed can be chosen arbitrarily, and we will generally express them in an adimensional system where $c = 1$ represents the maximum concentration and $c = 0$ represents the absence of solute.

2.2.2 Diffusion in disordered media

Since the present work has a lot of ties to groundwater mechanics, hydrology, and flow in disordered media, it is worthwhile to mention some particularities of solute dispersion in these systems. Dispersion in porous media was first studied independently by Saffman [84] and De Josselin De Jong [85], who modelled dispersion as random walks through a network of pores. In this work, molecular dispersion was assumed to be negligible when compared to dispersion by the flow in the media. More recent work has identified that randomly diffusing tracers diluted in a liquid which is itself flowing through a disordered media may not be described adequately by Fickian diffusion. Diffusion in fractures or disordered soil close to the percolation threshold instead behave following what has been called "anomalous dispersion" or sometimes "fractal diffusion", in such a phenomena, the characteristic time and length scale are linked by a law of the type [86]

$$l \sim \tau^{2/d_w} \tag{2.10}$$

Where $d_w > 2$. This relation concretely corresponds to a "slowing down" of diffusion over long distances when compared with normal Fickian diffusion, and it means that the partial differential equations describing the evolution of the concentration profile will depart from the simple Fourier law. Exhaustive treatment of anomalous diffusion is beyond the scope of this dissertation, but can be found in classic papers such as [87], [86], or [88], and applications to flow in fractured rock and porous media can be found in [34]. Beyond flow in porous media, anomalous diffusion phenomena have also found applications in description of human mobility patterns [89] and transport in cell biology [90].

Considerations of anomalous dispersion may become important when applying the results presented in this work to disordered media, be it in the study of flow through soils, dispersion in cell cultures, or in paper microfluidics.

2.2.3 Convection-Diffusion

The previously described heat equation appropriately describes the evolution of a concentration field for a dilute solution in a liquid in the absence of fluid movement. If the fluid is also in movement, a convective term has to be added to the mobility in 2.7, which gives us the convection-diffusion equation.

$$\frac{\partial c}{\partial t} = D\nabla^2 c - \mathbf{u} \cdot \nabla c \tag{2.11}$$

Convection-diffusion problems vary widely because of the presence of the convective term, and treatment of different problems may turn out to require different methods, depending on the type of flow at hand. In this work, we are studying 2D flow that can be adequately described by potential flow theory, such that $\mathbf{u} \sim \nabla\phi$. In steady-state, and using dimensionless quantities, the equation thus becomes

$$0 = \nabla^2 c - \mathrm{Pe}\nabla\phi \cdot \nabla c \tag{2.12}$$

Where the Peclet number $\mathrm{Pe} = \frac{L/u}{D}$ appears, with L and u representing characteristic length and velocity scales for the flow. The Peclet number represents the fraction of convective to diffusive transfer in the flow, and in the microfluidic systems we study it will generally be quite high, of the order of 100 to 10000. We note, however, that problems related to equation 2.11 are generally singular in the limite of infinite Pe, such that even in the limit of very convective flow, the diffusive term can never be entirely neglected, or we get solutions that fail to fulfill all boundary conditions. In practice, this is explained by the fact that there always remains a small boundary layer in the domain where diffusion dominates convection, and increasing Pe makes this boundary layer smaller and smaller but never eliminates it [23]. Mathematically, this singular behavior can be seen by the fact that taking the limit of infinite Pe effectively eliminates the Laplacian term, reducing the order of the partial differential equation by one and thus resulting in a problem that cannot fulfil the same boundary conditions correctly. Because of this behavior of convection-diffusion problems, their numerical resolution can be complexified, and some numerical methods suited for elliptic problems may become less precise or even unstable if used incorrectly [91] [92]. It is still often still valuable to consider the "pure convection" problem, given by

$$0 = \nabla\phi \cdot \nabla c \tag{2.13}$$

Whose solution is $c = f(\psi)$, where ψ is the stream function. In many practical applications, for instance when finding the footprint of a microfluidic probe or other similar device (see chapter 3), the pure convection solution can be sufficient, as it only requires us to know the streamline pattern of the flow to approximate the footprint. In problems at high Pe, the pure convection solution can also be the leading order term in a singular perturbation scheme.

Equations of the form 2.11 appear in other areas of physics beyond just transport of dilute analytes in fluid flow. We note for example vorticity transport in linearized versions of the Navier-Stokes equation [93] [94], the Fokker-Planck equation in statistical physics and the physics of plasma [95], transport equations for electrons and holes in semiconductors [96] or

the Black-Scholes equation in financial modeling [97].

Methods of resolution for convection-diffusion problems will generally depend on the exact nature of the convective term $\mathbf{u} \cdot \nabla c$ and the range of Pe we are looking at.

2.2.4 Taylor dispersion

A well-known effect of convection-diffusion in creeping flows is the smearing of concentration profiles by Taylor-Aris dispersion [98] [99]. A patch of concentration being carried by a parabolic flow will exhibit a "smearing" due to the uneven velocity profile (see figure 2.7), which will lead to an effective diffusivity that is higher than the measured molecular diffusivity D.

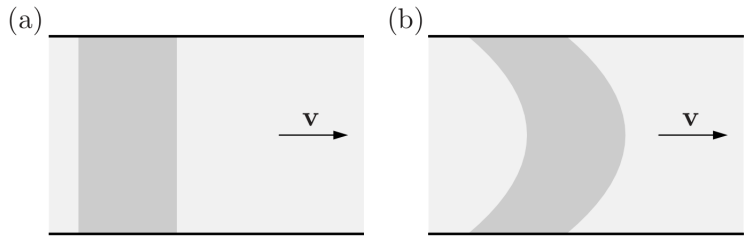

Figure 2.7 Smearing of concentration in a parabolic flow, illustrating the principle of Taylor-Aris dispersion, image from [5]

Taylor dispersion plays an important role in many microfluidic systems, as it causes heavy smearing of reagents carried through microchannels. However, most of the systems we study in this document are at steady-state, with diffusion happening in a roughly perpendicular direction to flow. In such a system, there is still modulation of the concentration profile by the parabolic flow (in the form of the so-called "butterfly effect" [4]), but Taylor dispersion can usually be neglected.

If, in future work, we start studying the details of the transient aspects of convection and diffusion in multipolar systems, it will become important to consider Taylor dispersion.

2.2.5 Conformal mapping for convection-diffusion problems

We are dealing with a convection-diffusion equation of the form 2.12, where the flow term is the gradient of a 2D scalar potential. It turns out that the system of equations 2.4 and 2.12 is actually conformally invariant [100]. This means that applying a conformal map to a solution of the convection-diffusion problem in a certain flow pattern described by a potential function Φ will yield an equally valid solution to a new convection-diffusion problem with flow

described by the transformed potential. Visual examples of this procedure are illustrated in figure 2.8

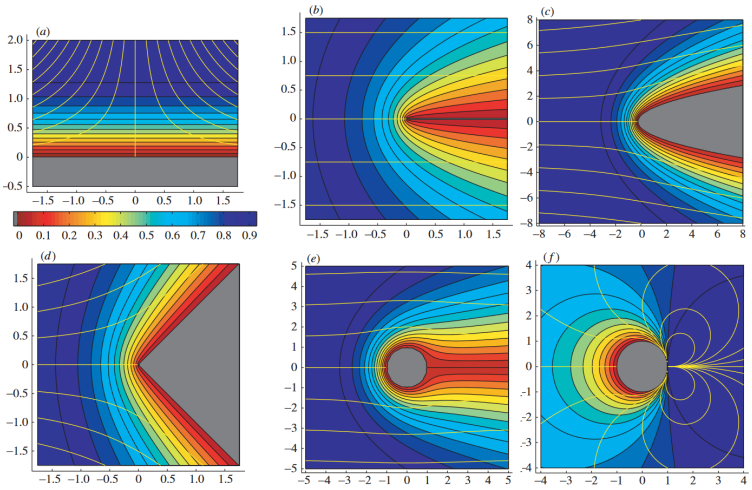

Figure 2.8 Solutions to convection-diffusion problems obtained using conformal maps. From [100]

Application of the method of conformal mapping to convection-diffusion problems dates back to Boussinesq's work in the early 1900s [101]. The strategy for a general problem will usually be to transform the problem to streamline coordinates (or Boussinesq coordinates), where the complex potential is $\Phi = z$, corresponding to simple plane flow. In such a simplified problem, boundary conditions will map to segments of constant ψ, and the convection-diffusion equation reduces to

$$\frac{\partial^2 c}{\partial \phi^2} + \frac{\partial^2 c}{\partial \psi^2} = \mathrm{Pe}\frac{\partial c}{\partial \phi} \tag{2.14}$$

This equation can be brought back, through a change of variable, to the Helmholtz equation, for which a number of solutions in terms of Green's function have been tabulated [102]. Notable work on the resolution of convection-diffusion problems through conformal mapping includes work on pollution transport [49], modeling of dispersion by porous obstacles [103], study of wakes behind rigid obstacles [104], moving boundary problems in growth phenomena [105], tracer dispersion in porous flows [53], or vorticity transport in the Navier-Stokes equation [93] [106].

The application of conformal maps to convection-diffusion problems will be the main analytical tool we use throughout this work to obtain analytical solutions to transport problems in microfluidic systems.

2.2.6 Diffusion from surfaces and boundaries

We briefly mention a few classic solutions to problems of convection-diffusion from surfaces and obstacles. Knowledge of these solutions will be useful in analyzing transport problems in microfluidics.

Transport from a surface in shear flow has been studied by Lévêque [107], who showed that the concentration profile could be expressed in the form of an exponential integral of the type

$$f(x) = \int_0^x \mathrm{e}^{-t^3} dt \tag{2.15}$$

The Lévêque solution is very useful in a number of microfluidic applications involving a reactive surface placed at the bottom of a microchannel, or under a probe-type system. Similar solutions for both leading edges [108] and trailing edges [109] have been found in terms of Wiener-Hopf methods. These solutions assume the edge to be much longer than the width of the boundary layer. Work has been done on the more difficult problem of a reactive absorber of finite length [110] [111], although such problems generally require numerical methods. Solutions to convection-diffusion from a semi-infinite leading edge in plane flow is given in [105] in terms of error functions. This solution will be useful in deriving closed-form solutions to the transport problems we are studying.

Acrivos and Taylor also obtained expressions for heat transfer for suspensions of spheres or cylinders in Stokes flow [112] using singular perturbation methods, which has found use in the physics of colloids as well as in the study of plankton and other swimming microorganisms.

2.2.7 Reaction-Diffusion

In addition to convection and diffusion, solute transport in microfluidic systems often involves the production or consumption of the diffusive species. Consumption or production of the dilute species that happens at the boundary of the domain can usually be modelled using appropriate boundary conditions to the convection-diffusion equation. Problems with constant concentration or constant flux from a surface can be modelled using the solutions mentioned in the previous section, for example the Leveque solution for transport from a reactive surface at the bottom of a microfluidic channel.

Addition of a volumetric source or sink term to the diffusion equation turns the problem into one of reaction-diffusion. Such a problem can be found, for example, when studying oxygen or nutrient consumption within cell cultures. Problems involving convection, diffusion, and reaction all at once are generally very difficult to tackle, and analytic treatment will generally

only work in regimes where one phenomena dominates the others. Useful information can usually still be obtained by observing the behavior of the dimensionless quantities dictating the ratio of each phenomena to the others. Such a treatment of convection-diffusion-reaction problems in the case of microfluidic systems is done in [113].

Reaction-diffusion problems with more than one reacting species constitute a vast domain of research in applied mathematics, due to the great variety of spatial patterns that result from them [114]. Among these complex reaction-phenomena are wavelike phenomena in the BZ reaction [115] and the well-known Turing patterns [116]. These reaction-diffusion systems have applications in the modeling of phenomena at a range of scales, from the dispersal of vegetation [117] [118] to the formation of patterns on the skin of certain animals [119] [120] to spatial distribution of animal populations [121]. Analogies have also been drawn between the sort of pattern yielded by diffusion reaction systems and the behavior of predator-prey dynamics in space [122]. While these systems received relatively little attention at the time of their publication in the 1950s, the advent of computer graphics and tools for easy simulation and visualisation of these reaction-diffusion systems has reignited interest in them in the past couple decades. Reaction-diffusion patterns have also been a tool of choice in the procedural generation of textures for computer graphics [123]. Examples of reaction-diffusion patterns are shown in figure 2.9

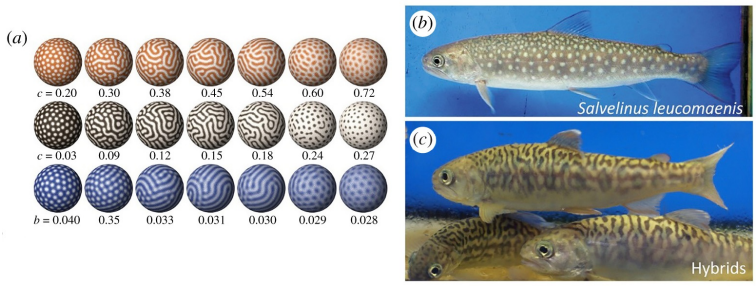

Figure 2.9 Reaction-diffusion patterns used to model the pigmentation of the skin of a zebrafishs. a) Simulations of reaction-diffusion equations on the surface of spheres. b) and c) Similar patterns observed on the skin of zebrafish From [120]

2.3 Similar work in the context of microfluidics

The main contribution of my PhD work has been not in inventing new mathematical tools but in taking existing tools and applying them to the context of microfluidics, where they had not found full applicability yet. In that spirit, to conclude this section, I will list some of the pre-existing work that was published in applying the mathematical concepts reviewed

above to microfluidic systems.

2.3.1 Hele-Shaw cells and potential flow

Modeling of flow in microfluidic chamber using Hele-Shaw cell formalism and superposition of point charges was a well-known topic in the early 2000s. Early publications on microfluidic probes recognized the flow to be modelled by superposition of point charges in Hele-Shaw cells, which allowed for the determination of the position of the stagnation point, as well as tracking of the probe's approximate footprint by identifying the streamline separating the "inside" and "outside" domains [8] [124]. Superposition of point charges in potential flow was used to track stagnation points in complex channel junctions, and was combined with predictive control loops to freely move particles around in 2D space [125] [13]. Potential flow formulation was also used to model flow in and around microfluidic droplets [126] [10]. Finally, chaotic advection has been studied in Hele-Shaw cell in the context of mixing applications [127].

2.3.2 Studies of diffusion

Studies of diffusion phenomena in microfluidic systems were also ubiquitous, at least in the context of networks of microchannels. Extensive work has been done studying lateral diffusion in microfluidic channels [128] [4]. These studies were applied to the design of the microfluidic mixers and gradient generators of the 2000s [129] [130] [131]. One-dimensional models have also been extended to more complex 2D microfluidic gradient generators in order to quantify mixing [132].

Some work, although more limited, had also previously been done in the context of 2D flow systems. Linearized convection-diffusion problems have been solved to obtain scaling behavior of concentration gradients near the stagnation points of microfluidic probes [124] [133]. Full 3D numerical models for convection-diffusion in microfluidic probes were also studied [14] [134]. Extensive study of the behavior of reactive patches at the bottom of microchannels, considering convection, diffusion, surface reaction and the aspect ratio of the system has also been conducted, both using dimensionless number analysis and through numerical computation [113].

2.3.3 Conformal transforms

Conformal mapping, although a very classic tool for the analysis of 2D flow, had been relatively unused in microfluidic applications at the time the work was started. Conformal

mapping had been used to study the permeation of solvent through bulk PDMS [135]. Otherwise, conformal mapping was also already well-known in the study of viscous fingering [32], which is closely tied to microfluidics. In particular, fingered growth processes related to diffusion limited aggregation (of which viscous fingering is a subset) have been thoroughly studied using iterated conformal maps [136] [137].

CHAPTER 3 MICROFLUIDIC MULTIPOLES

3.1 Outline

The theory we present in this dissertation was first developed to analyze what we called Microfluidic Multipoles. Using analogies borrowed from electromagnetism, we show how a number of microfluidic technologies, starting with microfluidic probes [8] and including several systems published in the late 2000s, can be conceived of as "multipoles", that is 2D flows constructed by a superposition of point-like injection and aspiration apertures.

The work presented in this chapter was chronologically the first impetus of the project, where I developped a theory for flow and diffusion in microfluidic probes, and then showed how it could be extended to arbitrary arrangements of point sources and sinks.

The theoretical work was backed by experiments by Pierre-Alexandre Goyette, who fabricated systems using 3D printing and then operated them first to compare theory and experiment, and then in an application involving immunoassays. The application, described in section 3.15, forms the template for newer research on highly multiplexed microfluidics that is currently being pursued in Thomas Gervais' research group [138] [139].

This chapter recapitulates results published in Nature Communications in 2019, in a paper co-authored by Pierre-Alexandre Goyette and myself [15].

3.2 Contribution

The text of the article was written in by Pierre-Alexandre Goyette and myself, in about equal proportions, with extensive feedback from Thomas Gervais. I wrote the introduction as well as the first half, concerning context and theory, and I produced the theoretical figures in the article. My main contribution for the work in this article consisted in developing the theoretical models for flow and diffusion in multipolar devices, and using conformal transforms to map simple solutions to more complex ones. Pierre-Alexandre did the work related to fabrication, experimental imaging, and the proof of concept immunoassay application.

3.3 Microfluidic Probes

The initial objective of the research project was to extend previous work, mostly done in the IBM research group by David Juncker , Govind Kaigala, and Emmanuel Delamarche on

microfluidic probes [8] [140].

Microfluidic probes consist of a pair of point-like apertures, generally connected to syringe pumps, located a short distance from each other on a flat mesa. The mesa is put in close proximity to a surface under analysis, and the system is submerged in water, creating a quasi-2D space in which flow can freely evolve, without being confined by walls.

If the aspiration aperture aspirates fluid at a higher flow rate than the injection aperture, and if the gap between the mesa and the processing surface is constant and small enough compared to the interaperture distance, the entirety of the injected fluid is reaspirated, and a steady-state flow profile is established. This regime, termed "hydrodynamic confinement", yields a footprint of finite size, whose shape can be adjusted by modifying the aspiration rate (see figure 3.1a).

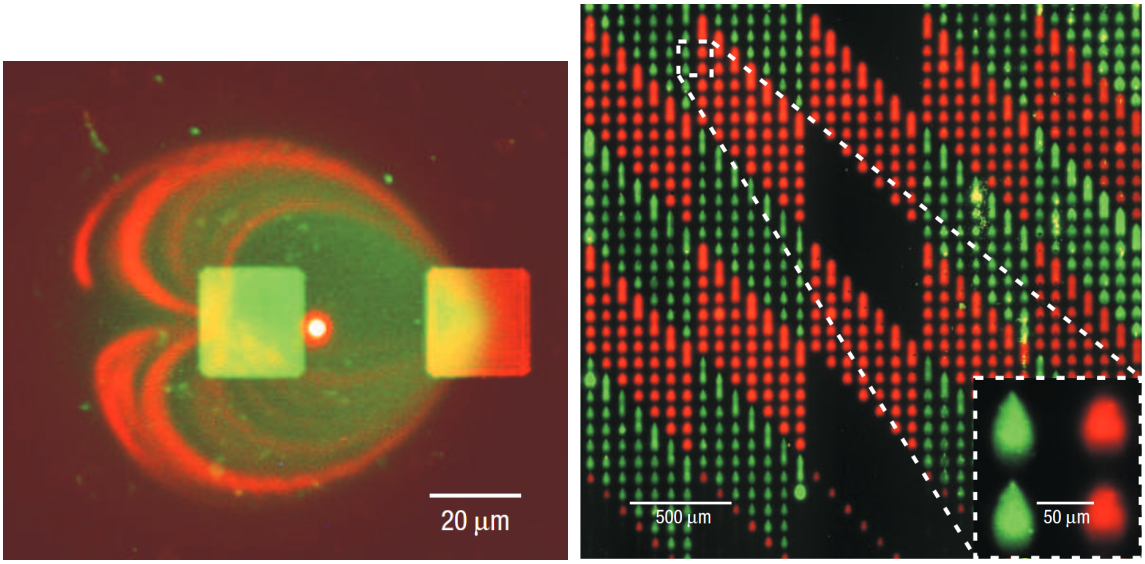

(a) (b)

Figure 3.1 Concentration footprint for a microfluidic probe (a), and an example of a large surface stained using the same probe (b). Images taken from [8]

The small footprint of the microfluidic probe, as well as the simplicity of its design, made it ideal for use in a scanning fashion in order to precisely stain biological surfaces [141] (see figure 3.1b).

While not the first published system to break away from the channel-based paradigm, microfluidic probes formed a great template for what would later be coined "Open-Space Microfluidics" [140]. As a technological tool, microfluidic probes' main selling points came in solving problems that could not be solved by typical networks of channels, namely the

non-destructive processing of large surfaces using flows with very small shear stresses (although some later applications did explore applications involving significant generation of shear stress [14]).

Although microfluidic probes were initially built out of silicon, Pierre-Alexandre's work in the Nature Communications article pioneered the fabrication of these systems using much more accessible photolithography 3D printing [142], which is what was used in all of our group's subsequent work. 3D printing of microfluidic probes and other open-space microfluidics systems has many advantages, some of which we discuss in section 3.11.

3.4 Microfluidic Quadrupoles

Shortly after the publication of the original microfluidic probe article, Mohammad Qasaimeh and Thomas Gervais published work on "Microfluidic Quadrupoles" [124]. Microfluidic quadrupoles were analogous to microfluidic probes, but had a set of 4 apertures instead of 2 (see figure 3.2).

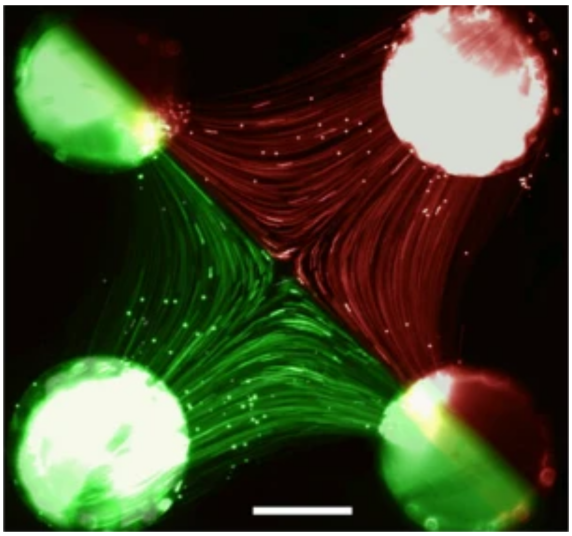

Figure 3.2 Experimental image of colored beads in a microfluidic quadrupole. Different colored beads are injected in each of the two injection apertures. Taken from [124]

Near the center of the microfluidic quadrupole, the flow is purely extensional. By injecting different fluids in each of the two injection apertures, a linear concentration gradient can be generated near that center. The original quadrupole article, published in Nature Communications, demonstrated fabrication and operation of the system to create tunable concentration gradients as well as providing in-depth discussion of the theory behind it. Later publications focused on more concrete applications, such as the use of microfluidic quadrupoles to study

the migration of neutrophils [143].

The quadrupole article is significant because it is the first to explicitly introduce the strong analogy between probe-type microfluidic flows and electric multipoles, an analogy which is central to this project.

3.5 Other scanning-probe systems and "Open-Space Microfluidics"

The 2010s saw the rise of a number of additional microfluidic technologies operating without the need for channel walls. Following the success of the initial microfluidic probe, IBM research group published several different designs for microfluidic probes and probe adjacent devices. These included vertical microfluidic probes that could be rapidly prototyped in silicon [144], probes based on hierarchical flow confinement, where a series of apertures were nested into each other to produce a more stable envelope [145], hydrodynamic thermal confinement [146], where microfluidic probes were used to inject heated liquid on surfaces, and linear arrays of apertures used to create comb-like patterns on surfaces [147].

Around the same time, other groups experimented with other scanning probe-type systems, finding different ways to process surfaces using minute volumes of fluids. These included chemistrodes [148] that could locally expose a surface to sequences of reagent pulses, fluidFM [149] combining nanofluidic channels and atomic force microscopy heads, pipetting systems [150], fluid-in-fluid deposition [151], etc.

All of these technologies were grouped under the "Open-Space Microfluidics" label [140], as a way to differentiate them form existing channel network systems. The label of "Open-Space Microfluidics" was adopted by a small number of research groups to self-describe parts of their research work. Most of these groups, including our own [152], contributed to a book on the subject, edited by Govind Kaigala and Emmanuel Delamarche [153].

3.6 Preexisting theoretical work

While most of the focus of open-space microfluidics research was on experimental setups and applications, some papers did focus on more theoretical analysis of flow and transport in these systems.

Extensive work on the position and control of stagnation point in multipolar flows was done by groups using channel junctions to precisely trap particles and move them around arbitrarily [13]. The same analysis was done very early on to identify the position of the stagnation point in microfluidic probes, and thus determine a good estimate on the size of its footprint [8].

Identification of key adimensional parameters in microfluidic probes, namely Reynolds number and Peclet number, was done from the initial article. Scaling laws for concentration gradients were obtained in analytical manner for microfluidic probes and quadrupoles by solving linearized versions of the convection-diffusion equation around the stagnation points of the flow [124] [133].

3.7 Preexisting numerical work

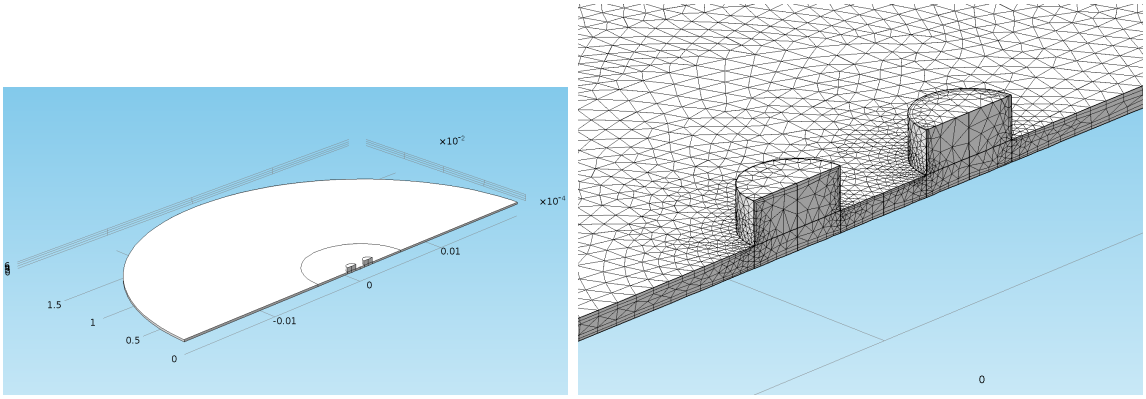

(a) (b)

Figure 3.3 Typical simulation domain for a microfluidic probe in Comsol Multiphysics. (a) Zoomed-out picture of the domain. (b) Zoomed-in version of the same domain, showing details of the mesh. In such simulations, compromise is often made between using realistic aspect ratios and minimizing the number of elements in the mesh.

Some groups presented finite element analysis of flow and diffusion in microfluidic probes and probe-adjacent systems [14]. However, these simulations' results were often not very precise, offering more of a qualitative insight into the features of the flow, and often being supplanted by simple dimensional analysis such as the one presented in [133] in terms of precision. This is mainly due to the highly multiscale aspect of these systems, which renders them difficult to directly analyse using full 3D CFD.

Indeed, one of the design rules for microfluidic probes and other systems, mentioned early on, is that the thickness H of the quasi-2D domain should be significantly smaller than the injection and aspiration apertures' radius r, which itself should be significantly smaller than the interaperture caracteristic distance d. Some early papers recommended that that $d \approx 10r$ and that $r \approx 10H$ [152], although in most practical setups the ratio is more of the order of $H \approx r$ and $d \approx 5r$. This requirement on dimensions is exacerbated by the fact that the domain that flows evolve in in most open-space microfluidics application is usually

considered to be infinite (that is, the 2D domain extends very far past the interaperture distance). In a typical simulation, to avoid significant edge effects, the simulated domain must be at least 5 to 10 times larger than the interaperture distance. See figure 3.3 for a schematic representation of the length scales at play. All of these factors compound together to generate simulated domains that are, in the best cases, approximately 100 to 1000 times wider than they are thick. This requirement is directly contradictory to the requirement of most CFD meshes, which requires individual elements to be, as much as possible, the same dimension in every direction. Resolution of the parabolic flow in the direction of the gap puts constraints on the types of elements used, forcing us to use higher order elements, or to use elements whose size is dictated by the very small gap dimension. Even in these cases, resolution of the 3d aspects of the flow underneath the apertures may be substandard. The associated diffusion problem is also singular in the limit of high Peclet, and leads to solutions where concentration is constant for most of the geometry, and then varies very fast in a thin boundary layer, putting additional strain on numerical methods. The exact position of this boundary layer changes depending on the parameters of the flow and is not known a priori in more complex geometries. For all of these reasons, most of the work that has been published on numerical analysis of microfluidic probes and other related multipolar systems has often been substandard in terms of resolution and theoretical precision. Of course, such simulations were still decent guides to design, but they often ended up being quite costly in terms of computing time for a yield that was not very precise. In the article presented in chapter 5, as well as in some of our conference papers and workshops, I have presented ways to attenuate this problem, by directly simulating the 2D problems where necessary.

Of course, these criticism are mostly related to "direct attack" of the numerical problem by commercial solvers. More sophisticated numerical methods do exist to tackle this sort of problems, but to my knowledge they were not used in the litterature related to microfluidic probes when I began work on this project. A thorough survey of numerical methods in the context of highly multiscale convection-diffusion (or convection-diffusion-reaction) problem would probably be interesting as an extension of the present work.

3.8 Microfluidic Multipoles

The main thrust behind our article on microfluidic multipoles [15] was threefold

- Present a unified theoretical model for diffusion in microfluidic probes and other analogous systems
- Fabricate versatile systems, using 3D printing, that could reproduce all of these flows

- Show that the fabricated systems held promises for biological applications by presenting an example experiment done with one of our newly designed devices

Important secondary results that came about while working on this article were the precise verification of the predictions of the theoretical model by comparing the predicted velocity and concentration fields to precise experimental PIV (Particle Image Velocimetry) data, as well as fluorescence microscopy photos. Another secondary result was the presentation of a procedure to explore, generate, and predict very complex flow patterns by starting from a known solution and iteratively applying conformal maps to it to obtain more complex ones.

We coined the systems presented in the article "Microfluidic Multipoles" to differentiate them from existing microfluidic probes, as well as to highlight explicitly the electric-fluidic analogy at play in our theoretical models. While the theory presented in the article allows us to model existing microfluidic probes, the systems we presented differed in that the device was fied in place and the flow was modulated during the experiment, rather than having the device attached to a scanning mechanical arm.

Another key difference between the systems we presented in this article and most existing "open-space microfluidics" systems was the use of 3D printing as a way to fabricate the devices, as opposed to traditional silicon etching. Not only did this method of fabrication enable very rapid prototyping in a context of university research, it also enabled the fabrication of monolithic systems with complex networks of channels within them, opening the door for the fabrication of systems that would be very difficult to engineer using traditional silicon etching methods. In our systems, apertures could be placed more or less arbitrarily around the 2D surface of the mesa, while previous silicon fabrication techniques favored designs where all of the apertures were lined up. This way of fabrication eventually opened the way for the complex systems that would come later, namely highly symmetrical flower-type probes, and pixelated chemical displays [19] (see chapter 7).

3.8.1 Flow in the Hele-Shaw cell

Flow under a microfluidic probe is exactly described by the Hele-Shaw cell [20]. The mesa of the microfluidic probe (or other multipolar system) forms the top plate, while the surface being processed forms the bottom plate. If both are held close together, and the gap between them is kept constant, it can be shown that the flow reduces to a potential flow in the direction of the plane, modulated by a parabolic profile in the direction of the gap. This allows us to use the theory of potential flows to analyze the system.

In this way, we reduce the three-dimensional problem to a two-dimensional one. Of course, by

doing so, we neglect several effects in the third dimension, namely the "Butterfly Effect" [4] that unevenly broadens the diffusion interface, as well as the specific geometry of the flow in the turning region under the apertures [133]. We discuss some of these effects in more detail in section 5.11.

The 2D flow problem is thus that of potential flow in an infinite domain, with injection and aspiration from a series of point sources. Since the equations are linear, we can determine the expression of the flow from a single point-like aperture, and then express the total flow as the sum of the contributions from each source.

The z-average flow from a single aperture can be determined using Gauss' theorem, and is given by

$$\vec{v_i}\left(\vec{r}\right) = \frac{Q_i}{2\pi H}\frac{\vec{r}-\vec{r_i}}{|\vec{r}-\vec{r_i}|^2} \tag{3.1}$$

Where Q_i is the volumetric flow rate from the aperture, H is the vertical gap, and $\vec{r_i}$ is the position of the aperture. This velocity field can be expressed as the gradient of a potential function Φ

$$\Phi\left(\vec{r}\right) = \frac{Q_i}{2\pi H}\log\left(|\vec{r}|\right) \tag{3.2}$$

We introduce dimensionless variables $q_i = \frac{Q_i}{Q_0}$, $\tilde{x} = \frac{x}{L}$, $\tilde{y} = \frac{y}{L}$, where L is a characteristic length scale in the plane (for instance the distance between the two apertures in a microfluidic probe) and Q_0 is a characteristic flow rate (usually taken as the injection rate in a microfluidic probe). We also represent the position vector $\vec{r}$ as a complex number $z = \tilde{x} + i\ \tilde{y}$. This will come in handy when solving the associated convection-diffusion problem.

3.8.2 Convection-diffusion equation

In order to obtain the concentration profile in the microfluidic probe, we need to solve the steady-state convection-diffusion problem associated with the flow in that geometry. The equation we have to solve for this 2D problem is given by

$$\nabla^2 c - \mathrm{Pe}\nabla\Phi\cdot\nabla c = 0 \tag{3.3}$$

Where c is the dimensionless concentration profile, and Pe is the Peclet number, given by $\mathrm{Pe} = \frac{Q_0}{2\pi H D}$, with D being the diffusion coefficient of the injected substance.

Equation 3.3 is normally intractable due to the algebraic term $\nabla\Phi \cdot \nabla c$, which complexifies it significantly. Fortunately in this specific form, the steady-state convection-diffusion equation is conformally invariant. If we express our coordinates as complex numbers $z = x + i\ y$, we can use the transform $f(z) = \Phi(z)$ to transform to a new domain where the flow is just a plane flow.

This new domain is called the streamline coordinate domain, the new coordinates ϕ and ψ are the real and imaginary parts of the complex potential $\Phi(z)$. They correspond respectively to the level set of the potential and the streamlines of the flow. In this domain, the boundary conditions from the initial problem become equivalent boundary conditions on horizontal segments and the convection-diffusion equation simplifies to

$$\frac{\partial^2 c}{\partial \phi^2} + \frac{\partial^2 c}{\partial \psi^2} = \mathrm{Pe}\frac{\partial c}{\partial \phi} \tag{3.4}$$

This equation is much more tractable than the original convection-diffusion equation. Specifically, it can be reduced to the Helmholtz equation through a change of variable. Solutions to the Helmholtz equations can then be obtained in terms of Green's functions, tabulated in partial differential handbooks [154]. In the limit of high Peclet, it is also possible to neglect the horizontal diffusion term $\frac{\partial^2 c}{\partial \phi^2}$, which makes the equation separable. We further explore solutions of equation 3.4 in chapter 4.

The main problem then becomes one of determining how the boundary conditions in the initial problem map to the streamline coordinate domain. Fortunately, we will see that many seemingly different systems can be represented by the same streamline domain diffusion problem, so that it is not always necessary to solve the entire problem from start to finish in order to analyze a new system.

3.9 Solution for the microfluidic probe

One of the simplest problems solvable with the above-described procedure is the problem of flow and diffusion in a microfluidic probe (which we called a "Microfluidic Dipole" in the article). The potential representing flow in a simple microfluidic probe is given by

$$\Phi = \log(z) - \alpha \log(z - 1) \tag{3.5}$$

Where α is the ratio of aspirated flow rate to injected flow rate. We are trying to solve the associated convection-diffusion problem for the case where the injected fluid is at a fixed concentration $c = 1$, and the surrounding fluid is at concentration $c = 0$. An illustration of

the streamline domain for this problem is given in figure 3.4

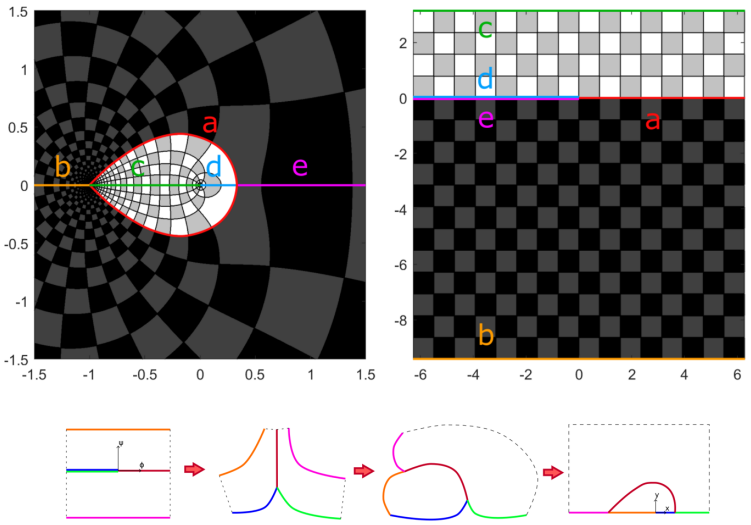

Figure 3.4 Schematic representation of the streamline coordinate domain for the microfluidic probe, left is the regular flow domain, right is the streamline coordinate domain. Bottom cartoon shows an illustration of how one domain gets unfolded into the other.

In the streamline domain, the diffusion problem becomes that of two channels of different concentration, initially separated, then put into contact and allowed to mix. The point where the two fluids are put into contact is the image of the stagnation point Φ_{stag}. In the limit of high Peclet, a very good approximation can be obtained by supposing that the point of contact of the two fluids (corresponding to the horizontal axis past the point Φ_{stag}) is kept at a constant concentration $c = \frac{1}{2}$. In this case, the solution is that of straight flow past a semi-infinite obstacle of fixed concentration, which is given in [105].

$$c(\Phi) = \frac{1}{2}\left(1 \pm \operatorname{erf}\left(\operatorname{Im}\sqrt{\operatorname{Pe}(\Phi - \Phi_{stag})}\right)\right) \tag{3.6}$$

By replacing Φ for its expression in terms of z (given in equation 3.5), we obtain the concentration profile at high Peclet everywhere in the microfluidic probe. This solution is illustrated in figure 3.5

This solution supposes that the concentration is constant along the separating line $\psi = 0, \phi > \Phi_{stag}$. This approximation always breaks down for sufficiently large values of ϕ (we expect that in the limit of infinite ϕ, both fluids are completely mixed and the concentration is uniform and equal to $\frac{1}{\alpha+1}$, which is the ratio of injected to aspirated fluid). However, the region where this approximation breaks down is confined to an exponentially small circle around the aspiration aperture, whose radius decreases with increasing Pe. In the ranges of

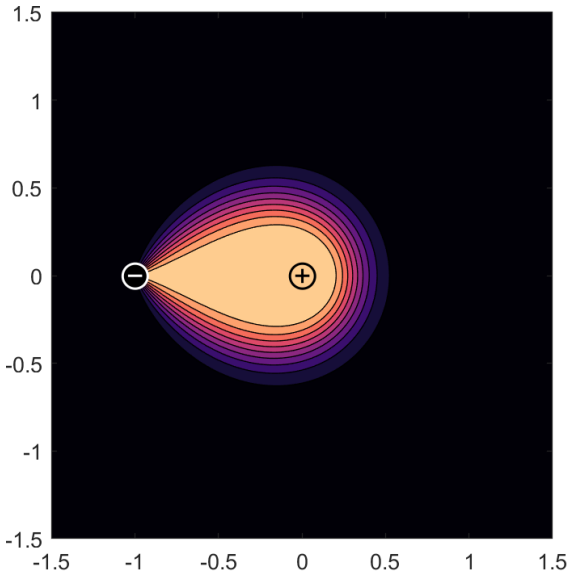

Figure 3.5 Solution for concentration in the microfluidic probe

Pe we are working with (which are of the order of 100 to 1000), this region is completely situated under the aperture and the solution is exact everywhere in the domain of interest.

3.10 Using simple transforms on the probe solution

Once we are in possession of a complete solution for flow and diffusion in the microfluidic probe, we can use conformal transforms to obtain other equivalent solutions for more elaborate systems. In this way, we can get concentration profiles for a large family of symmetrical systems "for free", just by transforming the solution for a single microfluidic probe. Examples of concentration profiles shown in the Nature Communications article are illustrated in figure 3.6.

In this first article, the focus was mainly on transforming the probe solution using power transforms of the form

$$f(z) = z^a \tag{3.7}$$

Where a is an integer. Such transforms produce a radial symmetry around the origin. When the origin is taken as the aspiration aperture, the transform yields a "flower"-shaped probe, with a single aspiration at the center, and a petals evenly distributed around it. With the origin at the injection aperture, the resulting shape is an a-sided polygon. With the origin taken halfway between injection and aspiration, the resulting flow is equivalent to a

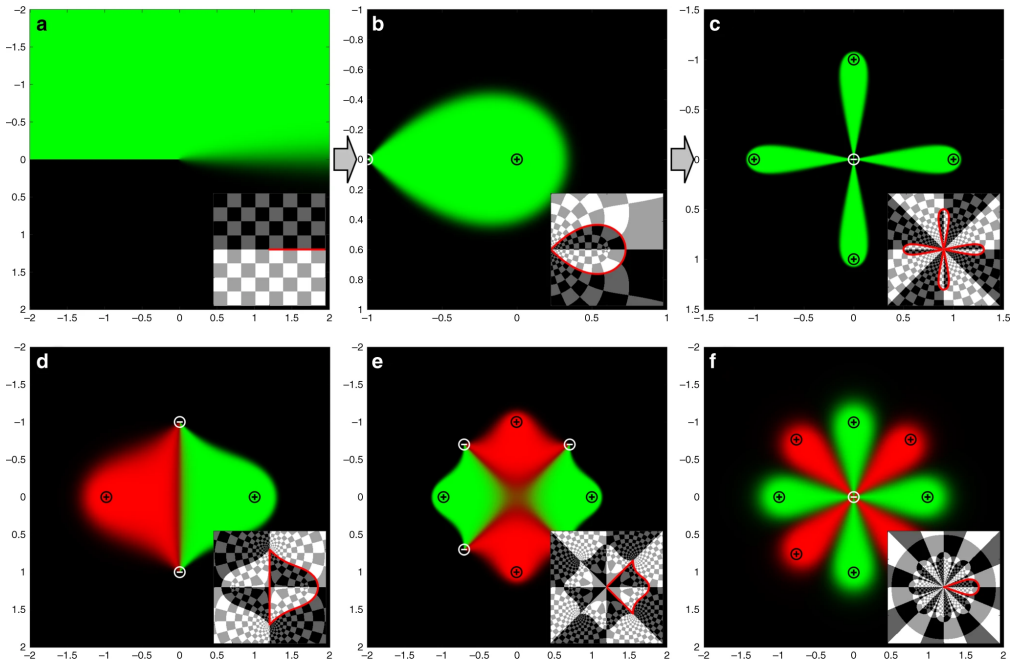

Figure 3.6 Concentration profiles obtained by solving the convection-diffusion equation and transforming it using conformal maps. a) Solution in the streamline coordinate domain. b) Solution for the microfluidic dipole or microfluidic probe. c) 4-petal "flower" probe obtained by applying a radial symmetry to the microfluidic probe solution. d) Solution for microfluidic quadrupole. e) "Poppy" probe obtained by applying radial symmetry to the quadrupole. f) 8-Petal "flower" probe. Insets in each figure illustrate how the streamline coordinate domain gets folded into the final flow domain.

microfluidic quadrupole in the case of $a = 2$, and to "poppy"-shaped probes in cases of larger a (see figure 3.7e). The transform $f(z)$ was also used on the dipole solution, yielding flow and concentration profile for a pair of injection apertures of different flow rate and concentration in the plane (a geometry which we termed "impinging flows").

3.11 System fabrication and operation

The solution procedure presented in previous sections easily allows the prediction of flow and concentration profiles in families of systems constructed as a series of injection and aspiration apertures over a surface. The experimental part, realized by Pierre-Alexandre Goyette, then consisted in fabricating a versatile device that could reproduce these same flow patterns experimentally. Most microfluidic systems on which we were basing our work (especially microfluidic probes and probe-adjacent systems) had been made of silicon up to that point. Silicon offers several advantages, namely extremely high precision in fabrication, cheap material, and high ease of mass production. The ability to mass produce several probe

heads at a low cost is also an important factor in a clinical setting, where you may have an expensive setup for which you only need to replace the probe head for each experiment. However, in a lab setting, silicon also has several disadvantages. In a research setting, where the focus is on fabricating a small number of systems, and iterating quickly, the economies of scale afforded by silicon mass-production are offset by the very high cost and complexity of the clean room. For this reason, we decided to fabricate devices using photolithography 3D printing. 3D printed systems can be fabricated in a matter of a couple of hours and iterated on quickly. An additional advantage of 3D printed systems, as opposed to silicon-based ones, is the possibility of fabricating monlithic elements with 3D channel structures within them. This will come in handy when fabricating systems with arrays of apertures distributed around the 2D plane. In previous microfabricated systems, the channel structure within the probe head was usually confined to a plane, because of the limitations of microfabrication techniques. This means that devices usually had apertures that were lined up in a single line, or limited to a small number of different lines. 3D printed systems allows the relatively straightforward fabrication of systems such as the "flower" probe, or the pixelated chemical displays presented in chapter 7, which would be nontrivial to fabricate using traditional silicon etching techniques. Of course, the relatively expensive photosensitive resin required by these printers and the fact that systems have to be printed one at a time puts limits on scaleability. There are also additional difficulties when printing features inside of a system (such as interior channels), which can be prone to clogging and end up having a poorer resolution than the advertised resolution of the printers. However, more sophisticated 3D printing techniques are being developped by research groups for the purpose of making integrated microfluidic systems [155], and these could open up the way to more sophisticated 3D printed probe heads.

Once fabricated, the systems are connected to a series of programmable syringe pumps using plastic tubing. Experiments involve injecting a mix of water and fluorescein solution, and are imaged using fluorescence microscopy.

In order for the system to behave properly, the gap between the probe head and the glass slide over which the experiment is conducted has to be kept constant. Initial experiments involved using a precision goniometer to adjust the angle, but later on it was decided to use spacers placed directly on the probe head, in a "picnic table" geometry. The probe head could then be directly placed on top of the glass slide and constant gap was ensured by the spacers. The experimental setup is illustrated in figure 3.7

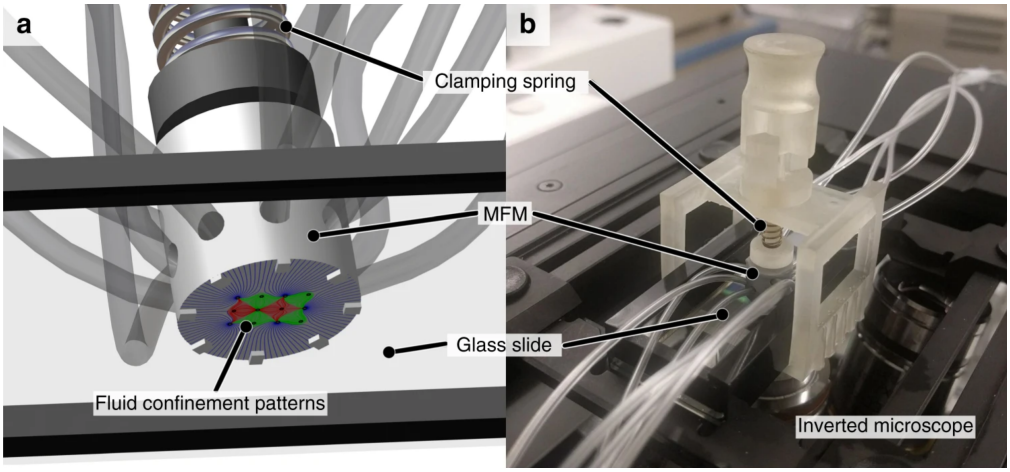

Figure 3.7 Experimental setup. a) CAD illustration of the probe head as seen from below the glass slide. b) Photo of the actual experimental setup

3.12 Validation of the theoretical model

The first systems that were fabricated served to validate the theoretical diffusion model. Fluorescence images of multipolar systems in different geometries and with different experimental parameters were taken and then compared with the theoretical concentration profiles. Match was found to be near perfect between theoretical and experimental profiles. The results of these comparisons are presented in figures 3.8 and 3.9. This match of predicted concentration profile to experimental results was a tremendous step in validating the use of the theory and opening up the way to using the theory for more elaborate systems.

3.13 Rectangular Arrays of Apertures

One of the main selling point of the article was the flexibility of the simple theoretical model we presented. In order to mirror this, we fabricated a reconfigurable system consisting of 12 apertures in a rectangular matrix, whose flow rate could be set independently of each other. In this manner, the fabricated system consisted in a first demonstration of a truly reconfigurable 2D microfluidic system. By injecting and aspirating in different apertures of the array, we were able to reproduce patterns similar to most previously published probe-type systems, as well as new ones, such as polygonal footprints. Examples of the different flow and concentration patterns obtained using this reconfigurable multipolar system are illustrated in figure 3.10.

This early system was reconfigurable in the sense that it could reproduce different flow pat-

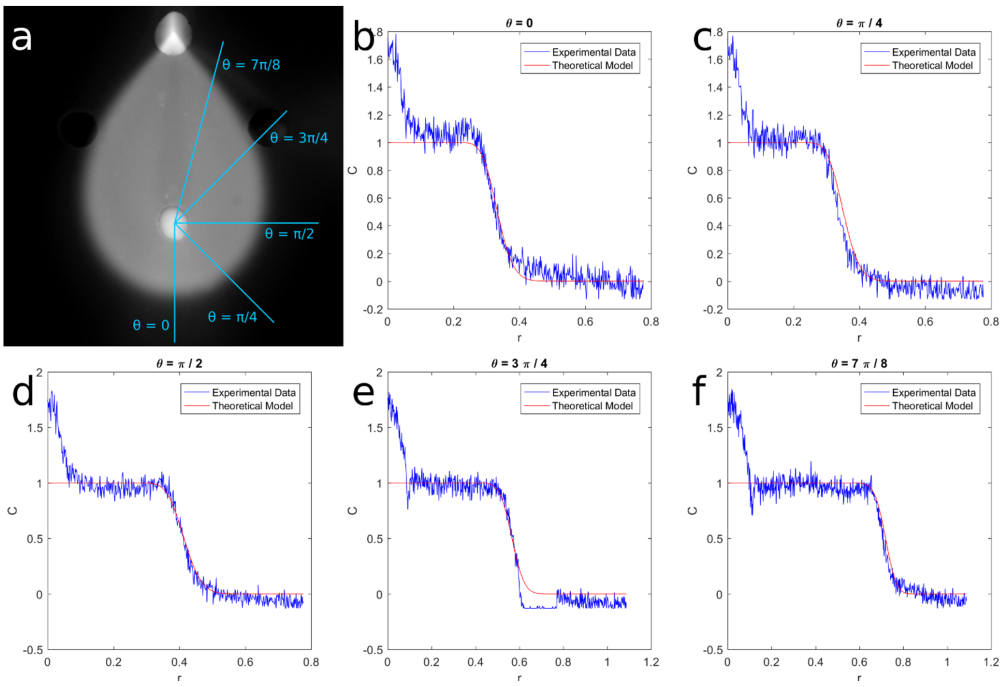

Figure 3.8 Comparison of theoretical transport model with experimental results. Predicted concentration is put side-by-side with experimental results for different angles from the injection aperture. Disrepency at $\theta = 3\pi/4$ is due to the presence of another aperture in the experimental image.

terns by injecting and aspirating different fluids from different combinations of apertures. Of course, the reconfigurability during a single experiment was still somewhat limited. Flow rate from a single aperture could be dynamically adjusted during the experiment, and apertures could be turned "on" or "off" dynamically, but a single aperture could not be used both to aspirate and inject during the same experiment. Likewise, a single aperture could not inject different reagents at different times in the same experiment. Many of these limitations were eventually lifted in microfluidic pixelated displays, which are presented in chapter 7.

3.14 Flower-type Arrays

A second "reconfigurable" system that was showcased in the same article is a flower-shaped radially symmetrical array of apertures. Fluid is injected from the surrounding apertures and reaspirated in a central aperture, creating distinct "petals" that have minimal crosstalk. This system allows for a smaller variety of different patterns than the rectangular array of the previous sections, but is in many ways more appropriate for real-life experiments due to the simplicity of its design and the absence of interaction between petals. In an experiment, each petal can have expose a surface to different conditions, such as different concentrations,

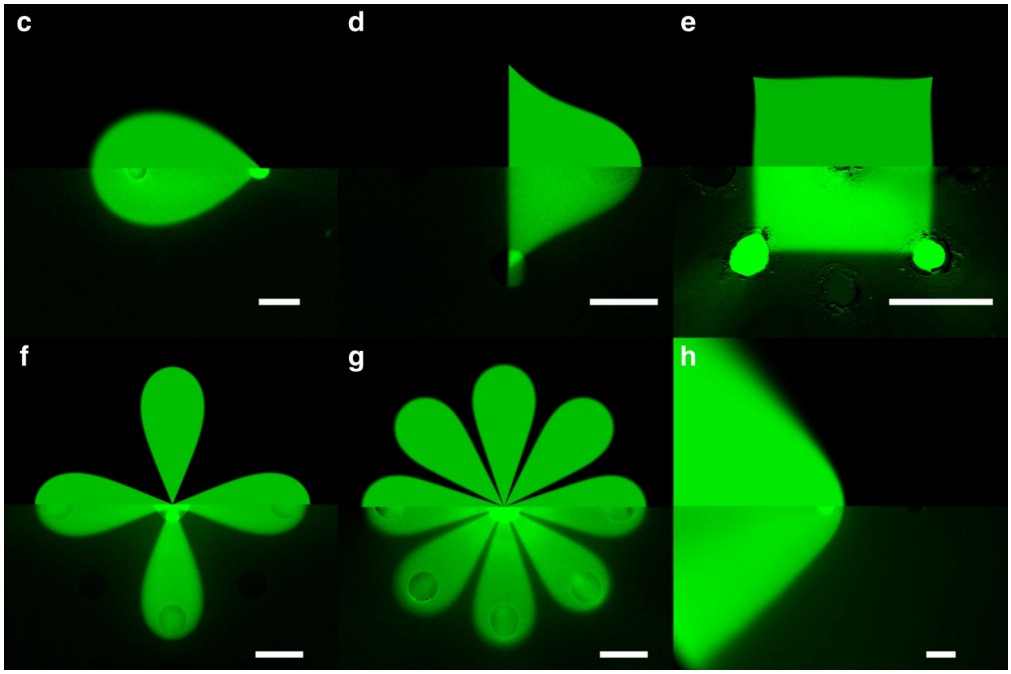

Figure 3.9 Side-by-side comparison of theoretical and experimental concentration profiles for different multipolar geometries. In each subfigure, the top half is the concentration profile predicted by theory and the bottom half is an experimental fluorescence microscopy image of the same geometry. Scale bar: $500\mu m$

different reagent, or similar reagents pulsed in time according to different frequencies or duty cycles. This was demonstrated in this article with a "one-step" immunoassay experiment, presented as a proof of concept, and is also the basis for further work by other students in the group [138].

3.15 Immunoassay Application

In order to demonstrate the application of the system in designing complex multi-step experiments on surfaces, Pierre-Alexandre Goyette designed and ran an experiment showcasing how an immunoassay binding curve could be obtained in a single experiment. The experiment was performed over a glass slide functionalized with goat IgG anti-mouse antibodies, obtained from David Juncker's group at McGill University. The surface was first exposed to 6 different concentrations of antigens, using the petals of a 6-sided flower for each concentration. After the initial incubation time of 50 minutes, another set of apertures exposed the entire surface to a solution of fluorescent antibodies which would bind on the antigens. A final step consisted in washing the entire surface by injecting water through a separate aperture. After these steps, the functionalized surface could be observed through fluores-

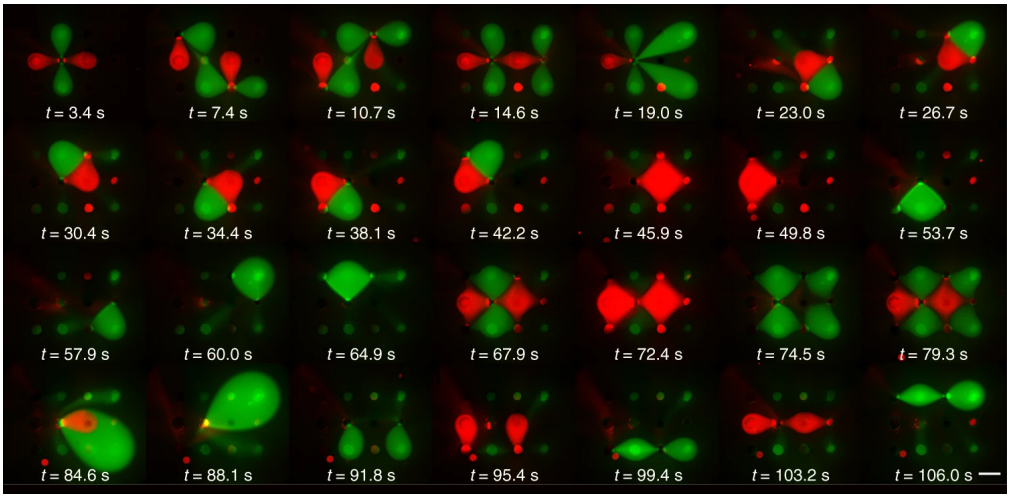

Figure 3.10 Demonstration of reconfigurability in a rectangular aperture array. Several different concentration patterns are obtained over a surface in a single minutes-long experiment.

cence microscopy, with the differen petals exhibiting different intensity of fluorecence. The link between initial concentration of antigen and final signal (fluorescence intensity), could then be mapped into a binding curve. The different steps of the experiment, as well as the results, are shown in figure 3.11. Normally, such a binding curve would require a separate experiment for each antigen concentration, but in this case the entire thing could be done in a single hour-long experiment. This thus demonstrates the ability of the multipolar system to automate and parallelize complex multi-step experiments involving a number of different conditions.

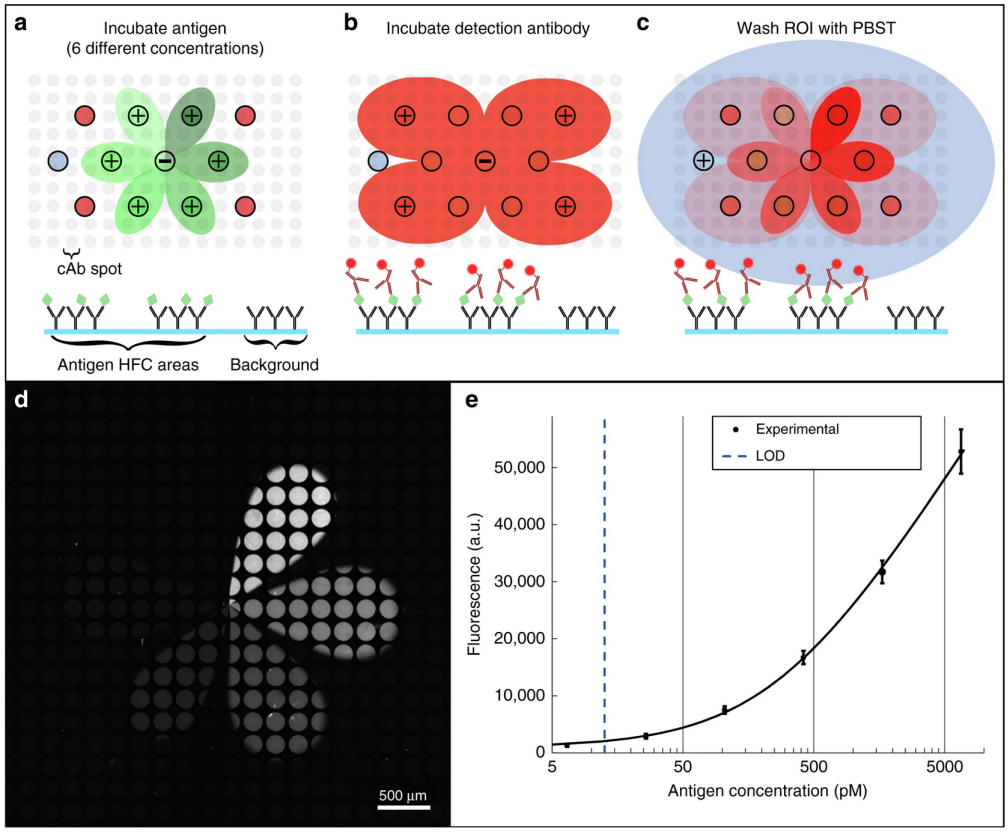

Figure 3.11 Immunoassay experiment performed using reconfigurable multipolar systems. a), b), and c) schematic illustration of the different steps of the experiment. d) Fluorescence image of the functionalized surface after the experiment. e) Experimental binding curve for the immunoassay.

CHAPTER 4 ARTICLE 1 - TWO-DIMENSIONAL CONVECTION-DIFFUSION IN MULTIPOLAR FLOWS WITH APPLICATIONS IN MICROFLUIDICS AND GROUNDWATER FLOW

4.1 Outline

This article, published in Physics of Fluids in 2020, contains a more exhaustive discussion of the theoretical tools presented in the previous section.

We tackle the general problem of flow field and convection-diffusion in potential flows containing a number of point sources, each injecting or aspirating fluid at a given concentration. We solve for the high Peclet case, which is the relevant one in most microfluidic systems, but also show how a solution can be constructed for low Peclet flows.

We also show how combinations of point sources, combined with a subset of conformal maps called Schwarz-Christoffel transforms, can be used to model diffusion in complex channel junctions, establishing links with well-known microfluidic systems such as hydrodynamic focusing systems [156], T-Mixers [128], and H-Filters [157].

In the introduction, we also describe how the solutions we develop could be of use to scientists working in other domains, mainly groundwater mechanics.

The text and figures of the articles are reproduced as they appear in the Physics of Fluids publication, published in December 1, 2020.

The text of the article, as well as all the results presented therein, were done by myself, with feedback from Thomas Gervais. The results presented are a logical extension of the work that was presented in our previous Nature Communications article (see section 3).

4.2 Contribution

Production of results, theoretical analysis, bibliographical research, production of figures, article redaction.

4.3 Introduction

Many 2-dimensional or quasi 2-dimensional flow problems can be approximated as arrangement of point sources and sinks in an unconfined 2D space. Transport in such planar multipolar flows is important in many areas of fluid mechanics. Multipolar flows appear in impinging

jet problems, for example in industrial cooling processes [158] or in the study of diffusion flames [159]. Transport in such flows has also been analyzed in the context of hydrocarbon recovery [53] [160] [35] and in the exploitation of aquifers in hydrogeology [161] [162]. Distributions of multipoles have been used as approximations for flow past rigid obstacles in the context of convection trough porous media [103], for the modelling of fluid interface in porous media [163], for approximating transport of suspended particles in quasi-2D colloids [164] or for the modelling of droplet suspensions in microfluidic channels [126]. In biology, multipolar flows can be found in the irrigation of the choriocapillaris [165]. In engineering, many devices include flow from thin pipes injected to a thin space between two plates. These include hydrostatic thrust bearings [166], radial diffusers [167] and injection molding processes [168]. Among multipolar flows, quadrupole flows are of special interest as the flow within them is purely extentional. They have been used to study the stretching of oil droplets [169] and as exact solutions of the Navier-Stokes equation for the study of vortex stretching [170] [106].

More recently, in the context of microfluidics, there has been a renewed interest in the study of passive transport in multipolar laminar flows. Arrangements of sources and sinks have been used to generate hydrodynamically confined flows with microfluidic probes [8] [145] or to generate tunable concentration gradients in microfluidic quadrupoles [124]. Similar devices have also been used in a non-confined operation mode to generate omnidirectional concentration gradients [171]. Outside of open-space devices, multipolar flow has been used to model intricate flow patterns in microchannel intersections [172] [13], and can be used to model planar concentration gradient generators [132]. Microfluidic multipoles have also been used as a building block to create reconfigurable concentration patterns on open surfaces [15] [173].

In light of these applications, there is a need for a deeper understanding of 2D transport processes in multipolar flows. Considerable work has already been done on the subject: Transit times have been found for particles in symmetrical dipole flows both without diffusion effects [161], as well as with diffusion for some geometries [53], scaling laws have been found for various physical parameters in microfluidic dipoles using linearized equations near the flow's stagnation point [133], analysis of the gradient at the center of microfluidic quadrupoles have yielded precise expressions for diffusion length [124] and thorough numerical simulations have been done for several multipole geometries [14] [152]. More recently, Zouache and Eames published an investigation of flow and passive transport in the turning region of multipolar flows as well as in triangular subcells of tesselated flows, such as are found in the human choriocapillaris [174]. However, despite these advances, there is still a need for a complete framework for the analysis of general 2D multipolar transport problems. Analytic approaches usually either neglect diffusion entirely and focus on material surface tracking

[175] [176], or find diffusion lengths for very specific regions of space [124] [133]. Neither of these methods allows for the analysis of complex 2-dimensional flow profiles and concentration gradients. On the numerical side, calculations are made laborious by the highly multiscale aspect of multipolar flow problems [152], which puts strict constraints on the meshing of the geometry and makes calculations very resource intensive. Recently, we presented a theoretical model for the complete 2D concentration profile in microfluidic multipoles at high Pe as well as a method for generating more elaborate solutions using conformal transforms [15]. This model was restricted to high Peclet flows with hydrodynamic confinement (meaning problems in which the net aspiration rate is larger than the net injection rate), as is found in microfluidics applications. In this paper, we present a complete analysis of the problem of 2D convection-diffusion in planar multipolar flows at low Re. We then give solutions to the problem for both high and low Pe regimes, valid for problems both with and without hydrodynamic confinement. We then show how the same solution procedure can be applied to problems confined in chambers and microchannels. Combined with conformal transforms, 2D multipolar problems can serve as a building block to understand a great variety of flow configurations. We find that in practice, the "high" Pe approximation yields precise results for values of Pe as low as 1.

4.4 Theory

4.4.1 Hele-Shaw flow

Starting from the incompressible Navier-Stokes equation, we can demonstrate that, for a flow of sufficiently small Reynolds number confined in a thin space between two parallel plates, the velocity field is [20]

$$\begin{aligned} u &= -\frac{1}{2\mu}\frac{\partial p}{\partial x} z\,(d-z) \\ v &= -\frac{1}{2\mu}\frac{\partial p}{\partial y} z\,(d-z) \\ w &= 0 \end{aligned} \tag{4.1}$$

Which is the product of a potential flow in the xy direction and a parabolic profile in the z direction. Averaging over the z direction, we get streamlines that are exactly analogous to field lines in a 2D electric field [28]. The 2D flow field can thus be written as

$$\boldsymbol{u} = \nabla\phi \tag{4.2}$$

With the potential ϕ proportional to the pressure field, and obeying

$$\nabla^2 \phi = 0 \tag{4.3}$$

We can use Gauss' theorem to obtain the adimensional potential generated by a point source or sink

$$\phi_i = Q_i \log\left(|\boldsymbol{x} - \boldsymbol{x_i}|\right) \tag{4.4}$$

Where Q_i is the adimensional flow rate at the aperture and $\boldsymbol{x_i}$ is its position. Since the governing equations are linear, the flow generated by a set of point sources and sinks is simply given by the sum of the contribution of each source and sink.

Transport of a passive tracer such as heat or a dilute molecule in the flow is described by the 3-dimensional convection-diffusion equation

$$\nabla^2 c - \mathrm{Pe}\ \boldsymbol{u} \cdot \nabla c = 0 \tag{4.5}$$

Our analysis assumes no flux from either the top or bottom wall, such that the only source of tracer comes from prescribed concentration at the inlets. We are interested in the behavior of the 2D, depth-averaged, concentration profile. In cases where the chamber height is much smaller than the diffusion caracteristic length, the passage from 3D to 2D depth-averaged is a direct one, as interdiffusion can be assumed to keep the concentration constant along the vertical dimension at all time. At very high values of Pe, when the interdiffusion length becomes comparable to the chamber height, the concentration profile starts varying in the z direction according to the butterfly effect [177]. In such a case, precise determination of the full 3D profile is best done by first assuming a pure convection solution, then modifying the interface cross-section by using a solution analogous to the well-known Leveque solution [107].

Provided the supposition highlighted above stands, the 2D concentration profile is described by

$$\nabla^2 c - \mathrm{Pe}\ \nabla\phi \cdot \nabla c = 0 \tag{4.6}$$

Equation 4.6 accurately describes transport in a large host of microfluidic devices, be they open-space scanning probes or gradient generators in large chambers. This equation can also be directly applied to a number of Darcy flows, namely for groundwater flow in quasi-

planar aquifers or in paper microfluidics applications [178], provided there is little interaction between the porous matrix and the concentration field.

Equation 4.6 neglects the 3D aspect of the flow and is thus inappropriate for capturing effects along the z-axis such as diffusion very near the turning region or effects of prescribed concentration on the top or bottom plate. Both these effects have been thoroughly analyzed by Zouache & al in [174].

Reducing the flow to a 2-dimensional potential flow allows us to rewrite position vectors as complex numbers $z = x + iy$. We can then rewrite spatial derivative operators using

$$\nabla = \frac{\partial}{\partial x} + i\frac{\partial}{\partial y} \tag{4.7}$$

The complex potential ϕ thus becomes a function of a single variable z. The contribution of point sources becomes simply

$$\Phi_i = Q_i \log(z - z_i) \tag{4.8}$$

The system of equations 4.3 and 4.6 is conformally invariant [101] [100]. This allows us to use conformal transforms to map simple known solutions to more complex geometries. This will be the main approach we use when solving transport problems in multipolar flows.

4.5 Multipolar flows

We are interested in convection-diffusion in multipolar flows, that is flows generated by discrete sets of point-like injection and aspiration apertures. In practice, these can be fabricated by having small circular channels deliver or aspirate fluid from the top plate of the Hele-Shaw cell. The difference in flow profile between a finite circular aperture and a point-like source is negligible outside of the radius of the aperture [152].

4.5.1 Finite-size dipoles

The simplest case of a multipolar flow for which a steady-state concentration profile exists is the flow illustrated in figure 4.1, consisting of a single injection of unit flow rate and a single aspiration of flow rate $\alpha > 1$, separated by a finite distance. We label this configuration the finite sized dipole to differenciate it from the usual dipole source where injection and aspiration are separated by an infinitesimal distance. Flow and concentration in the finite sized dipole are exactly equivalent to those in the microfluidic probe [8], and provide the

starting point for our analysis. The flow field and an example of a concentration field in the finite dipole are illustrated in figure 4.1. The complex potential in a finite dipole is given by

$$\Phi = \log(z) - \alpha \log(z+1) \tag{4.9}$$

In cylindrical coordinates, the convection-diffusion equation for the dipole flow becomes

$$\frac{\partial^2 c}{\partial r^2} + \frac{1}{r}\frac{\partial c}{\partial r} + \frac{1}{r^2}\frac{\partial^2 c}{\partial \theta^2} = -\mathrm{Pe}\left(\frac{1}{r\left(r^2 + 2r\cos\theta + 1\right)}\left(\left((\alpha-1)r^2 + (\alpha-2)r\cos\theta - 1\right)\frac{\partial c}{\partial r} - \alpha\,\sin\theta\frac{\partial c}{\partial \theta}\right)\right) \tag{4.10}$$

The concentration is fixed a $c = 1$ for the injection aperture, $c = 0$ at infinity and zero flux at the aspiration aperture. Several approaches exist to solve this equation. The classic method is to use perturbation methods to analyze the behavior of c in the limits of very high or very low Pe. This problem has to be solved using singular perturbations, similar to the approach used by Acrivos and Taylor to analyze convection-diffusion around a spherical obstacle [112]. This is feasible when $\alpha = 2$ and the boundary layer separating the region of high concentration from the region of null concentration takes the form of a circle of radius 1. However, for general values of α, the boundary layer's position is not trivial, which makes it hard to obtain a solution in terms of singular perturbations. Another solution avenue is to use material surface tracking, which is often used in groundwater problems involving point sources and sinks [179]. However, this method usually neglects the effects of lateral diffusion, which we want to account for in our analysis.

4.5.2 The problem in streamline coordinates

To simplify the problem, we use a transformation to Boussinesq coordinates [101]. Since the system of equations 4.3 and 4.6 is conformally invariant, we can use the complex potential Φ as a map from the domain $z = x + iy$ of dipolar flow to the streamline coordinate plane $\Phi = \phi + i\psi$ where the flow is a simple, constant plane flow. This is similar to the hodograph method used in interface problems for groundwater flows [180] [181] [52]. In the streamline coordinate domain, the convection-diffusion equation is reduced to the simpler form

$$\frac{\partial^2 c}{\partial \psi^2} + \frac{\partial^2 c}{\partial \phi^2} - \mathrm{Pe}\frac{\partial c}{\partial \phi} = 0 \tag{4.11}$$

This represents convection-diffusion in a uniform plane flow. There remains to impose the proper boundary conditions on 4.11. To determine these boundary conditions, we must

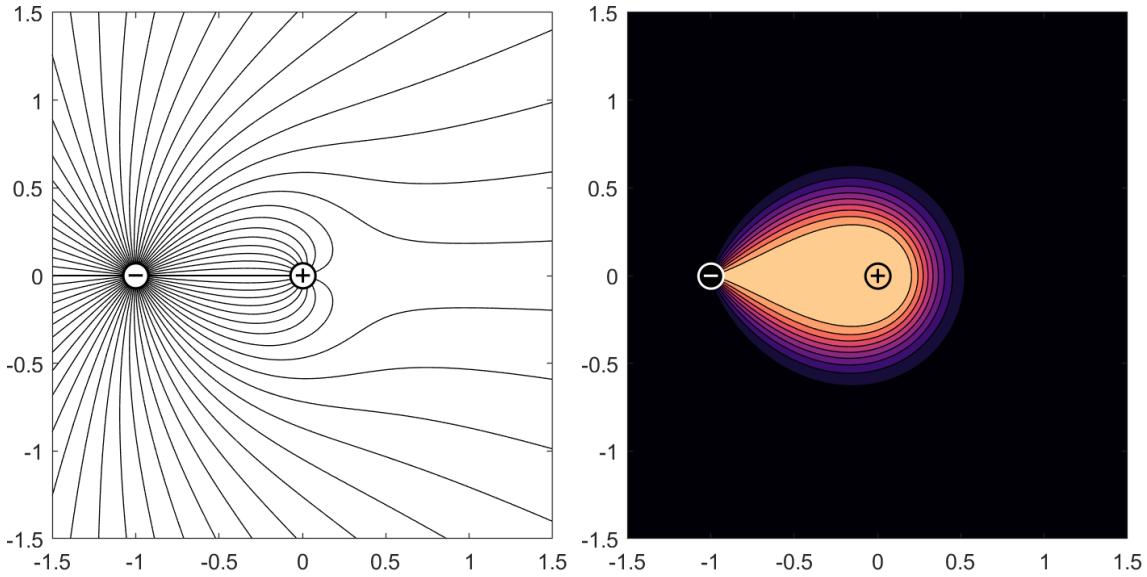

Figure 4.1 Streamlines (a) and concentration profile (b) for a finite sized dipole with $\alpha = 4$ and $\mathrm{Pe} = 10$

determine where the important features of the dipole flow map in the streamline coordinate domain. These important features are the symmetry axis at $x = 0$, split in 4 different segments by the two apertures and the stagnation point, as well as the streamline going from the stagnation point to the aspiration aperture. The map of each segment in streamline coordinate can easily be obtained by using the complex potential to map each endpoint. By the definition of our map, any segment of a streamline maps to a straight segment of constant ψ in the Φ domain. These features are illustrated in figure 4.2.

The equivalent problem to solve is thus the problem of convection-diffusion inside of a strip with zero-flux (symmetry) conditions on the top and bottom walls. In addition, the strip is separated by a semi-infinite segment of zero flux around $\psi = 0$, which separates a region for which $c \to 0$ as $\phi \to -\infty$ and one for which $c \to 1$ as $\phi \to -\infty$. This semi-infinite boundary condition makes the problem particularly hard to solve analytically, even if the underlying equation is relatively simple. We will give solutions to this problem in the limits of high and low Peclet numbers, and use these solutions to obtain concentration profiles for different multipole geometries.

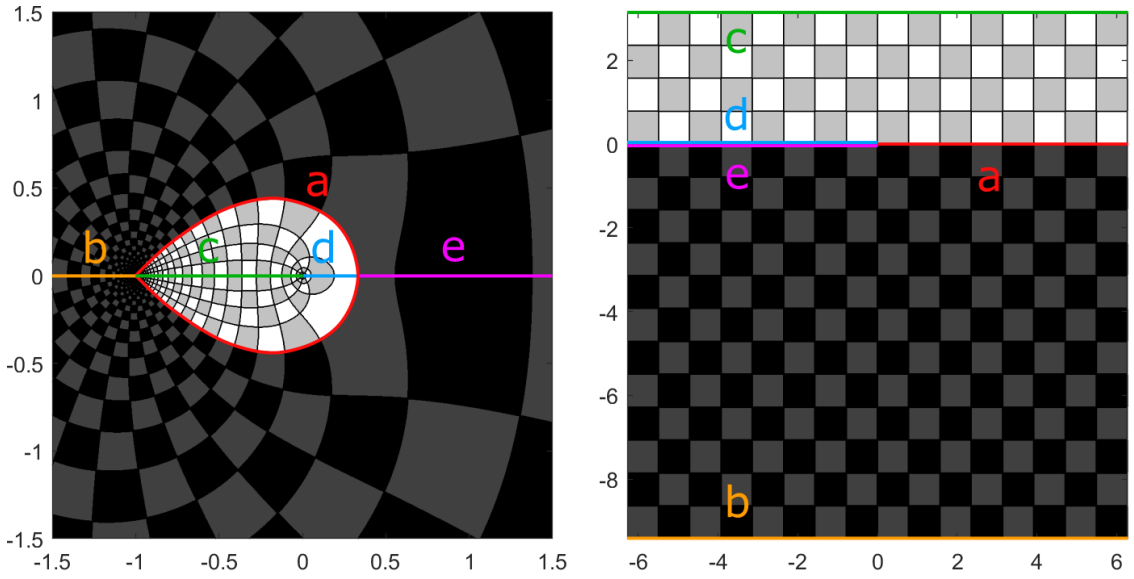

Figure 4.2 Map of the important features of the finite dipole domain (a) and their equivalent in the streamline coordinate domain (b)

4.5.3 Position of the stagnation point

In the streamline coordinate domain, there is a semi-infinite strip of zero flux at $\psi = 0$ going from $\psi \to$ to $\phi = \phi_{stag}$, where ϕ_{stag} is the image of the stagnation point in the dipole flow. The stagnation point represents the point in the dipole flow domain where the velocity field vanishes. It can be shown that is position is given by

$$z_{stag} = \frac{1}{\alpha - 1} \tag{4.12}$$

Its image in the streamline domain is thus given by

$$\Phi_{stag} = \log\left(\frac{1}{\alpha - 1}\right) - \alpha \log\left(\frac{\alpha}{\alpha - 1}\right) \tag{4.13}$$

For the remainder of the text, we will use $\psi + i\phi = \Phi + \Phi_{stag}$ as a transformation, so that the semi-infinite boundary ends at the origin in the streamline domain.

4.5.4 Approximation for large Peclet

We first approach the problem in the high Pe limit. This regime is the one most commonly found in microfluidics applications, where Pe is usually in the range of 10^2 to 10^4. The semi-infinite boundary condition at $\psi = 0$ seems to suggest that we could use the Wiener-Hopf method to solve this problem, as in [108] [109] [182]. However, the addition of symmetry conditions at $\psi = \pi$ and $\psi = (1-\alpha)\,\pi$, as well as the different limit conditions for c as $\phi \to -\infty$ makes the problem difficult to pose using this formalism. We thus look for a simplified formulation of the problem that still captures the important features of the solution. To do so, we first observe the behavior of the solution near $\Phi = 0$, that is near the edge of the semi-infinite no-flux boundary. At high Pe, there is a region around this point where the effect of the boundaries at $\psi = \pi$ and $\psi = (1-\alpha)\,\pi$ are negligible. A local solution valid in this region can be obtained by solving the simplified boundary value problem consisting of equation 4.11 with the boundary conditions

$$\begin{aligned} \frac{\partial c}{\partial \psi} &= 0 \quad \phi < 0, \psi = 0 \\ c &= 1 \quad \phi \to -\infty, \psi > 0 \\ c &= 0 \quad \phi \to -\infty, \psi \leq 0 \end{aligned} \tag{4.14}$$

By symmetry of the problem, we can deduce that c will be equal to $1/2$ for $\psi \geq 0, \phi = 0$. This allows us to independently solve both halves of the plane. Specifically, the problem in both halves becomes identical to the leading-edge problem from [105]. We can thus apply the solution directly and obtain the complete concentration profile as a piecewise solution. The solution obtained is continuous on the entire domain apart from the semi-infinite BC.

$$c\left(\psi, \phi\right) = \begin{cases} 1/2\left(1 - \operatorname{erf}\left(\operatorname{Im}\sqrt{\operatorname{Pe}\left(\Phi\right)}\right)\right) & \psi < 0 \\ 1/2\left(1 + \operatorname{erf}\left(\operatorname{Im}\sqrt{\operatorname{Pe}\left(\Phi\right)}\right)\right) & \psi \geq 0 \end{cases} \tag{4.15}$$

This solution is illustrated in figure 4.3a

The solution 4.15 is valid near the origin and for high values of Pe, however it breaks down for sufficiently large values of ϕ. This can be seen intuitively by observing that very far downstream, the solution yields a uniform concentration of $c = 1/2$ while a simple first principle analysis of the original problem shows that far enough down the channel, the concentration must be $c = 1/\alpha$ everywhere. More specifically, we have neglected the effect of the symmetry conditions at $\psi = \pi$ and $\psi = (1-\alpha)\,\pi$, which don't influence the wake near the mixing region, but eventually must be considered sufficiently far downstream. We have previously

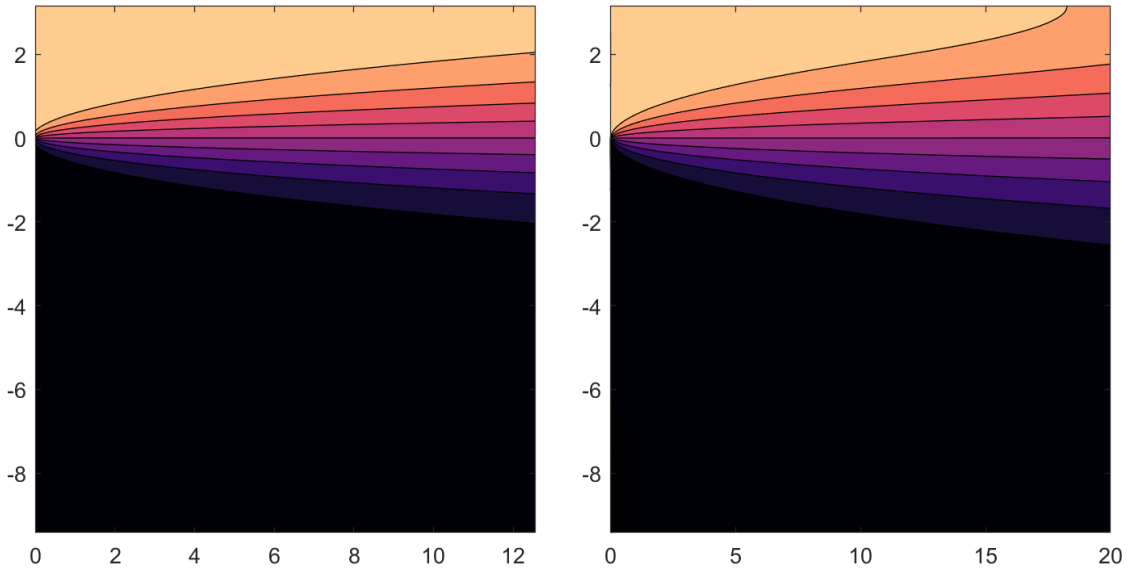

Figure 4.3 Streamline coordinate solutions for the finite dipole at high Pe. a) Solution 4.15, valid around the stagnation point and breaking down far downstream and b) Solution 4.19 valid far downstream but breaking down near the stagnation point

shown [15] that this breakdown region happens when $\psi > O(\mathrm{Pe})$. When the solution is transformed back to the dipole domain, the breakdown region where the solution is no longer valid is confined to a circle or radius $O\left(e^{-\mathrm{Pe}}\right)$ around the aspiration aperture.

4.5.5 Second approximation for large Peclet

In some cases, we may be interested in solutions for the highly convective regime in which we need accuracy far downstream. In this case, we can use different approximations for the problem in streamline coordinates and obtain a second solution. For very high values of Pe, we can be justified in assuming that no mixing of the fluid happens before $\phi > \phi_{stag}$. In that case, we can assume that concentration will be constant in each channel region for $\phi < \phi_{stag}$. We can then solve equation 4.11 for the semi-infinite strip $\phi > 0$, $\psi \in](1-\alpha)\pi, \pi[$.

Using the change of variable $c(\phi,\psi) = \exp(1/2\mathrm{Pe}\ \phi)\, U(\phi,\psi)$, we can bring 4.11 to the form of the helmholtz equation

$$\frac{\partial^2 U}{\partial \psi^2} + \frac{\partial^2 U}{\partial \phi^2} = \frac{1}{4}\mathrm{Pe}^2 U \tag{4.16}$$

The Green's function for this boundary value problem is known and is given by [154]

$$G\left(\phi,\psi,\phi',\psi'\right)=\frac{1}{2\alpha\pi}\sum_{n=0}^{\infty}\frac{\epsilon_n}{\beta_n}\left(\exp\left(-\beta_n|\phi-\phi'|\right)-\exp\left(-\beta_n|\phi+\phi'|\right)\right)\cos\left(\frac{n}{\alpha}\left(\psi-\pi\right)\right)\cos\left(\frac{n}{\alpha}\psi'\right) \tag{4.17}$$

With $\beta_n=\sqrt{\frac{n^2}{\alpha^2}+\frac{\mathrm{Pe}^2}{4}}$, $\epsilon_0=2$ and $\epsilon_n=1$ for $n\neq 0$. This Green's function can be convoluted with the value of c at $\psi=0$ to obtain the concentration profile. Since we approximate the concentration profile at $\psi=0$ to be simply a step function, we obtain

$$c\left(\phi,\psi\right)=\int_0^{\pi}\frac{\partial G}{\partial\phi'}\left(\phi,\psi,\phi',\psi'\right)|_{\phi'=0}\,d\psi' \tag{4.18}$$

Which can be simplified to

$$c\left(\phi,\psi\right)=\frac{1}{\alpha}+\frac{2}{\pi}\sum_{n=1}^{\infty}\frac{1}{n}\exp\left(\left(\frac{\mathrm{Pe}}{2}-\sqrt{\frac{n^2}{\alpha^2}+\frac{\mathrm{Pe}^2}{4}}\right)\phi\right)\sin\left(\frac{\pi n}{\alpha}\right)\cos\left(\frac{n}{\alpha}\left(\psi-\pi\right)\right) \tag{4.19}$$

About 10 terms are required to have an error of less than 10^{-3} everywhere except near the branch cut at $\phi=0$, where the solution is already not valid. Adding further terms beyond that only resolves the region around $\Phi=0$ more. This solution, illustrated in figure 4.3b breaks down in a region of order $O\left(\sqrt{\mathrm{Pe}}\right)$ around the branch cut since it neglects retrodiffusion in that region.

4.5.6 Error for each approximation

We have obtained two different approximations of the concentration profile in streamline coordinates for the dipole problem. Both break down in different regions and in general, we will use the one which is valid in the region of interest, depending on the problem. For multipolar devices with hydrodynamic flow confinement, solution 4.15 is perfectly appropriate, as the breakdown region will be confined to an exponentially small region under the aspiration aperture. If however, we want the concentration profile for non hydrodynamically confined devices such as impinging flows (presented in section 4.7), we may use the second solution, valid far enough downstream. In figure 4.4, we compare both solutions to finite element simulations to determine the error along the ϕ axis. We notice that the value of ϕ for which the error is larger for the self-similar solution is of the order $O\left(\mathrm{Pe}\right)$. We also note that by using a combination of the two solutions, we can use the high Pe solution for values of Pe as low as 1 while keeping an average error that is smaller than 2 %. The maximum error

committed decreases approximately with $\mathrm{Pe}^{-1.5}$, as shown in figure 4.4d.

4.5.7 Approximation for very low Peclet

In the limit of very low Peclet number, we may approximate that diffusion in the ψ direction happens much faster than convection, and that at any point in the streamline domain the fluid is completely mixed along any vertical line so that c is only a function of *phi*. This approximation allows us to separate the streamline domain in 3 1-dimensional subdomains and solve a simplified equation for each.

The first subdomain we analyze is the part of the strip defined by $\phi \geq 0$, corresponding to the region after the separating cut of zero derivative. In the very low Peclet regime, we can approximate that this region is perfectly mixed and has constant concentration everywhere. The concentration in this region will be the equilibrium concentration, that is $c = 1/\alpha$. As Pe increases, this approximation will break down in a region around $\Phi = 0$, where mixing will not yet be complete.

Once we have fixed the concentration for $\phi \geq 0$ to a constant $c = 1/\alpha$, the top and bottom half of the strip for $\phi < 0$ can be independently solved as separate 1-dimensional problems. In both cases, we are solving the 1-D convection-diffusion equation

$$\frac{\partial^2 c}{\partial \phi^2} - \mathrm{Pe}\frac{\partial c}{\partial \phi} = 0 \tag{4.20}$$

With $c = 1/\alpha$ at $\phi = 0$ and concentration at $\phi = -\infty$ fixed at either 0 (top half-strip) or 1 (bottom half-strip). This gives us a piecewise definition for the streamline coordinates solution at very low Peclet numbers

$$c\left(\phi, \psi\right) = \begin{cases} \frac{1}{\alpha} & \phi \geq 0 \\ \frac{1}{\alpha} e^{\mathrm{Pe}\phi} & \phi < 0 \;\&\; \psi > 0 \\ 1 - \frac{\alpha - 1}{\alpha} e^{\mathrm{Pe}\phi} & \phi < 0 \;\&\; \psi < 0 \end{cases} \tag{4.21}$$

This solution can be taken back to the dipole flow domain using the complex potential as a transformation, as was done for the high Pe solution.

4.6 Transforming the dipole solution

The dipole solution, be it for high or low values of Pe, can be used as a starting point to generate more elaborate solutions without needing to solve new transport problems. We

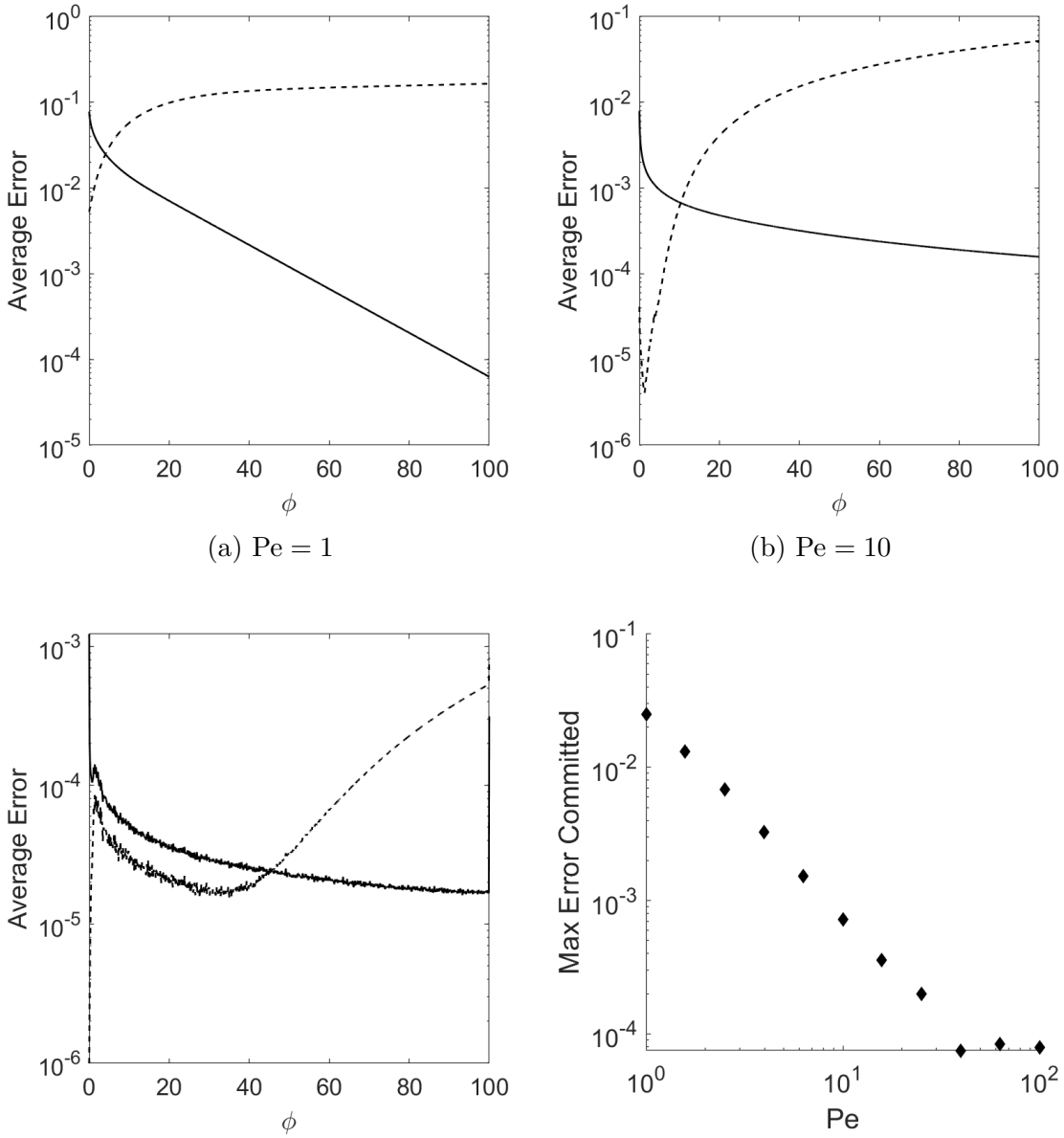

(a) Pe = 1

(b) Pe = 10

(c) Pe = 100

(d) Maximum error committed

Figure 4.4 Error averaged along ψ axis for different values of Pe for the self-similar solution (dashed) and series solution (full line) for $\alpha = 4$ and different values of Pe. Subfigure d shows the maximum error committed by combining both approximations. The error for each graph was obtained by comparing with 2D finite element simulations of the streamline problem done in COMSOL multiphysics. For each value of ϕ, the error was integrated along the ψ axis

can once again exploit the fact that the plane convection-diffusion equation and the Laplace equation describing the flow field form a conformally invariant system of PDEs. This allows us to use simple conformal maps to map the dipole flow to other multipolar flows with more apertures and obtain solution of the transport problem in those flows directly. Examples of simple transforms that can be used include power transforms for generating rotationally symmetrical geometries, inversion transforms to obtain nonconfined flow profiles, or schwarz-christoffel transforms to obtain confined channel geometries, as will be described in the following sections. A selection of concentration profiles obtained from the dipole solution are illustrated in figure 4.5.

4.7 The impinging flows solution

The finite dipole solution can be transformed to obtain concentration profiles in geometries without hydrodynamic confinement. For instance, starting from the solution 4.15 for the dipole flow geometry 4.9, we can use the transformation

$$z = z^{'-1} - 1 \tag{4.22}$$

To obtain the concentration in a flow caracterized by an injection aperture of rate $\beta = \alpha - 1$ rate and null concentration at the origin and another injection aperture of unit rate and unit concentration at $z = 1$. The flow profile for the impinging flows is given by the gradient of the potential function

$$\Phi(z) = \log(z - 1) + \beta \log(z) \tag{4.23}$$

In the case of $\beta = 1$, the two singularities inject at the same rate, and a vertical line of concentration $c = 1/2$ appears around $z = 1/2$. Very close to this stagnation point, the flow behaves like a purely extensional flow and the concentration profile approaches the well-known y-independent solution [100] [124]. However, as $|y|$ increases, the velocity decreases and a broadening of the concentration gradient is observed. In the case of $\beta > 1$, a hyperbolic wake is formed around the aperture at $z = 1$, and a similar wake is observed around $z = 0$ when $\beta < 1$. Different solutions for the impinging flows are illustrated at figure 4.6.

This solution can be used to model transport from two jets of different temperature impinging on a 2D plate, or temperature in an aquifer with two different cylindrical injection wells. In microfluidics, impinging flow devices can be used to generate long adjustable concentration gradients in an open-space context.

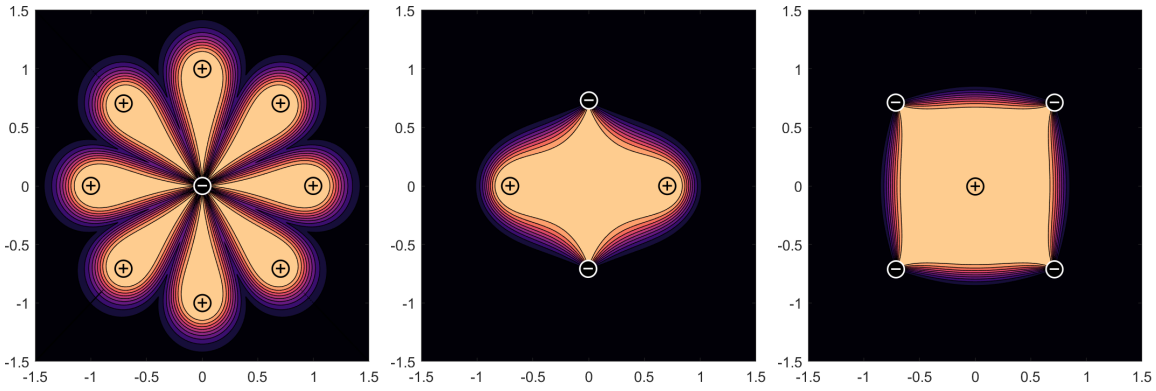

(a) $z = z'^8 - 1$ (b) $z = z'^2 - 0.5$ (c) $z = z'^4$

Figure 4.5 Concentration profiles obtained using combinations of translations and power tranforms

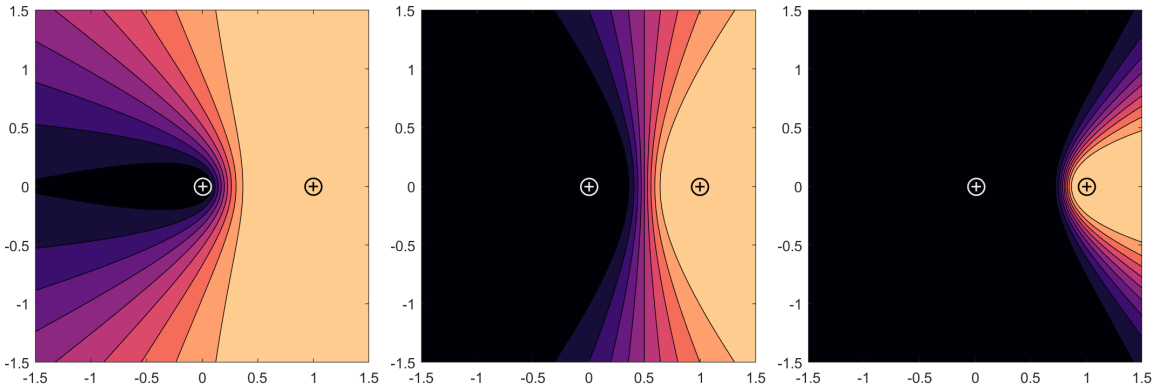

(a) $\beta = 1/4$ (b) $\beta = 1$ (c) $\beta = 4$

Figure 4.6 Solutions for impinging flows at Pe = 10 for various values of β

4.8 Other starting geometries

In the previous sections, we have been exploiting the solution to the dipole geometry problem described in 4.5.1, and finding derived solutions by using conformal transforms. However, the method outlined here is quite general and can easily be extended to more complex starting geometries. In cases when the arrangement of sources and sinks cannot be obtained by transforming an already known solution, we have to start by mapping the problem to streamline coordinates and see how the branch cuts map in the channel geometry. Once the problem is properly posed in the streamline coordinate domain, it can be solved using appropriate approximations and then mapped back to the multipole flow. This includes, but is not limited to, applications where there are injection apertures injecting more than a single reagent or reagent concentration. Examples of solutions obtained from different starting geometries are illustrated in figure 4.7.

4.8.1 Single source in straight flow

One example of a different starting geometry is the case of a single injecting source in a straight flow. This geometry can be found in problems of injection of cold water in aquifers, for example waste from groundwater heat pumps or in the analysis of the contamination of underground water sources. This arrangement cannot trivially be obtained by applying simple transforms to the dipole solution presented in the previous sections. However, we can apply the same reasoning as we did in section 4.5.1 to find the form of the problem in streamline coordinates. The obtained streamline coordinate problem is very similar to the finite dipole one, and the same solution procedure can be applied.

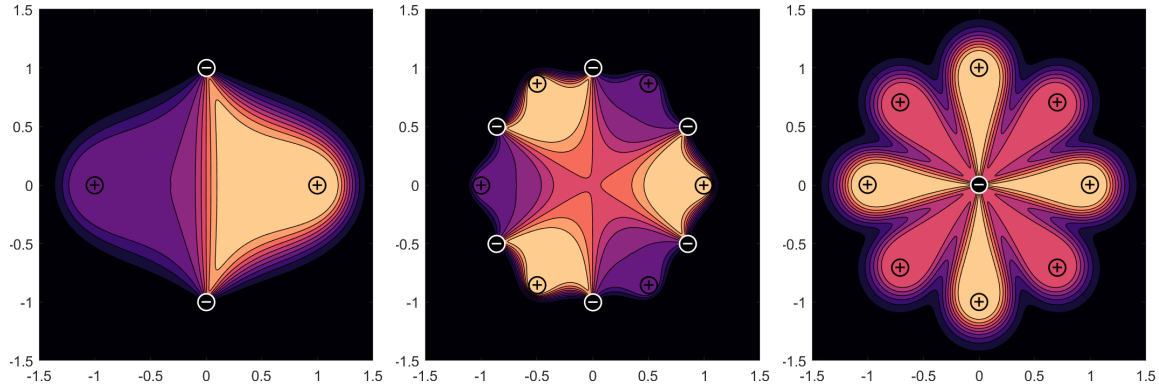

Figure 4.7 Concentration profiles for multipolar geometries not obtainable from the simple dipole solution.

Flow in the thermal plume arrangement is described by the complex potential

$$\Phi = z + \alpha \log(z) \tag{4.24}$$

Which corresponds to a dipole source of unit strength at infinity and an injection aperture of rate α at the origin. This flow possesses a single stagnation point at $z_{stag} = -\alpha$. This stagnation point transforms to the point Φ_{stag} given by

$$\Phi_{stag} = -\alpha + \alpha \log(-\alpha) = \alpha(\log(\alpha) - 1) + i\ \alpha\ \pi \tag{4.25}$$

The first high Pe approximation 4.15 is applicable directly to this problem. To obtain a high Pe solution valid far downstream, we must modify the results of section 4.5.5 to account for the fact that the domain is now semi-infinite in the ψ direction. This solution can again be obtained by using the Green's functions for Helmholtz' equation in the quadrant, with Dirichlet boundary conditions on one axis and Neumann boundary conditions on the other. Because the domain in streamline coordinates is semi-infinite, the low Pe regime is harder to analyze than the strip domain of the dipole solution. We leave to future work the determination of the diffusion profile for the thermal plume at very low values of Pe, which would have to be done using matched asymptotic expansions (as the approximation of complete mixing in the ψ direction has to break down for sufficiently high ψ).

An example of high Pe solution for a thermal plume in a straight flow is illustrated in figure 4.8a. The solution can again be transformed using simple conformal maps to obtain concentration profiles for more elaborate flow patterns. This is illustrated in figure 4.8b, where we use a simple power transform on the plume solution to obtain the concentration profile of a single injection aperture placed over a purely extensional flow.

We note that this solution is different to the well-known Green's function for convection-diffusion in a straight flow [183], given in terms of Bessel functions, since it includes the effect of physical displacement by the injected fluid.

4.9 Application to closed channel geometries

So far we have used power transforms and inversions to obtain rotationally symmetrical geometries that can be used to model flows in unbounded 2-dimensional domains. The main application of these being in open-space microfluidics. However, the same models can be used to model diffusion profiles in closed channel microfluidic devices. This is due to the fact that a majority of microfluidic devices operate in channels much wider than they are tall, making

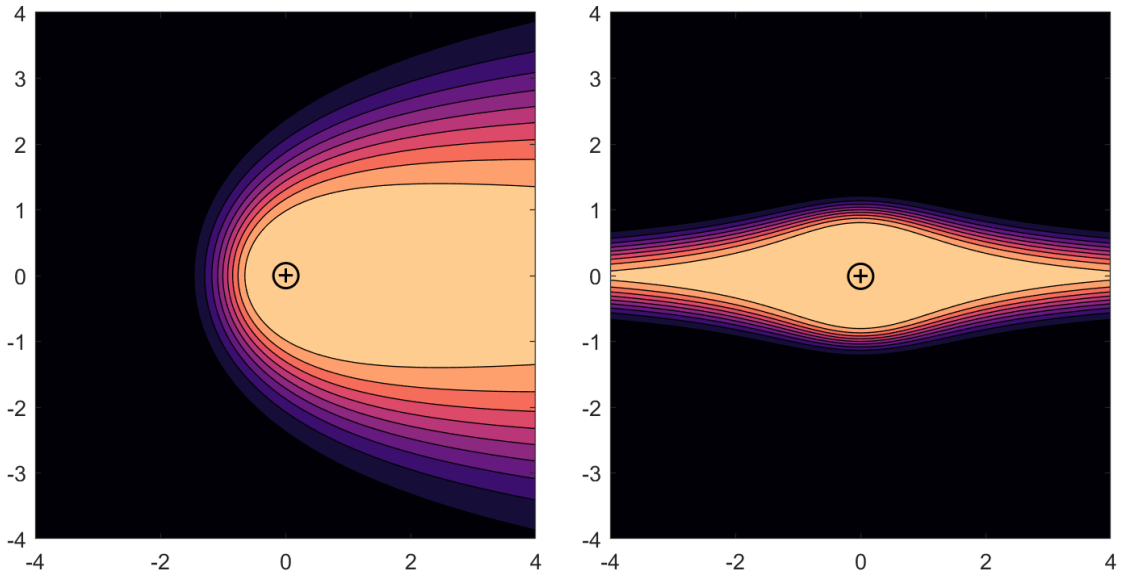

Figure 4.8 Concentration for a thermal plume in a straight flow with Pe = 10 and $\alpha = 1$ (a) and concentration for a single injection aperture superimposed over a purely extensional flow (b), obtained by applying the power transform $z = z'^2$ to the solution illustrated in (a)

them suitable for modelling with 2D flows. In particular, classic passive mixers such as the T-mixer [128], hydrodynamic focusing [156] or the H-filter [184] can easily be modelled using our formalism. The main difference between closed-channel microfluidic devices and open-space devices is the presence of no-slip walls, which can throw doubt on the legitimacy of the method. Indeed, the potential flow formulation is inadequate for modelling no-slip walls and the 2D Stokes equation, which is usually used to describe such flows, is not conformally invariant. However, it has been shown that the potential flow approximation only breaks down in a thin boundary layer near the walls [185]. Since in most passive mixing devices, the region of interest is near the center of the channel, this means our approximation can safely be used and the 2D flow can be considered a potential flow in the bulk of the channel.

The general strategy for modelling diffusion in closed-channel junctions is to begin with an arrangement of point sources on the real axis in an unbounded plane, the solution of which can be easily obtained using the previously outlined method. The obtained concentration profile is then transformed using Schwarz-Christoffel maps, such that real axis is mapped to the edges of the channel, and point sources are placed on the edges, approximating incoming flow from side inlets. The general method is illustrated in figure 4.9.

From the same starting geometry, a variety of channel geometries can be obtained. We

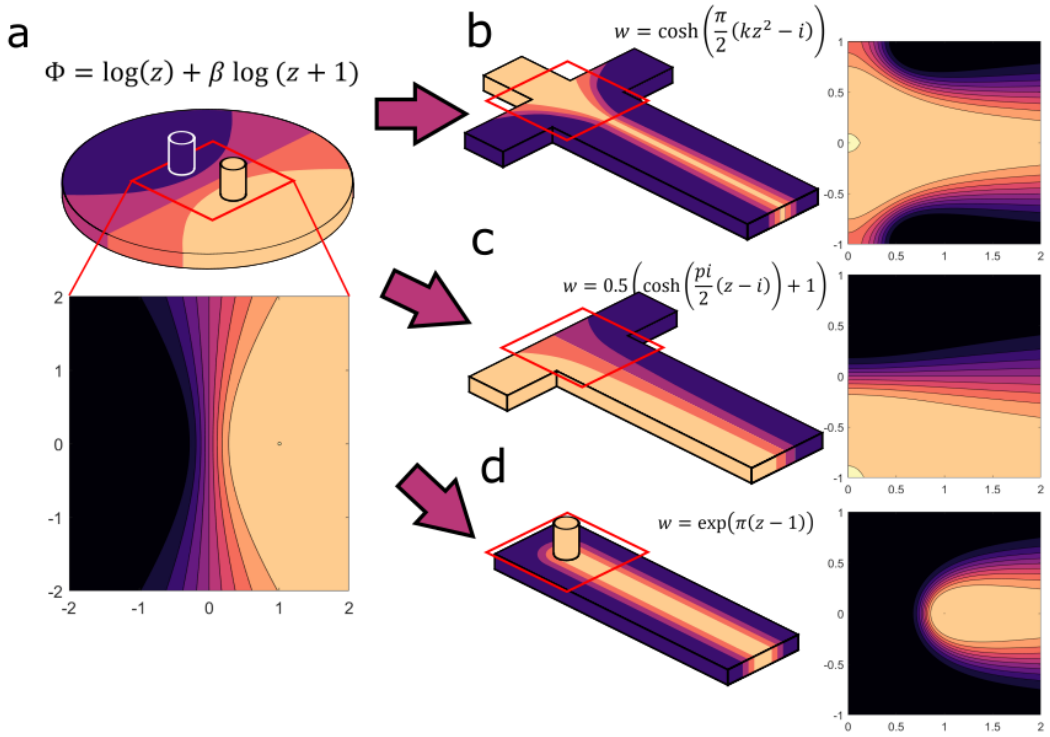

(a)

Figure 4.9 General outline of the closed channel model. We begin with a known solution for impinging flows in unconfined 2d space (a) and use 2 and 3-vertices Schwarz-Christoffel maps to obtain profiles for a T-mixer (b), hydrodynamic focusing (c) and a point source injecting from above in a closed channel (d)

contrast these models, which yield complete concentration profile for the turning region of passive mixers, to the quasi-1D lump models usually used to model such devices [128]. By combining both approaches, it is possible to obtain a complete picture of transport in closed channel microfluidic devices, even those including junctions with several inlets and outlets. The same Schwarz-Christoffel mappings, to either 2-vertices channels or 3-vertices semi-infinite slots, can also be used to model diffusion patterns from multipolar arrangement with translational symmetry. This way, for example, the solution illustrated in figure 4.9d can represent a point source in a closed channel or an array of point sources in a plane flow. This kind of strategy could be used to model symmetrical arrays of multipoles such as those used to mark tissues in [147].

4.10 Mapping to closed polygons: diffusion in chambers and pixelated displays

In the previous section we showed how simple Schwarz-Christoffel mappings to 2 and 3-vertices polygons could be used to map multipolar flows from the open space to known channel geometries. In all of the presented cases, at least one vertex was projected to infinity, so that the resulting geometry as unbounded in at least one direction. We now look at examples of Schwarz-Christoffel mappings to polygons that are bounded in all directions. This can be used to model either diffusion in large 2d chambers in which fluid is injected and aspirated from point-like apertures or small channels on the edges of the chambers, or to model open-space multipolar geometries with 2D translational symmetry, such as those used in hydrocarbon recovery from thin aquifers or in microfluidic pixelated displays [19].

Unfortunately, not many Schwarz-Christoffel maps to bounded polygons have closed analytical expressions. It is possible to approximate any mapping using easy to implement numerical methods such as those presented in [59], however this may prove to have diminishing returns when compared to directly solving the corresponding diffusion problem numerically. In some cases, due to the highly singular nature of diffusion problems in multipolar flows, the numerical determination of the transformation may turn out to be more stable and precise than the numerical resolution of the differential equation system.

One transformation for which there exists a well-defined closed form for both the direct and inverse mapping is the map from the semi-infinite plane to a square, given in terms of elliptical functions [65]. While the map is slightly unwieldy, most scientific computation packages include implementations of both the jacobi elliptic sine and elliptic integral that are necessary for the direct and inverse map, which makes its implementation very simple. We show in figure 4.10 how the method is applied to obtain diffusion profiles in rectangular arrays of apertures. The details of the calculation are given in [19].

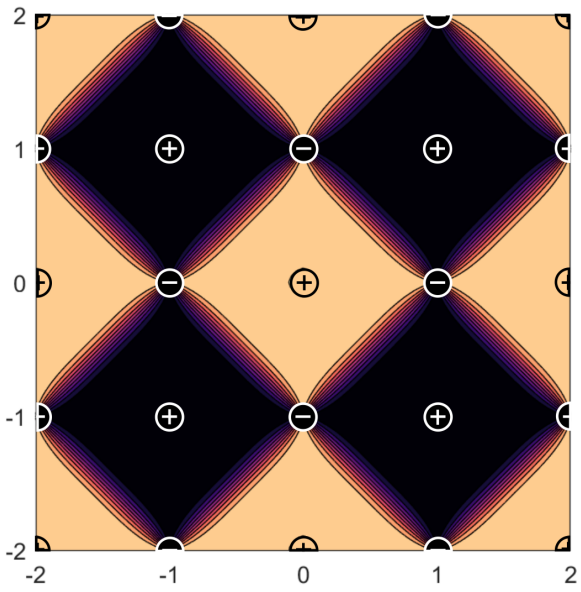

Figure 4.10 Concentration profile for a translationally symmetrical array of injection and aspiration apertures, generating concentration "pixels"

4.11 Concluding remarks

We have analyzed the problem of tracer dispersion in 2D multipolar flows and shown solutions to the problem for both high and low Pe limits. We have shown two high Pe solutions, valid respectively downstream and upstream, and which can be combined to obtain an approximation valid everywhere in the flow domain. We have shown how simple solutions for transport in multipolar devices can be extended to obtain 2D concentration profile in a variety of geometries. These solutions allow for a more sophisticated, 2-dimensional description of convection-diffusion in many transport problems. Specifically, they give us complete concentration profiles in domains where we previously relied on material surface tracking or limited scaling arguments. These include open-space microfluidic applications such as microfluidic probes or multipoles, reinjection problems in groundwater flows found in groundwater heat pumps or aquifer contaminations and in interface tracking problems in porous media and diffusion in microfluidic channels and chambers. Moreover, the technique demonstrated here is not limited to the few arrangements of sources and sinks we have illustrated. By using the same transformations with more elaborate initial geometries, we could generate concentration profiles for increasingly sophisticated devices. We hope that a more thorough knowledge of 2D exchange phenomena in open-space system will allow engineers and experimentalists from

a wide range of fields to design devices that exploit the full features of 2D convection-diffusion, without being limited by unidirectional lump models.

Acknowledgements. E.B. acknowledges funding from the Fonds de Recherche du Québec (FRQ) "Bourse de doctorat en recherche" and from the National Science and Engineering Research Council of Canada (NSERC) "Bourse Alexander Graham Bell". T.G. acknowledges funding from the Fonds de Recherche du Québec (FRQ), "Établissement de nouveaux chercheurs" and "Équipe" programs, and the National Science and Engineering Research Council of Canada (NSERC – RGPIN - 06409). We thank the Canadian Microsystems Center (cmc.ca) for access to a shared computational infrastructure.

Declaration of Interests. The authors report no conflict of interest.

Data Availability The data that support the findings of this study are available from the corresponding author upon reasonable request.

CHAPTER 5 ARTICLE 2 - THE 2D MICROFLUIDICS COOKBOOK - MODELING CONVECTION AND DIFFUSION IN PLANE FLOW DEVICES

5.1 Outline

This article, published in Lab on a Chip in 2023, is a tutorial review describing how tools of complex analysis, namely conformal transforms, can be combined with simple solutions of the Laplace equation and convection-diffusion equation, in order to obtain complete descriptions of transport in a range of microfluidic systems.

The article begins with an extensive survey of 2D microfluidic technologies, then presents a general solution procedure that can be used to precisely analyze transport in them.

The target audience for this article is engineers and scientists working in the field of microfluidics, especially graduate students. These microfluidics experimentalists are often called on to be jack of all trades, manipulating fabrication, biological experiments, fluid control, etc. As such, the idea was to provide a didactic explanation of simple tools that they could use in their systems, without having to become fluid mechanics experts.

The article is a good synthesis of the entirety of the project and its applicability to different areas of microfluidics.

The text and figures of the articles are reproduced as they appear in the Lab on a Chip publication, published in February 10, 2023.

5.2 Contribution

The text of the article, as well as all the results presented therein, were done by myself, with feedback from Thomas Gervais.

Contribution: Production of results, theoretical analysis, bibliographical research, production of figures, article redaction.

5.3 Introduction

Ever since the inception of microfluidics, and continuing to this day, the basic building block for microfluidic systems has been the microchannel [2]. Microfluidics initially developped in the 1970s as an offshoot of the emerging domain of microsystem [186]. The rapid development of microelectronics led to the invention of sophisticated techniques for working with

silicon, and these techniques were then reappropriated by engineers working on MEMs and Microfluidics to develop not just electronic circuits, but also mechanical and fluidic systems. Because of this close proximity with microelectronics, it makes sense that early microfluidics devices were designed as networks of microchannels. Microfabrication techniques easily allow for the etching of rectangular channels in silicon. Such channel networks are also reminiscent of the already familiar pipe networks of the macroscopic world. Moreover, as in electronic circuits, a channel network based logic allows for the decoupling of key functions in a microfluidic systems. Such a system can be thought of as an assembly of basic units which can then be sequenced into complex arrangements. Nowadays, transport in microchannels is extremely well-understood. Flow profiles are mapped for almost any imaginable channel cross-section [3], allowing for the determination of pressure gradients and hydraulic resistance in basic microchannel elements [5]. Diffusion in simple channel junctions has also been studied extensively [4] [156]. Using dimensional arguments and 1D models, diffusive exchange between different fluids put in contact over a distance can be accurately quantified, allowing for the design of passive mixers [128], filters [157] and chemical gradient generators [129]. Once the precise behavior of individual microchannels is known, they can be assembled in complex networks. These networks can then be analyzed using fluidic analogs to Kirchhoff's laws. This allows us to use the entire body of knowledge that exists for analyzing linear electric circuits, available in any undergraduate electric circuit textbook, "for free" and to apply it directly to the study of channel networks.

The combination of the theoretical understanding of the channel as an isolated unit with the high level rules for assembling them using circuit theory forms a solid, self-contained body of knowledge which can powefully tackle extremely complex channel networks. Pushed to its extreme, this framework has been the backbone of impressive systems mimicking microelectronics [7] reproducing complex ecosystems on chips [6], accomplishing multi-step lab operations on chip [187], as well as many more. However, while this paradigm is extremely strong and has allowed for the development of important technologies, it has its limits. By using circuit theory, we conceptualize elements in our systems as either point-like or 1-dimensional, abstracting away any 2D or 3D behavior the fluid could have. In recent years, a number of new technologies have emerged that break away from this 1-dimensional paradigm. Precisely engineered channel junctions have been used to generate and distort both rotational and extensional flows [188] [172], which can then be used to precisely study complex fluids [189]. Similar junctions have also been used to generate flows with precisely controllable stagnation points, which are then used to trap and move around small particles in 2D space [190] [13]. Flow in large chambers has been used to generate complex chemical gradients that are impossible to realize in simple channels [9] [132]. Outside of chambers,

entire families of microfluidic systems which use flow not confined by walls at all have been developped. Microfluidic probes [8] use pairs of point-like apertures to precisely stain large biological surfaces. From there, more complex arrangements of point-like apertures are used to generate increasingly complex flows over surfaces, microfluidic quadrupoles for the study of chemotaxis [124], reconfigurable multipoles for the automation of biological assays [15], even periodic arrays of apertures for a microfluidic analog to pixelated LCD screens [19].

A theoretical framework for such field-based microfluidic systems would be of great help to engineers working in the field, and would allow the push for more elaborate technologies that fully exploit the intricacies of 2D flow and transport. Fortunately, it turns out that such transport is already well-known to mathematicians working in various fields related to fluid mechanics [49] [191] [103], porous media [45] [34] or heat transport [192] [23]. The goal of this article is to gather this knowledge, that is currently scattered piecemeal over various fields, and collect it in one place easily accessible to engineers working in the field of microfluidics. This will enable us to describe flow and transport in 2D microfluidic systems in a systematic way, and thus facilitate the analysis of existing system, as well as the invention of new ones. Another goal of this article is to show examples of applications of simple transport theory as a way to further understand microfluidic systems. By the end of this tutorial review, the reader should have a solid grasp on the tools needed to examine flow and diffusion in a wide range of different microfluidic technologies. Of course, the framework described here can also be of interest to engineers working in different fields, namely groundwater mechanics, diffusion-limited growth phenomena, or heat transfer to name a few.

While the 2D technologies summarized above cover a wide array of applications, we can identify a number of recurring factors about them. By breaking them down to their most basic building blocks/phenomena, we can obtain a list of relevant physical phenomena that can be analyzed independently of each other. We will see that these basic phenomena, such as flow, diffusion and interfacial tension, are quite few in number, and can often be studied using the same set of tools. This will enable us to define a basic workflow that is a great starting point in the study of any 2D microfluidic system.

We begin this tutorial review by showing an overview of "field-based" microfluidic systems that operate using transport in 2D space. We then show a simple framework to analytically model flow in these systems. From there, we introduce conformal transforms, a mathematical tool with which we generate complex solutions from simpler ones. We then show how this mathematical framework can be extended to model diffusion, then interface effects. We end with a brief overview of some of the important 3D effects that happen in these quasi-2D systems.

Example matlab scripts for all of the applications demonstrated in this tutorial review are provided as supplemental material. We strongly encourage readers to experiment and play with them.

5.4 Field-Based Microfluidics

Many different families of systems exhibit 2-dimensional flow, we briefly review the most important ones here. An overview of these different systems is found in figure 5.1

5.4.1 Channel Junctions

Perhaps the first microfluidic system where 2-dimensional flow fields make their appearance is the center of channel junctions. Very early microfluidic mixers and filters consisted of simple channel networks where fluids of different concentration were put in contact over a certain distance and allowed to passively exchange before being reseparated. Examples of such devices include the well-known T-Mixer [128], H-Filter [157] as well as early hydrodynamic focusing systems [156]. In early passive mixing application, the downstream, knowledge of the quasi-1D behavior of flow and diffusion was important. The transport properties of such a flow were precisely characterized using classical transport theory [177] [4]. Later on, similar channel junctions were used in multiphase systems to generate regular droplet streams [196] [197]. In these applications, the 2D aspect of the flow at the junction is crucial, as it ultimately determines the shape of the droplets obtained. Flow at the junction in these systems also constitutes a nontrivial interface problem, which has been extensively studied [36]. Other groups used similar channel junctions with the express purpose of generating 2D flows in their center. Taking inspiration from G.I. Taylor's four-roll mill [169], a system initially invented to study the deformation of macroscopic droplets, research groups engineered various junction-based devices to generate extensional flows, shear flows, or even rotational microfluidic flows [188] [172] (Fig.5.1.a.i and Fig.5.1.a.ii). Such systems have then been applied to rheometry and caracterization of complex fluids [189]. Instead of adjusting flows to control shear, some groups used similar flow generating systems to generate stagnation points whose position can be adjusted. These hydrodynamic traps allows for the trapping and moving around of particle in 2 dimensions [190] [13] (Fig.5.1.a.iii). Such microfluidic traps have been proposed for use in single-cell analysis [198] and as ways to study complex polymer formation [199]. The analysis of such adjustable stagnation point flows remains a topic of interest to this day [200].

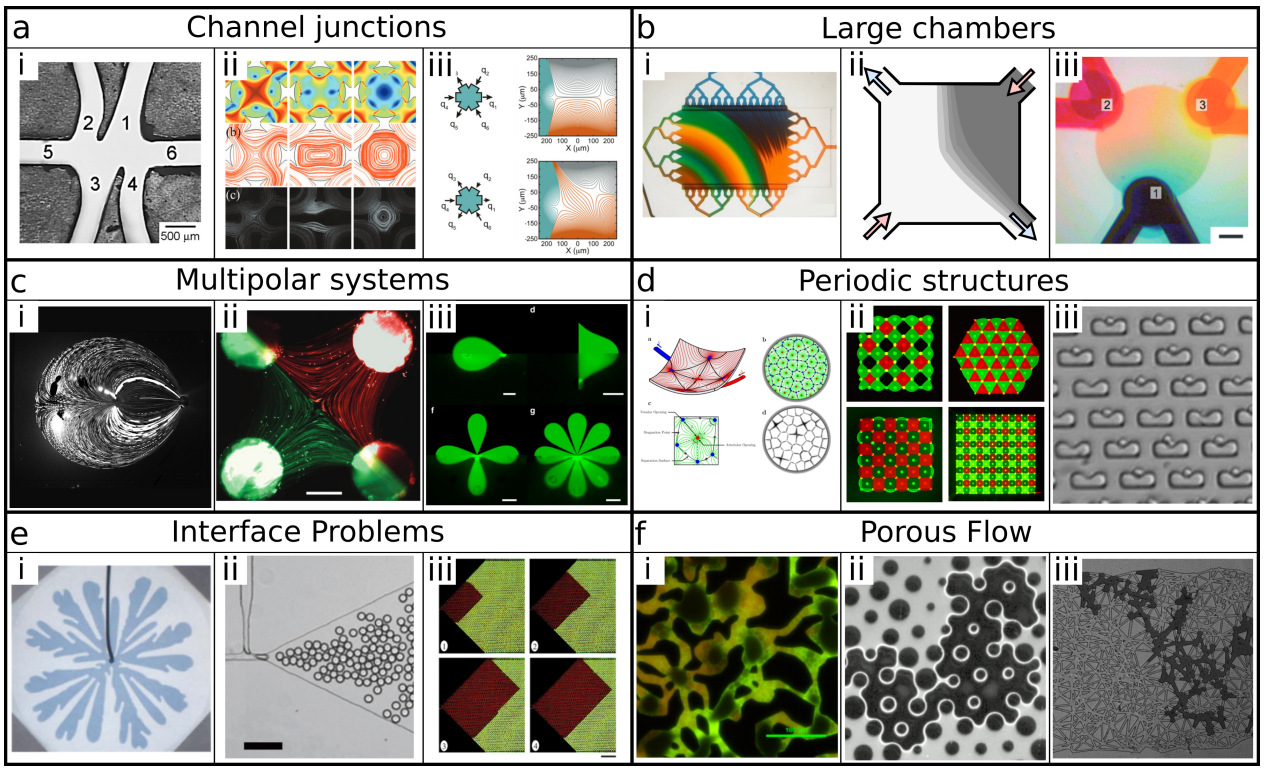

Figure 5.1 Microfluidic technologies operating with 2D flow fields. A) Flow in channel junctions: i) and ii) Microfluidic four-roll mills [188] [172], iii) Stokes traps [13]. B) Complex flow in large chambers: i) 2D concentration gradients in chambers, image courtesy of Folch Lab, ii) moving interface system [9], iiii) microfluidic palette [132]. C) Multipolar systems: i) Microfluidic probe (Image courtesy of Pierre-Alexandre Goyette), ii) Microfluidic quadrupole [124], iii) Reconfigurable multipoles [15]. D) Periodic structures: i) Irrigation of the human choriocapillaris [165], ii) Pixelated chemical displays [19], iii) Cell traps in microfluidic chambers [11] E) Complex interface systems: i) Radial viscous fingering [31], ii) droplet-based microfluidics [10], iii) 2D capillary pumps [193]. F) Models for Porous Flow: i) Silicon wafer models for sandstone [194], ii) Post arrays for the simulation of 2D multiphase flow [37], iii) PDMS micromodels for fractured rocks [195].

5.4.2 Large Chambers

A natural extension of channel junctions as a way to generate 2D flow fields is flow in large chambers. Early microfluidic gradient generators were used to create controlled gradients along one direction in large microfluidic chambers [129] [130]. One key application of such generators was the construction of artificial chemical environments in order to study chemotaxis [201], replacing the need for macroscopic gradient generators such as Boyden [202] or Dunn chambers [203]. While early systems for generating chemical gradients in chambers were an extension of channel-based systems, and functioned in a quasi-1D manner, with diffusion decoupled from convection, later systems involved transport in 2-dimensions (Fig.5.1.b.i). Examples of such systems include microfluidic palettes [132](Fig.5.1.b.iii) generating complex 2D gradient with minimal flow and shear stress, adjustable extensional flows in chambers for movable gradient interface [9](Fig.5.1.b.ii), as well as systems where parallel inlets inject fluid that is then free to evolve in a much wider chamber, creating intricate concentration patterns [204] [205] [206].

5.4.3 Multipolar Systems

A breakthrough in field-based microfluidics is the use of so-called multipolar systems, that is systems in which the fluid is confined in a thin region between two plates, and flow is generated by point-like apertures injecting or aspirating fluid from either the top or bottom plate. The simplest such device is the microfluidic probe [8] (Fig.5.1.c.i), in which a pair of apertures generates a confined flow. Such probes have been used for micro-immunochemistry [141], localized perfusion of brain slices [207], or single-cell analysis [134]. Several variants of the original design have been developped, using either precise silicon etching [144] or more recently 3d printing [142]. Variants with nested apertures for tighter confinement [145] or probes delivering heated liquid [146] have also been created. However, multipolar systems are not just used as a way to engineer probes to mark tissues. Several other problems can be elegantly solved through a multipolar approach. Using four apertures to create a purely extensional flow, microfluidic quadrupoles have been used to generate tunable linear concentration gradients [124](Fig.5.1.c.ii) which were then used to study cell chemotaxis [208], radial arrays of apertures were used to create directionally tunable gradients in chambers [171], flower-shaped systems were used to create multiplexed environments for complex experiments [15](Fig.5.1.c.iii) and mass-balanced doublets were used to generate shielding systems enabling the selective protection of sensitive surfaces in microfluidic chambers [18]. Moving from point source to line-source, micro-flow generators were developped to study the shear response of cell walls [14].

5.4.4 Periodic Structures

Multipolar systems based on periodically repeating arrays of aperture also exist and serve to generate complex flow and concentration environments. Microfluidic probes based on linear arrays of apertures were proposed as a way to expose surfaces to several conditions at once [147]. More recently, periodic arrays of apertures were proposed to fabricate pixelated chemical systems [19](Fig.5.1.b.ii). Such pixelated systems are also reminiscent of the irrigation of the choriocapillaris in the human eye [165](Fig.5.1.d.i), an example of a biological microfluidic system using periodic multipolar principles. In the domain of single-cell analysis, a number of cell trapping systems are also based on periodic systems, be they arrays of wells [209], "pachinko"-style systems to passively trap cells [11](Fig.5.1.d.iii) or traps based on suction through arrays of point-like apertures [210].

5.4.5 Interfaces

We have listed several technologies that exploit flow and diffusion in field-based microfluidics for single-phase system. However, a significant fraction of the research done today in microfluidics involves multiphase systems [36]. The study of multiphase flow in plane channels was pioneered by Saffman and Taylor [29], who studied the way a fluid displaced by a less viscous one generates unstable "finger" structures. The instability of the interface was further investigated in the context of point-like apertures injecting in large chambers [31](Fig.5.1.e.i), and found applications in porous media and oil recovery [34] [35]. In the context of microfluidics, such unstable interfaces are used to generate controllable streams of droplets [12] that can then be used as microreactors for complex reactions or assays [211]. Several of the flow problems involved in droplet microfluidics have been closely examined: flow inside droplets has been modelled as dipoles in order to study their long-range interactions [126] [10](Fig.5.1.e.ii), the interface problem involved in the generation of droplets, and the impact of flow parameters on droplet size and throughput is also well-characterized [197]. Another common use of multiphase flows in microfluidic systems is in the design of capillary pumps. Initial designs for capillary pumps were 1-dimensional, following channel paradigms [212]. In such pumps, a meniscus pulls the fluid through a linear channel through Laplace pressure. However, very soon, more complex pumps involving periodic 2D arrays of posts were designed [193](Fig.5.1.e.iii). In such pumps, the flow is pulled in a nontrivial way through a large chamber. Similar principles to those involved in these capillary pumps, as well as ideas from the original Saffman-Taylor experiments were also exploited to create self-coalescing modules, allowing the reconstitution of dried reagents in channels without mixing by Taylor dispersion [38]. The same modules were later used to create elaborate 2D concentration pat-

terns in microfluidic systems [213]. Lastly, microfluidic flow fields involving multiple phases have been used extensively for rheometry [189] [214]. These applications also form an extensive body of knowledge that has been reviewed elsewhere [21]. Problems involving multiphase flow, even in 2D and at low Reynolds number, are generally extremely complex, and form their own area of research [32], but the tools we present in this review are often applicable to understand the functioning of simple multiphase flow, as has been done previously by other authors for the case of droplets [10] and of complex capillary flows [38].

5.4.6 Models for Porous Flow

One final area in which 1-dimensional models break down is in microfluidic systems studying porous media. Flow in porous media is an extremely vast area of research [34], and one of the main challenges behind it is the determination of continuous models for flow in complex rocks, soils, and other disordered mediums. To solve this problem, research groups are creating complex analogs of fractured rocks on chips, and studying how fluid flows in them [215](Fig.5.1.f.i, Fig.5.1.f.ii, and Fig.5.1.f.iii). These systems sit at the interface between 1D channel based microfluidics and 2D field-based flows, and the groups fabricating them study how complex arrays of the former can lead behavior modelled by the latter. Similar chips can also be used to model complex disordered environments, as is the case for "soil on a chip" [216] systems, where flow in the chip becomes coupled with growth phenomena from living bacteria, fungus or plants.

5.5 The Hele-Shaw Cell: A Basic Unit for 2D Flow

In order to break free of the channel paradigm, we need to "step up" one dimension and study systems that are inherently 2-dimensional. Instead of a microchannel that has a width and height that are significantly smaller than its length, we study large chambers, which have one shallow dimension and extend significantly in the other two directions. Such a large, shallow chamber has been described in the past by Henry-Selby Hele-Shaw [28]. In his experiments, Hele-Shaw showed that the streamlines of a fluid confined in a thin domain between two flat plates behaves in a manner exactly analogous to field lines in a 2D electric field. This was actually proposed as a way to "simulate" electric fields in complex capacitors in an era where numerical simulations did not exist. The Hele-Shaw cell has remained an object of scientific interest up to this day. We cite for instance its use as a model for flow in porous rocks [217], its interest as an environment to study fluid-fluid instability and the fractal behavior that happens at an interface [32], or its role as a model for string theory [218]. The Hele-Shaw cell is of special interest for microfluidics as it represents a perfect model for flow in a large number

of systems. Indeed, a number of the systems listed in section 5.4 operate with flow in large shallow chambers, or with flow confined between a plane surface and a slab from which flow is injected or aspirated, creating a quasi-planar domain. Even regular microfluidic channels, because of the way they're fabricated, are often much wider than they are tall, allowing the use of the Hele-Shaw framework to study flow within them. We have shown elsewhere how, while flow and diffusion in microchannels can easily be explained by 1-dimensional models, the behavior of fluid in junctions of channels will have an inherently 2D aspect for which the Hele-Shaw cell is a more appropriate model [16].

5.6 Flow in the Hele-Shaw Cell

5.6.1 Potential flow can be used for microfluidic systems

Flow in the Hele-Shaw cell is relatively simple to model analytically, especially in microfluidic systems where Reynolds numbers are usually extremely small. When the thickness of the domain d, which is the characteristic dimension in the z direction, is much smaller than the characteristic dimensions of the flow in the x and y direction, and when inertial effects are negligible, flow in the Hele-Shaw cell is given by [20]

$$\mathbf{u} = -\frac{1}{2\mu} z\,(d-z)\left(\frac{\partial p}{\partial x}\,\hat{\mathbf{x}} + \frac{\partial p}{\partial y}\,\hat{\mathbf{y}}\right) \tag{5.1}$$

Where $\mathbf{u}$ represents the flow field, p the scalar pressure field, μ the fluid viscosity, and $\hat{\mathbf{x}}$ and $\hat{\mathbf{y}}$ the unit vectors in the x and y directions. This corresponds to a parabolic flow in the z direction modulating an irrotational 2D flow field in the xy plane. The 2D flow can be described as the gradient of a potential function which is proportional to the pressure field. Flow thus becomes expressed as the gradient of a potential function Φ, which, in the absence of sources or sinks, satisfies Laplace's equation

$$\nabla^2 \Phi = 0 \tag{5.2}$$

In this way, flow in the Hele-Shaw cell can be exactly modelled using the tools of potential flow theory, which are analogous to those used to study 2D electric fields. With this formulation, we can use the entire gamut of tools of classical electrostatics to study flow in microfluidic systems. We also note that equation (5.2) is the same as the equation describing Darcy flow in two dimensions [41]. The tools we present in this review are thus analogous to tools that have been used to study flow in 2D aquifers and flow in porous media, and solutions from

one can be often readily transferred to the other, despite the enormous difference in scale.

5.6.2 Flow can be modelled as a superposition of point sources

One of the main advantages of the potential flow formulation is the linearity of the equations involved. Very complex flows can be expressed as the sum of contributions from a library of simple base elements. Similarly to how electric fields can be modelled as sums of point sources. The 2D flow yielded by a single point source can easily be found using Gauss' theorem. For a point source at the origin, it is given by

$$\mathbf{u_i} = \frac{Q_i}{2\pi d\sqrt{x^2+y^2}}\ \hat{\mathbf{r}} \tag{5.3}$$

Where Q_i is the flow rate through the aperture, d is the domain thickness, and $\hat{\mathbf{r}}$ is the unit vector pointing away from the point source. Using our potential flow formulation, we find that this flow represents the gradient of a dimensionless potential contribution given by

$$\Phi_i = \frac{Q_i}{Q_0}\log\left(\frac{\sqrt{x^2+y^2}}{L}\right) \tag{5.4}$$

Where Q_0 is a characteristic flow rate and L is a characteristic distance in the xy plane. We define $q_i = \frac{Q_i}{Q_0}$, $\tilde{x} = \frac{x}{L}$ and $\tilde{y} = \frac{y}{L}$ in order to work in a simpler dimensionless system. The total potential can then be given by the sum of individual contributions

$$\Phi = \sum_i q_i \log\left(\sqrt{(\tilde{x}-\tilde{x_i})^2 + (\tilde{y}-\tilde{y_i})^2}\right) \tag{5.5}$$

Where $\tilde{x_i}$ and $\tilde{y_i}$ are the dimensionless coordinates of each individual point source. Examples of microfluidic devices modelled as sums of point sources are given in figure 5.2, where the method is used to model a channel junction (Fig.5.2.a), a microfluidic probe (Fig.5.2.b), a microfluidic "lighthouse" (Fig.5.2.c), Stokes traps (Fig.5.2.d), and microfluidic quadrupoles (Fig.5.2.e).

Point sources are sufficient for modelling flow in most devices. As long as the aperture's size is significantly smaller than the flows characteristic length, it can be modelled as a point source without loss of precision. Moreover, we can show that this is independent of the aperture's exact shape (be it circular, polygonal or otherwise) [152]. We have also shown elsewhere that small channels connected to larger chambers can be modelled as point sources without inducing significant errors [16]. However in some cases more elaborate source terms may be needed. For instance, liquid may be injected from an aperture of non-negligible size, either

a line source [14] (Fig.5.2.f) or from a large 2D aperture whose radius is comparable to the flow's caracteristic length. For such cases, analytical expressions for the contribution often exist, and can be found in groundwater mechanics textbooks such as [45], which compiles a large number of individual source elements that can be assembled into more complex flows through linear superposition. An example of simple script used to generate streamline plots from superposition of point sources is given in supplementary materials.

5.6.3 Shear stress is proportional to the 2D flow field

Precise knowledge of shear stress can be critical in several applications of 2D microfluidics, especially when treating sensitive biological surfaces. Chambers of varying width have been used to create Shear stress gradients in order to study the adhesion of human lymphocite [219] [220]. As another example, we cite the use of microfluidic probes devices for studying adhesion of single cells to surfaces [221]. Shear stress at the bottom surface of a Hele-Shaw cell is related to the slope of the velocity profile in the z direction.

$$\tau = \mu \left(\frac{\partial |\mathbf{u}|}{\partial z} \right)_{z=0} \tag{5.6}$$

Since flow velocity in the Hele-Shaw cell is given by the product of a parabolic flow in the z direction and a 2D potential flow (see equation (5.1)), it follows that at any point in the Hele-Shaw cell, shear stress is simply proportional to the 2D flow field [133]. This simple observation is very powerful as it means that any 2D flow problem that can be modeled using a potential flow function has an associated shear stress map described by the same potential. Away from walls, knowledge of the 2D flow field is thus sufficient to completely characterize shear stress. The areas of higher shear stress will correspond to the areas of faster 2D flow, generally located near the injection and aspiration apertures. It is to be noted that the models we provided for point source contributions (equation (5.3)) have a 2D velocity that goes to infinity as we get closer to the point source. In reality, apertures have a finite size and the point source model breaks down under the aperture. Accurate shear stress information can still be extracted from the point source model by evaluating the 2D velocity profile at a distance from the point source equal to the radius of the aperture.

5.6.4 Conformal transforms turn simple results into complex ones

One of the most powerful tools we can use to analyze transport in 2D microfluidic systems is conformal transforms. Conformal transforms are a tool of complex analysis that enable us to reformulate partial differential equation problems in different, often simpler, domains. They

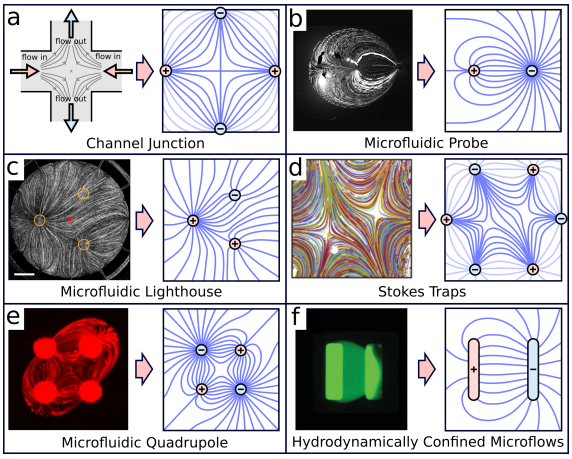

Figure 5.2 Various microfluidic systems modelled as sums of point sources. a) Channel junctions with movable stagnation points [190], b) Microfluidic Probe [8], c) Microfluidic Lighthouse [171], d) Stokes Traps [13], e) Microfluidic Quadrupole [124], f) Hydrodynamically Confined Microflows [14], an example of system where line sources have to be used in order to model the entire 2D flow.

have been used exhaustively in various domains of engineering to solve problems related to the Laplace equation in 2D, be they in heat transfer, electromagnetism, fluid flow, theory of elasticity, etc. [59] Since we have seen that flow in the Hele-Shaw cell is described by a potential function that respects the 2D Laplace equation (from equation 5.2), we can directly apply the tools of conformal mapping to our theory.

In order to do so, we rewrite our dimensionless position vector $\tilde{\mathbf{r}}$ as a single complex number z

$$z = \tilde{x} + i\tilde{y} \tag{5.7}$$

In such a formulation, the potential for a point source at the origin becomes simply

$$\Phi_i = q_i \log(z) \tag{5.8}$$

The complex potential $\Phi = \phi + i\psi$ has the convenient property that its imaginary part ψ exactly corresponds to the stream function of the flow. From the complex potential, the dimensionless velocity field can be obtained using $\tilde{\mathbf{u}} = \frac{d\Phi}{dz} = \tilde{u}(\tilde{x}, \tilde{y}) + i\tilde{v}(\tilde{x}, \tilde{y})$. This has the added advantage of giving us a very simple way of plotting streamlines in a system, as the streamlines are just the lines of equal ψ, ψ being the imaginary part of a generally quite simple analytical function.

The Laplace equation describing $\Phi(z)$ is invariant under conformal transforms [222]. Conformal transforms are a subset of transformations of 2D space which preserve angles. Conformal invariance of equation 5.2 means that, if we possess a valid solutions of 5.2 and a transformation of space which is conformal, we can immediately use the transformation to generate a new solution, which is itself also physically relevant. The transformations of complex space $\mathbb{C}$ which are conformal, and thus preserve solutions of Laplace's equation, are just the set of analytical functions of a complex variable. In practical terms, this means that if we possess a complex potential $\Phi(z)$ which describes flow in a 2D microfluidic system (for example one that was obtained by adding point source contributions as was described in section 5.6.2), then any potential of the form $\Phi(f(z))$ will also describe a possible system, provided $f(z)$ is an analytic function (which includes any familiar mathematical functions).

We show in figure 5.3 how we can take a catalog of known flow profiles and transform them using simple functions to obtain an entire array of different solutions. Four source images, a flat grid (Fig5.3.a), a straight flow(Fig5.3.b), flow around a cylinder(Fig5.3.c), and dipole flow in a microfluidic probe(Fig5.3.d) are transformed.

Each of these source images is first transformed using a power transform $f(z) = z^2$. Such a map has the effect of "folding" the half-plane into a quarter plane, adding a new axis of symmetry to the system, as is seen in its effect on the flat grid (Fig5.3.e). This power transforms maps the straight flow to a purely extensional flow (Fig5.3.f), the straight flow around a cylinder to purely extensional flow around a cylinder (Fig5.3.g), such as is found in experiments on droplet deformation [169], and the microfluidic probe is mapped to a microfluidic quadrupole, which is a geometry consisting of two injection and two aspiration apertures [124]. If an inversion transform $f(z) = \frac{1}{z}$ (Fig5.3.i) is applied to the same origin images, points near the origin are mapped to points near infinity, and inversely points far from the origin are mapped to points near the origin. This maps the straight flow to a 2D dipole flow (Fig5.3.j), the flow around a cylinder to dipole flow inside a cylinder (Fig5.3.k), where the exterior and interior of the cylinder have been "swapped", and the microfluidic probe to an impinging flow geometry, where two point sources inject fluid towards each other at different flow rates (Fig5.3.l). Such an impinging flow geometry has been described in our previous publications [16]. Finally, a logarithm transform is equivalent to switching from cartesian to polar coordinates, as is seen in its effect on the straight grid, transforming it to a polar grid (Fig5.3.m). This maps the straight flow to the flow from a point source (Fig5.3.n), and the flow around a cylinder to a point source near a rounded obstacle (Fig5.3.o). The logarithm transformation can be applied to the microfluidic probe image, but the result doesn't have any interesting immediate physical significance.

These are some examples of applications of simple conformal maps to real flow profiles. Of course, there exists many more possible maps. Extensive catalogues of conformal maps are given in textbooks such as Schinzinger and Laura [59], Driscoll [65], or in more classic texts such as Abramowitz and Stegun [223]. A small catalog of simple transforms can be found in supplementary table 1.

We use conformal transforms in two ways when studying flow profiles. The first use is to simplify a flow problem, bringing it from a complex geometry to a more straightforward one. This allows us, for example, to find flow solutions for symmetrical geometries with a large number of apertures without having to resort to long sums of point sources [15]. This can also allow us to find stagnation points in complex flows without having to solve complex algebraic equations. This use of conformal maps to simplify geometries will become very important when we analyze diffusion problems in section 5.7.

The second use of conformal transform is to take a known solution and "complexify" it. Once we are in possession of a valid flow potential, we can apply our entire library of known conformal transforms to it to immediately generate a number of other, equally valid solutions "for free". This sort of exploration can be extremely useful in the design and invention of new microfluidic systems. Examples of this procedure are shown in our previous publication [16].

5.7 Diffusion in Hele-Shaw Cell

As shown in the previous section, potential flow formulation models almost any conceivable 2D flow in microfluidic devices. However, the operation of many microfluidic systems relies not only on control of flow within them, but also on the precise diffusion of solutes within these flows, be they fluorophores, drugs, reactive species, etc.

The concentration c of a diffusive species in a 2D flow is described by the 2D convection-diffusion equation

$$\nabla^2 c - \mathrm{Pe}\ \tilde{\mathbf{u}} \cdot \nabla c = 0 \tag{5.9}$$

Where $\mathrm{Pe} = \frac{Q_0}{2\pi d D}$ is the Peclet number, representing the ratio of convective to diffusive transport [113]. The main difficulty in solving this equation comes from the algebraic term $\tilde{\mathbf{u}} \cdot \nabla c$, which renders the equation extremely complicated for all but the simplest flow. Analytical solutions rarely exist, and the typical way to analyze such an equation is in terms of singular perturbations [23]. Such methods are quite advanced, and typically only yield results in limited regions of interest, for example bulk transport properties around boundary

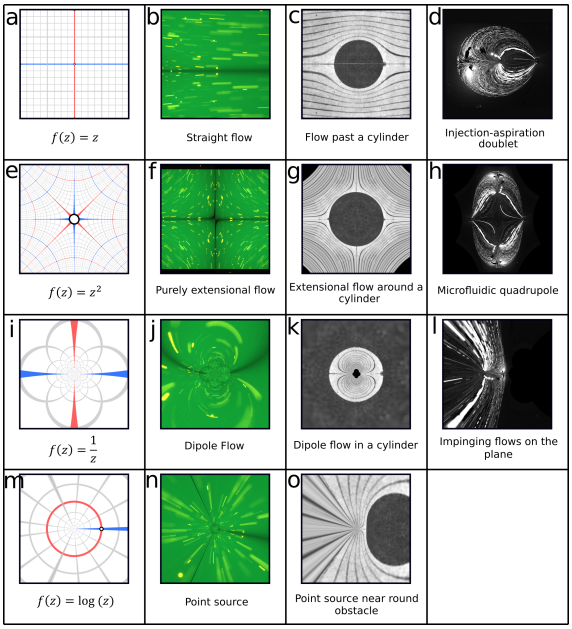

Figure 5.3 Application of simple conformal maps to various initial images. First row is the untransformed image, respectively a plain grid (a), an experimental image of a straight flow with fluorescent beads in it (b), flow around a cylindrical obstacle from Hele-Shaw's original article [28] (c), microfluidic probe (d). Second row is each of these images transformed using $f = z^2$ transform (illustrated in subfigure e), leading to a purely extensional flow (f), extensional flow around a cylinder (g) and flow in a microfluidic quadrupole [124] (h). Third row is the images transformed using an inversion transform (i), leading to a 2D dipole flow [20] (j), dipole flow inside a cylinder, which can be used as a model for recirculation in a droplet [10] (k), and impinging jets of different concentrations [15] (l). Final row is the images transformed using a logarithmic transform (m), leading to 2D flow from a point source (n), flow from a point source near a rounded obstacle (o).

layers.

In the case of Hele-Shaw flows however, much simpler solutions can be found. The flow field $\tilde{\mathbf{u}}$ can be rewritten as $\nabla\Phi$, making the convection-diffusion equation

$$\nabla^2 c - \mathrm{Pe}\ \nabla\Phi \cdot \nabla c = 0 \tag{5.10}$$

This form of the convection-diffusion equation is actually conformally invariant [101] [100]. This crucial fact allows us to extend the entire toolbox elaborated for flow patterns in section 5.6 and directly apply it to the diffusion problem, which would otherwise be impossible to solve directly.

As mentioned in section 5.6, we can use conformal maps in two different directions: either to exploit known results and generate more complex ones from them, or conversely to simplify complex problems to tractable geometries.

5.7.1 Using conformal transforms to complexify results

The first direct use of conformal maps we can make is to "complexify" known results. Similar to what was shown for flow patterns in figure 5.3, if we are in posession of a known concentration profile in a Hele-Shaw cell, we can apply our library of conformal maps to generate a host of new solutions to more complex geometries. While this strategy was useful for flow patterns, it is absolutely crucial for concentration profiles, as the constitutive equations otherwise rapidly become unsolvable for all but the simplest geometries.

This strategy is applicable to any form of diffusion pattern in Hele-Shaw cell. In the best of case, if we possess an analytical result for diffusion in a microfluidic device, it can immediately be transformed to obtain analytical concentration profiles in a myriad other geometries. However, even in the absence of analytical results, conformal maps can be used to explore possible configurations. Any representation of a concentration profile can be transformed and used to make predictions, this includes concentration profiles obtained via numerical methods (see section 5.9) but this can also include experimental fluorescence images (as was done in the last column of figure 5.3). Examples of such a technique are shown in figure 5.4.

5.7.2 Using conformal transforms to simplify and solve convection-diffusion problems

Conformal maps can be used in the converse direction as well, taking complex problems and simplifying them in order to obtain tractable equations. In previous publications [15] [16]

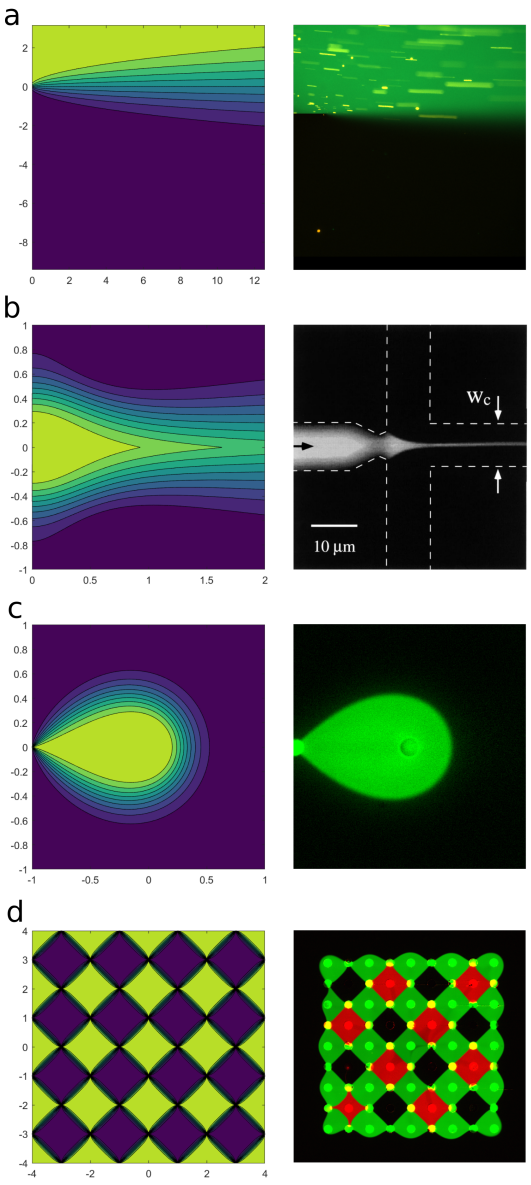

Figure 5.4 Analytical concentration profiles for various 2D microfluidic systems. a) Streamline coordinate solution for 2 fluids of different concentration put in contact in a horizontal plane flow. This solution is then transformed using conformal maps to obtain b) Concentration profile in a hydrodynamic focusing system [156], c) Concentration in a microfluidic probe (Experimental image courtesy of Pierre-Alexandre Goyette), d) Concentration in a pixelated chemical display [19]. All of the analytical maps are obtained by transformations of the simple plane flow concentration profile shown in a).

[19] [18], we have shown how this can be used to obtain complete concentration maps for very elaborate microfluidic systems. We summarize the procedure in this section.

The key to the solution procedure lies in realizing that the complex potential $\Phi(z)$ is itself an analytical function of a complex variable, and can thus be taken as a conformal map. By taking the map $f(z) = \Phi(z) = \phi + i\psi$, we get a description of the flow not in terms of the space coordinates $\tilde{x}$ and $\tilde{y}$ but in terms of the new coordinates ϕ and ψ, representing equipotentials and streamlines. In terms of these new coordinates, equation (5.10) becomes

$$\frac{\partial^2 c}{\partial \phi^2} + \frac{\partial^2 c}{\partial \psi^2} = \mathrm{Pe}\frac{\partial c}{\partial \phi} \tag{5.11}$$

Explicit passage from equation (5.10) to equation (5.11) requires the definition of complex gradient operators and is made in [100]. The crucial factor is that in the streamline coordinate domain, described by coordinates ϕ and ψ, the flow becomes a simple plane flow, and the boundary conditions are transformed to conditions on horizontal segments [101] [52].

Equation 5.11 is much simpler to analyze than 5.10. Specifically, through the change of variable $C(\phi, \psi) = \exp\left(\frac{1}{2}\mathrm{Pe}\phi\right) c(\phi, \psi)$, it can be brought back to the form of the 2D Helmholtz equation

$$\frac{\partial^2 C}{\partial \phi^2} + \frac{\partial^2 C}{\partial \psi^2} = \frac{1}{4}\mathrm{Pe}^2 C \tag{5.12}$$

Which can often be solved in rectangular domains using tabulated Green's functions [154]. In simpler domains, solutions of equation 5.11 may sometimes already be known and expressible in terms of simple functions, see for example [105]

The strategy for approaching convection-diffusion in an arbitrary Hele-Shaw geometry thus becomes

- Determine the complex potential for the flow
- Use the complex potential to determine how individual features of the flow map to segments in the streamline coordinate domain
- Solve the simplified convection-diffusion problem in the streamline coordinate domain
- Map back to the flow domain to obtain the complete solution for the concentration profile

The general outline of the strategy is illustrated in figure 5.4, where we show the analytical

solutions of equation 5.10 in the case of a simple plane flow (Fig5.4.a), and proceed to transform it to obtain profiles for the turning region in a hydrodynamic focusing channel junction (Fig5.4.b), a source-sink doublet (Fig5.4.c) and a pixelated chemical display (Fig5.4.d). In all three cases (the hydrodynamic focusing, the source-sink doublet, and the pixelated chemical display), the diffusion problem was simplified back to the same streamline coordinate problem. We give more detail as well as step-by-step resolution for a large number of possible geometries in [16]. In many cases, the resulting solution can be expressed as a simple combination of elementary functions such as logarithms, square roots and error functions. An example Matlab script used for generating concentration maps is provided in supplemental files. We also provide a script used to transform digital images using conformal maps, allowing the user to generate image such as the ones shown in figure 5.3.

One important thing to note is that very often, devices which appear at first to be very different will all simplify back to the same problem in streamline coordinate. This creates very strong functional analogies between families of devices which are in appearance very different.

For example, the streamline coordinate problem for a H-Filter is the same as the one for a dipole source in a plane flow [18]. In both geometries, two fluids of a different concentration are initially separated, then put in contact over a certain distance, then reseparated. This suggests the use of such a dipole source in a chamber as a way to generate wall-free microfluidic filtering systems. Similarly, we can show that a lot of "probe" type devices reduce to the same streamline domain problem as a traditional T-Mixer [16].

These sorts of analogy present us with a strategy for transfering functionality of channel-based systems to the "open-space". We note here that often the simplest open-space geometry that achieves the desired function is not necessarily the one we might have thought of at first.

5.8 Worked-out example: Diffusion from a cylindrical obstacle of fixed concentration

In order to demonstrate the tools presented in the previous sections we show a worked out example using complex potential theory to model flow and diffusion around a circular obstacle. This could be a cell in a chamber, a reactive post, or a slowly dissolving pellet of reagent. Straight flow around a circular obstacle can be modelled by the potential function

$$\Phi = z + \frac{1}{z} \tag{5.13}$$

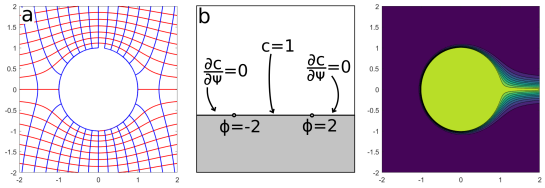

Figure 5.5 Worked-out solution to the problem of diffusion around a circular bead. a) Streamlines (red) and equipotentials (blue) given by the complex potential 5.13. b) Domain in which the transport problem given by equation (5.11) has to be solved. c) Concentration profile given by equation (5.15)

Which is the sum of a straight flow and a dipole source. The streamlines and equipotentials of this flow profile are shown in figure 5.5.a. In the streamline domain, the problem reduces to straight flow in a semi-infinite chamber with a single finite strip of fixed concentration in the middle of the domain (see figure 5.5). This strip is the image of the contour of the cylindrical obstacle, and its end points can be found by finding the complex potential of the two stagnation points of the flow Since the flow exhibits two stagnation points, one at $z_1 = -1$ and one at $z_2 = 1$, we find the corresponding points in the streamline domains to be $\Phi_1 = -1 + \frac{1}{-1} = -2$ and $\Phi_2 = 1 + \frac{1}{1} = 2$. The convection-diffusion problem at hand is thus to solve equation (5.11) with $c \to 0$ as $\sqrt{\psi^2 + \phi^2} \to \infty$, a symmetry boundary condition for the entire $\psi = 0$ axis, except for the range $\phi \in]-2, 2[$, where the boundary condition is that $c = 1$. The Peclet number for the transport problem can be computed using $\mathrm{Pe} = \frac{Q_0}{2\pi d D}$. If we know the average velocity in the channel we can replace Q_0 with the expression $u_{ave} \cdot r \cdot d$ where r is the caracteristic distance in the xy plane, here the radius of the cylinder. For example, if we are studying a bead of radius $r = 1mm$ in a chamber of height $d = 500\mu m$ with an average fluid velocity in the chamber of $u_{ave} = 1mm/s$, and if the bead is diffusing fluorescein in the chamber ($D = 4.2 \cdot 10^{-10} m^2 s^{-1}$), we find a Peclet number of $\mathrm{Pe} \approx 380$.

The domain in which equation (5.11) must be solved is shown in figure 5.5.b. The complete solution to the transport problem turns out to be quite difficult due to the mixed boundary condition on the axis $\phi = 0$, but approximate solutions do exist in the litterature [110] [111]. However, for our purpose, we can use a solution for a semi-infinite strip to obtain a concentration profile that is valid at high Pe around the surface of the obstacle.

$$c(\Phi) = \left(1 - \mathrm{erf}\left(\mathrm{Im}\left(\sqrt{\mathrm{Pe}\,(\Phi + 2)}\right)\right)\right) \tag{5.14}$$

Which is a classic solution of the problem of diffusion from a semi-infinite strip [105], offset so that the origin of the semi-infinite strip lines up with the point $\phi = -2$, $\psi = 0$, which corre-

sponds to the image of the front of the cylinder. From this solution in the streamline domain we can directly find the concentration profile in the regular flow domain by substituting in equation (5.13). We find

$$c(z) = \left(1 - \mathrm{erf}\left(\mathrm{Im}\left(\sqrt{\mathrm{Pe}\left(z + \frac{1}{z} + 2\right)}\right)\right)\right) \tag{5.15}$$

Which is illustrated in figure 5.5.c. Strictly speaking, this solution fails to completely model the wake behind the cylindrical obstacle, but can be largely sufficient for most practical purpose. For instance, even without knowing the full functional behavior of the wake, the quantity $\frac{\partial c}{\partial \psi}$ can be integrated along the length of the strip to obtain the total amount of reagent that is transported from the surface of the cylinder to the wake downstream, thus obtaining the Nusselt number (we give more detail on this procedure in [18]).

5.9 Use of numerical tools

The tools we have presented so far have allowed us to get a pretty complete analytical modeling of a variety of field-based microfluidic systems. Using conformal transforms, we have also seen how solutions for simple systems can be extended and used to analyze very elaborate geometries, while keeping solutions for flow and transport that are expressed in terms of single functions. Simple analytic solutions are of course always preferable to numerical calculations, they can give us the exact local scaling behavior of the flow and concentration as a function of operational parameters, and can be used to generate models that are computationally very light, that can then be used in controlling software (see for example [13]). There are times where the use of numerical tools is practical, if not necessary, when designing new systems. Moreover, the first preliminary analysis of a new system very often involve numerical investigation.

One crucial problem we face when using numerical methods to analyze 2D microfluidic systems is that the highly multiscale aspect of the problems makes their resolution by "direct attack" extremely difficult. Indeed, field-based microfluidic systems operate in a regime where the flow is evolving in a domain much thinner than it is wide. However, this clashes with the demands of classic numerical methods such as finite volume methods and finite element methods to have individual mesh elements be as "square" as possible. A 3D finite element method resolution of a problem of flow and diffusion in a Hele-Shaw cell will require at least 5 or 6 elements along the short direction of the domain in order to fully resolve the parabolic flow happening there. This means that the required resolution of the mesh is driven not by the characteristic length of the flow, but by the much smaller gap that the quasi-2D flow

exists in. This rapidly leads to extremely fine meshes, even for simple flows, and solution times that are extremely impractical, even for moderately precise results.

A solution to this problem is to sidestep the 3D aspects of the flow and directly solve the 2D equations, such as (5.2) and (5.10). Solving the 2D equations allows for the use of a mesh that is extremely refined in regions of interest, and more coarse outside of them. The removal of one dimension also means that even for extremely fine meshes, solving times will be orders of magnitude faster than for the equivalent 3D domain.

As an added bonus, since equations (5.2) and (5.10) are conformally invariant, solutions for flow profile or concentration maps obtained using numerical methods can be transformed using the tools of section 5.6.4, allowing a single simulation's result to be exploited in predicting several more complex systems.

5.10 Interfacial effects

The mixing of immiscible liquids and the effects of surface tension in Hele-Shaw cells is a very vast domain, and we give here only a couple of notes on it, as it has been thoroughly reviewed elsewhere [32] [39]. It is however worth showing how the tools presented in this review, namely conformal mapping anf potential flow theory, can be applied to analyze complex multiphase systems.

While the general problem of multiphase flow in Hele-Shaw cells is intractable, most phenomena appearing in microfluidic systems can be reduced to one of a couple of simpler flow types, which we list here.

The simplest multiphase phenomena found in microfluidic systems is certainly washburn flow [224], which is the driving force behind capillary pumps [212]. Washburn calculated the precise velocity of an advancing meniscus in a small cylindrical capillary using the laws of Poiseuille flows. This model also has the advantage to sit well within the quasi-1D channel paradigm, which makes it very simple to analyze, but not always descriptive enough for more complex 2D flows.

Another simple example of multiphase flow is viscous fingering in a rectangular channel, first studied by Saffman and Taylor [29]. When a less viscous fluid is pushed into a rectangular channel filled with a more viscous one, the interface is unstable and forms families of finger-like protrusions, eventually stabilizing with a single "main" finger advancing in the cell. The phenomena has been further analyzed by saffman and can be modelled using the tools of conformal mapping shown in section 5.6.4 [30] [225]. Extensions of the ideas behind viscous fingers have been used to create self coalescing flow modules [38], which have also been

analyzed in terms of conformal maps. Similar effects have been observed when the fluid is injected from a point-like aperture in a large chamber, leading to a radial fractal pattern [31]. Similar interfaces have been observed in porous rocks, for instance in fossil fuel extraction applications [35].

Lastly, one of the most common use of multiphase flow in microfluidics is in the formation and control of droplets. Flow of liquid in and around droplets is a complex problem studied elsewhere [226]. However, in many regimes, simple dipole flow can serve as a good approximation for flow both inside a microfluidic droplet as well as around it [10]. This formulation has been used to accurately model the behavior of large ensembles of droplets in microfluidic chambers [126]. This means that the framework developped in this article can be of use when analyzing flow and diffusion in problems involving microfluidic droplets and droplet ensembles.

5.11 Beyond 2D, effects in the third dimension

This review focuses on 2D effects in microfluidic devices but it is important to remain aware that we are treating systems that exist in the 3D world. This is compounded by the fact that standard fluorescence images, or microscope pictures of our systems are often taken either from the top or the bottom, so that what we see is a signal that has been integrated over a vertical direction, eliminating the third dimension from the picture (and from our minds). Even when using simplified models of behavior in 2D. It is important to remain aware of what happens in that third direction as it can very often be the driving factor in our system. We briefly mention here a couple of important effects that happen in the third dimension, even in planar microfluidic systems.

5.11.1 Turning region under apertures

One region where flow is decidedly not 2-dimensional is in the turning region under point-like apertures. In modelling systems as combinations of point sources in the plane, we implicitly assume that the characteristic distance separating each of these point sources is much larger than the radius of the aperture itself, or the thin gap of the Hele-Shaw cell. When these assumptions are not fulfilled, small errors in the predicted flow pattern can occur. This can manifest, for example, in errors on the predicted position of stagnation points [124] [133]. If the region of interest in the system is situated directly under one of the apertures, then the fully 3D aspect of the flow has to be considered. The problem of the turning region under a tube-like aperture has been studied in the past in various engineering applications such as

radial diffusers [227], hydrostatic trust bearings or injection moulding [228] [229].

5.11.2 Butterfly effect at the diffusion boundary layer

In section 5.7, we have tacitly assumed concentration in the microfluidic systems we study is constant along the vertical axis, allowing us to treat the convection-diffusion problem as a purely 2-dimensional one. This is a useful simplification with which we tackle very complex problems, but it does neglect effects that happen at higher Peclet numbers. Specifically, at high Peclet number, diffusion broadening happens due to "the butterfly effect" [177], where analytes will tend to diffuse more near the top and bottom surfaces of the Hele-Shaw cell. This is due to the lower velocity of flow in this region, which leads to comparatively more molecules diffusing out, leading to a characteristic "C" shape of the diffusion interface in the vertical direction.

5.11.3 Surface reactions

Another case in which concentration cannot be assumed to be uniform through the vertical section of the Hele-Shaw cell is in cases where surface reaction happens on either the top or bottom surface of the system. Surface reaction is bound to happen in a large number of microfluidics application, be they related to sensors [230], immunoassays [231] or surface patterning [232] [233] to name a few. In addition to involving a third dimension, the resulting convection-diffusion-reaction problem is much more complex than simple convection-diffusion, as it involves a reaction time scale to keep track of in addition to the convective and diffusive time scales. This leads to a very large number of qualitatively different situations depending on the relative scales involved [113]. The problem of molecule absorbtion on a surface in a shear flow, such as happens in microfluidic surface reaction applications, has been studied in classic transport theory litterature. We cite for example Leveque [107], Springer and Pedley [108] as well as classic transport textbooks such as Deen [73] for in-depth solution procedures.

5.11.4 Interaction with porous media

Finally, we briefly mention the situation when there is a porous surface at the bottom of the Hele-Shaw cell. This is the case,for example, when processing biological tissues, for example brain slices [207], adherent cell matrices [234], or cancer cells [235] [141], but could also happen in soil-on-a-chip systems [216], or systems modelling flow in a granular bed [236]. In such systems, we might be interested not only in what happens in the Hele-Shaw cell, but

also what happens within the tissue. In most cases, like in staining applications, permeability mismatch between the tissue and the Hele-Shaw cell is high, and it is sufficient to consider pure diffusion from the fluid to the tissue. However, in some cases, we might be interested in penetration of the fluid from the Hele-Shaw cell to the porous medium.

Behavior of the fluid at the porous interface is a complex problem that has been formulated by Beavers and Joseph [237] as well as Saffman [238] in the 1970s. While some theoretical litterature exists on this problem [239] [240], as well as experiments in macroscopic conditions [241], this last point has not been studied thoroughly in the context of microfluidics. This could be an important area of research, both in the study of perfusion and in the context of microfluidics being used as models for porous soils [215].

5.12 Conclusions

In conclusion, we have shown how a large number of microfluidic systems operate using similar principles of quasi-planar flow. We have shown how a handful of simple theoretical tools, namely potential flow, superposition of charges, conformal transforms and convection-diffusion analysis can be used to obtain thorough information on these systems' design and operation. We hope that this review makes these tools accessible to a greater public of engineers and experimentalists, and opens the door to a new generation of 2D microfluidic technologies.

Author Contributions

Study design, E.B., T.G.; writing—original draft preparation, E.B., T.G.; writing—review and editing, E.B., T.G.; Figures: E.B.; supervision, T.G. All authors have read and agreed to the published version of the manuscript.

Conflicts of interest

There are no conflicts to declare.

Acknowledgements

E.B. acknowledges funding from the Fonds de Recherche du Québec (FRQ) "Bourse de doctorat en recherche" and from the National Science and Engineering Research Council of Canada (NSERC) "Alexander Graham Bell Canada Graduate Scholarship". T.G. ac-

knowledges funding from the Fonds de Recherche du Québec (FRQ), "FRQNT Team Grants #205993 and #284621", and the National Science and Engineering Research Council of Canada (NSERC – RGPIN - 06838). We thank the Canadian Microsystems Center (cmc.ca) for access to a shared computational infrastructure.

CHAPTER 6 TECHNOLOGICAL APPLICATION - MICROFLUIDIC SURFACE SHIELDS

6.1 Outline

The toolbox developed in my PhD was first developed to model microfluidic probes and probe adjacent systems. In chapter 3, we showed how microfluidic probes could be caracterized as microfluidic multipoles, meaning arrangements of point sources and sinks distributed in a quasi-2D space. In chapter 5 we showed how the framework could be applied to a range of microfluidic systems.

This chapter, as well as the following one, showcase examples of new microfluidic systems that were designed using the theory of multipolar flows. Both of these systems were first predicted analytically, using potential flow theory, before being fabricated and operated by experimentalists in the group. Once these systems were fabricated, their operation and caracterisation was guided by the theory of diffusion in such systems. These two examples thus showcase a clear example of how strong theory can be used in service of technological development, and how solid understanding of the physical principles underlying our systems can hint at possible new devices.

In this chapter, we present the microfluidic surface shield. The work presented here was the subject of a peer-reviewed article in PRA [18], for which I was second author.

6.2 Contribution

The article related to this chapter [18] was written in around equal parts by myself and Oscar Boyadjian. I wrote the first half, including introduction and theoretical context, and Oscar wrote the second half, focusing on fabrication and applications. My contribution consisted in providing theoretical framework and analysis, and Oscar did the work related to fabrication of the systems, as well as take all of the experimental images shown in the article.

6.3 Initial Justification

As with other multipolar systems we designed, the initial idea for the microfluidic surface shield was to exploit the analogy between electric fields and flow in plane microfluidic systems. Specifically, we could look at other applications of conformal mapping in the domain of electrostatics and optics. One idea that got a lot of traction in the late 2000s is that of

engineering materials to generate conformal maps that could redirect light rays in arbitrary manners. A seminal paper on the subject is Ulf Leonhardt's "Optical Conformal Mapping", published in Science in 2006 [61]. This article, as well as J.B. Pendry's article in the same issue of Science [242], kickstarted the domain of "optical cloaking", where one uses varying refaction index in microengineered materials to redirect light around an obstacle. Ulf Leonhardt showed how spatially varying refraction index in a material could be conceived of as a conformal map that would deform the path of light rays, and Pendry showed how such a controllable refractive index could be achieved. These systems opened the way for many applications in optics, but "cloaking", that is the redirection of light rays around an obstacle so that it is rendered "invisible", became especially popular, thanks to its analogies with science fiction and fantasy concepts of "invisibility cloaks".

In the years following the publication, research groups proceeded to fabricate "invisibility cloaks" for several different wave phenomena, including acoustic waves [243], elastic waves [244], seismic waves [245], waves at the surface of water [246], quantum mechanical matter waves [247], etc.

Transposition of the cloaking principle to other wavelike phenomena is (theoretically) straightforward: as long as the phenomena can be described by the wave equation, the physics is the same, and the problem becomes one of engineering an appropriate microstructured material to modify the refractive index. However, shortly after, research groups started broadening the definition of "cloaking" and applying the terminology to phenomena that were not controlled by the wave equation exclusively.

Specifically, groups started developing "cloaking" systems for phenomena governed by parabolic differential equations such as heat flow [248], reaction-diffusion [249], and Darcy flow [250]. While not described by the wave equation, these systems are still modelled by equations that are conformally invariant, which enables the general methodology of applying a conformal transform on a flow (of heat, diffusive species, or fluid in a porous media) to deform it around an obstacle.

This, combined with our previous work on conformal transforms applied to microfluidic flow, led logically to the idea of "microfluidic cloaking". Using a pair of point-like apertures, an excluded volume can be created in an incoming straight flow. The surface under this excluded volume is thus only exposed to the injected fluid, and is separated from the rest of the flow. The streamlines of the flow are deflected around the excluded volumes in a manner analogous to the electric field lines around a conductor.

6.4 Rankine Body

Ulf Leonhardt's original article proposes a conformal transform given by

$$f(z) = z + \frac{1}{z} \tag{6.1}$$

As a way to deflect incoming light rays around a circular obstacle. In potential flow formulation, this map corresponds to a dipole source placed in an incoming plane flow. The main characteristic of this map is that there is a clear separation between the streamlines within the circle and those coming from the plane flow, with the two never mixing.

This flow pattern is something that we can reproduce quite easily in a Hele-Shaw cell by using point sources. We can build a large rectangular chamber in which a horizontal flow is driven using a syringe pump. If the Hele-Shaw cell is much thinner than it is wide, the resulting flow (away from the walls) is a straight flow modulated by a parabola in the vertical direction.

A dipole source can then be placed at the center of this chamber, and can be turned on or off, toggling the system between a state of undisturbed plane flow and one where a circular region is isolated from the rest of the flow.

In the "real" system, instead of a dipole source, we use a pair of mass-balanced injection and aspiration apertures separated by a finite distance. Instead of a perfectly circular exclusion zone, this creates an ovoid shape that is called a "Rankine Body", known for its application in early ship design [48]. The shape and size of the Rankine body can be adjusted by changing the ratio of the plane flow incoming flow rate to the flow rate injected by the injection aperture.

The potential function describing the flow in the microfluidic surface shield is thus

$$\Phi(z) = \beta z + \log(z+1) - \log(z-1) \tag{6.2}$$

Where $\beta = \frac{\pi d Q_{plane}}{W Q_{point}}$ is the ratio of the plane flow velocity to the caracteristic velocity of the point source. In the limit of pure convection, there is no mixing between the inside of the recirculation zone and the incoming flow. In cases where diffusion is present, the mixing can be rendered arbitrarily small (see section 6.8). An illustration of the microfluidic surface shield is shown in figure 6.1.

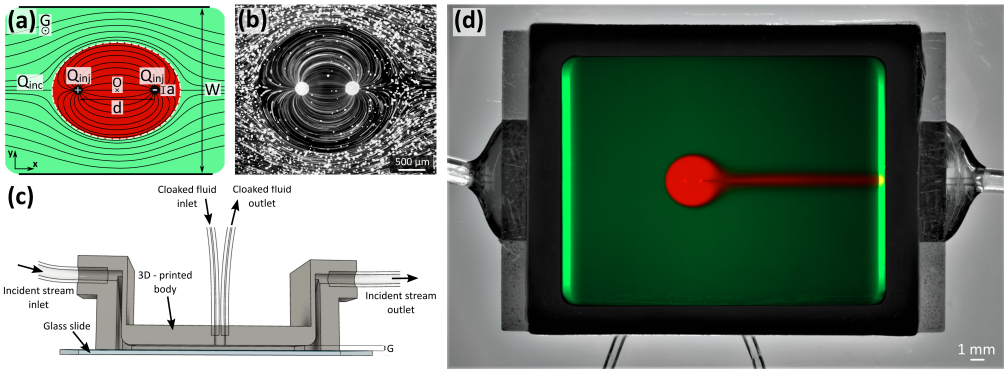

Figure 6.1 Illustration of the microfluidic surface shield. a) Conceptual figure of the streamlines in the system, with the excluded volume colored in red. b) Experimental image of the system in an experiment involving fluorescent beads, clearly showing the separation between the interior and exterior volume. c) CAD image of the system (side view) d) Composite fluorescence image showing the system from a top view, in a situation involving non-negligible diffusion

6.5 System fabrication and operation

The experimental part of this work was realized by Oscar Boyadjian. The system was first designed in CAD and manufactured using stereolithography. The device was connected to 4 plastic tubes connected to syringe pumps, one for each point-like inlets, and one for each end of the chamber. The central cell consisted of a 3D printed part mounted on a glass slide. The chamber had dimensions of 1.6 cm by 2 cm and a depth of 500 μm, and the two apertures, of radius 50μm were pierced in the 3d printed part, and separated by a distance of 1 mm. The system was sealed using UV-sensitive glue, and was operated using ethanol-dilute fluorescent solutions. Working with ethanol simplified the problem of air bubbles getting trapped in the system, and was sufficient for the proof-of-concept we presented in the article. Of course, in biological applications, the system would have to be run using water solutions rather than ethanol. This would involve more problems with trapped bubbles but could be solved by using functionalized surfaces and a more streamlined operation protocol.

Schematic of the system is shown in figure 6.1b.

6.6 Applications in surface chemistry

The proposed use of the system is to isolate a sensitive surface from an incoming flow. For example, a sensor could be placed on the surface underneath the pair of apertures, and be selectively exposed to an incoming flow, in a manner that could be adjusted dynamically

during the experiment. Such experiments, involving surface-based sensors, are common in domains like SPR sensing [251], Whispering Gallery Mode sensing [252], or quartz crystal microbalance sensing [253]. Outside of sensing application, this system could also be of use in other biological experiments involving reactive surface, namely in manipulating 2D cell cultures [254], or patterned antibodies [255]. In general, the problem of reaction from a surface to a microfluidic flow is one that has been studied in-depth [230] [113], and technologies allowing more precise control of the exposition of a reacting surface could prove to be a useful toolbox in the development of complex microfluidic systems. The work we presented in the Physical Review Applied article, however, was mostly conceptual in nature, and avenues of application for the system to real sensing experiments still remain to be done.

6.7 Analogy with Groundwater Heat Pumps

Before moving on to analysis of diffusion in the microfluidic surface shield, we mention that the problem of a plane flow intersecting a pair of mass-balanced point sources has been studied in the past in the domain of groundwater heat pumps.

Groundwater heat pumps are heat exchange systems in which hot water is extracted from an underground aquifer through an aspiration well. The water is then used to heat utilities, and the cold water is reinjected in the aquifer through a second well. As a first approximation, the aquifer can often be approximated as a mostly plane region described by a Darcy flow, which is another form of potential flow. In the presence of a plane current in the aquifer, different scenarios can occur, depending on the spacing of the apertures and their orientation relative to the flow. Some of these scenarios are illustrated in figure 6.2.

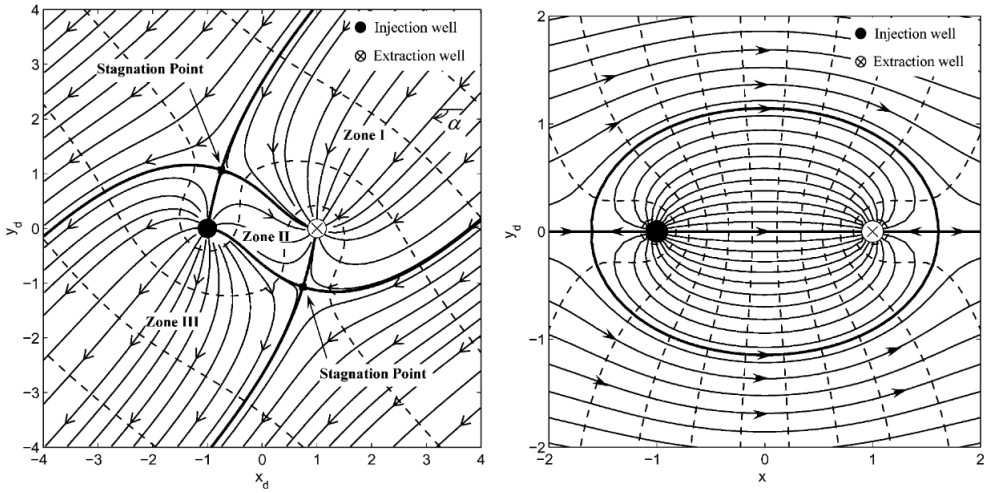

Figure 6.2 Flow in a planar aquifer with a pair of wells in a plane flow. From [161]

It is interesting to note that the second case shown in figure 6.2 is exactly equivalent to the flow in our microfluidic surface shield. Of course, in most groundwater heat pump applications, it is generally desirable to minimize feedback between the two apertures, so that the reinjected cold water is not reaspirated by the injection well, whereas in our microfluidic surface shield application we are doing the exact opposite: reaspirating the entirety of the injected fluid. In the case of planar aquifers perfectly described by 2D Darcy flow, the determination of the flow pattern is direct, however the analogy between the two systems could open the way to using microfluidic systems as miniature physical models for more complex aquifers with known distributions of wells, owing to the similarity of the equations describing flow in both.

6.8 Diffusion in the Microfluidic Surface Shield

In the limit case of pure convection, there would be no exchange between the exterior and interior of the Rankine body. However, in real experiments, if the plane flow and injected flow are at different concentrations, a thin diffusion boundary layer is established at the interface between the two regions. A small amount of reagent will thus diffusively "leak" from this boundary layer and be convected downstreams. In order to quantify this leakage, we need to solve the convection-diffusion problem associated with this system.

Diffusion in the microfluidic surface shield is analyzed using the same methodology we have presented in previous sections. The potential function (given in equation 6.2) for the flow is obtained by a superposition of a plane flow and two point sources. This potential function can then be used to map the problem to the streamline coordinate domain, where flow is plane and the boundary conditions map to horizontal obstacles.

In the systems we analyzed in previous sections, problems often mapped to variations of the same streamline coordinate domain: two strips of different concentration initially separated, then brought into contact and allowed to mix over an arbitrary distance. In section 4, we showed how a range of different systems could be reduced to this one problem, and how this problem could be solved in a number of different regimes.

In the case of the microfluidic surface shield, however, the problem is a little more complicated. The streamline coordinate domaine still features two strips of of different concentration, initially separated and then put into contact. However, the two strips are then reseparated at another point further downstream, so that they are only allowed to mix over a finite distance. A complete analytical solution of this problem is much more involved, and is analogous to what is called the "finite strip problem" in heat transport [110], where heat is transported in a flow from a strip of finite distance. The streamline coordinate problem

for the microfluidic surface shield is shown in figure 6.3.

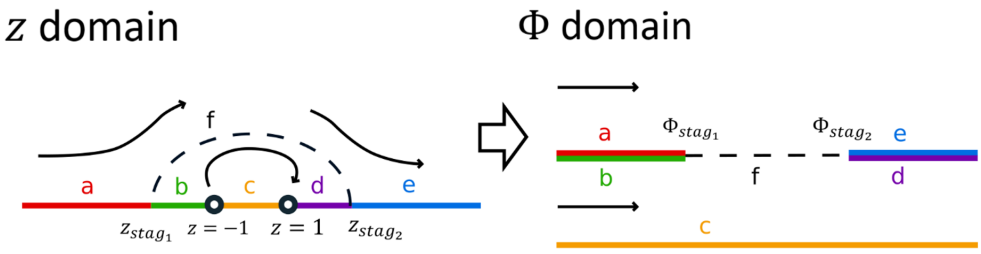

Figure 6.3 Features of the flow for the diffusion problem in the regular flow domain (z domain), and in the streamline coordinate domain (Φ domain). Segments a, b, c, d, e represent symmetry boundary conditions. Complete description of the coordinate for each segment in both domains is given in [18]

No analytical solutions for this problem, or analogs to it, exist. There are, however, approximate analytical methods. In cases where the strip is significantly longer than the characteristic diffusion length, the Wiener-Hopf method can be used to obtain approximate solutions on each end [108] [108]. A similar method was used to obtain approximate solutions for diffusion problem around finite obstacles in potential flows [111]. Iterative procedures for the determination of the Green's function have also been studied for some problems involving simple flow [110]. All of these methods usually yield a solution that is either an infinite series, or an integral that has to be approximated numerically (for instance an inverse fourier transform of a given function). Fortunately for us, in most practical cases, we do not need the exact analytical concentration profile everywhere. In the case of the microfluidic surface shield, we are mainly interested in the amount of exchange that happens through diffusion between the inside and outside region of the excluded volume. This quantity will allow us to determine how much reagent leaks out in the "tail" of the surface shield, shown in figure 6.1d. Examples of such a determination using scaling arguments can be found in [113], for problems that are very similar to the streamline problem shown in figure 6.3.

When the Peclet number is high enough (which is always the case in our experimental setup, with Peclet numbers varying from around 100 to 1000), the solution presented in equation 3.6 can yield a good approximation for the leading edge of the problem. This solution assumes that the concentration at the point of contact between the two strips remains constant at $c = \frac{1}{2}$, and is only approximately valid until the fluids are reseparated. However, by neglecting retrodiffusion, this solution can be integrated at the point of re-separation to obtain a very good approximation of how much reagent leaks out and isn't recaptured by the Rankine body.

This method is used to obtain the dimensionless flux from the Rankine body at arbitrary Peclet numbers, this flux is computed for a number of different conditions, and compared with experimental results, in figure 6.4.

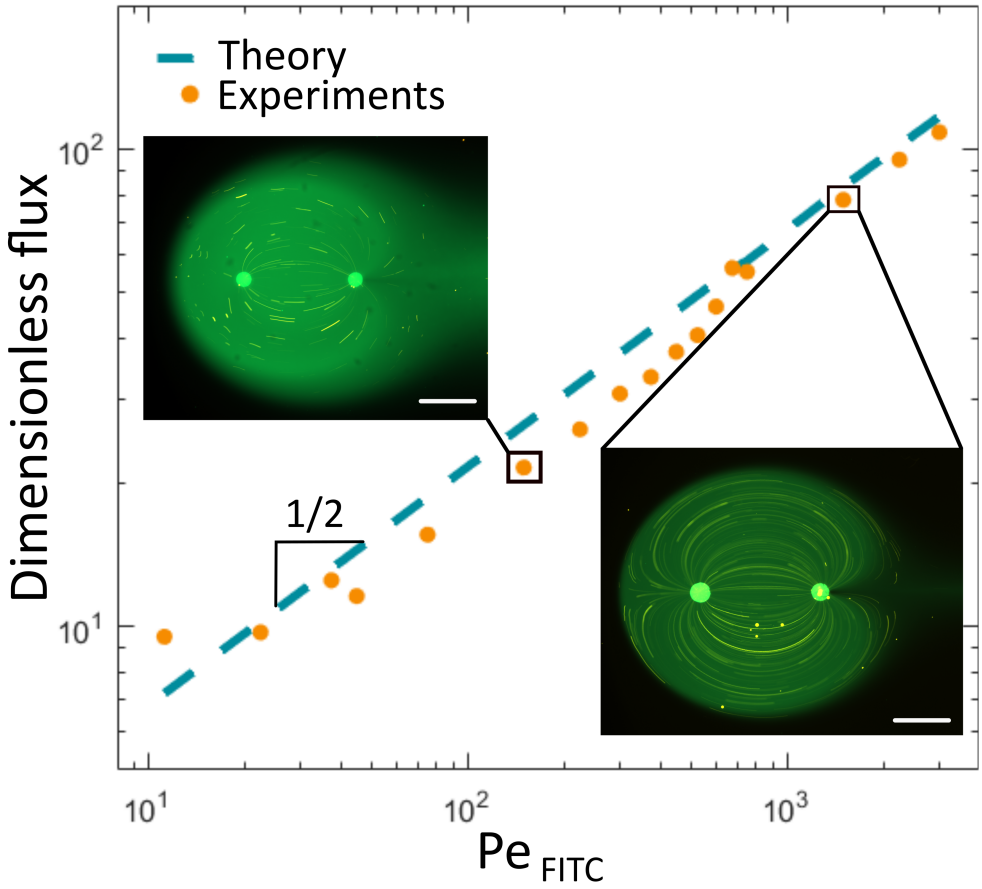

Figure 6.4 Experimental verification of dimensionless flux from the microfluidic surface shield. Dimensionless flux predicted from the theoretical model is compared to experiental results. Experiments used an FITC solution, and flux was calculated by integrating the concentration profile in the tail downstream

6.9 Analogy with H-Filters

Examination of the problem in streamline coordinates also reveals a striking analogy between the microfluidic surface shield and the well-known microfluidic H-Filter [157]. In both systems, two fluids of different concentration are put into contact, allowed to mix over a finite distance, then reseparated. In fact, using conformal transforms, we can see that the two systems reduce to the same streamline coordinate problem. This analogy suggests the use of microfluidic surface shields as systems for doing diffusion-based filtration and separation

in setups without channel walls, thus representing a sort of "open-space" analog to the H-Filter (which we dubbed the "O-Filter"). This is significant, as other groups in the past have attempted to reproduce such functionality using probe-type systems, and coming up with elaborate systems requiring a large number of apertures. Our conformal analogy shows that such elaborate systems are, in a sense, not required when one thoroughly understands the physics of diffusion at play in 2D microfluidic systems.

The analogy between the microfluidic surface shield and H-Filter is illustrated in figure 6.5.

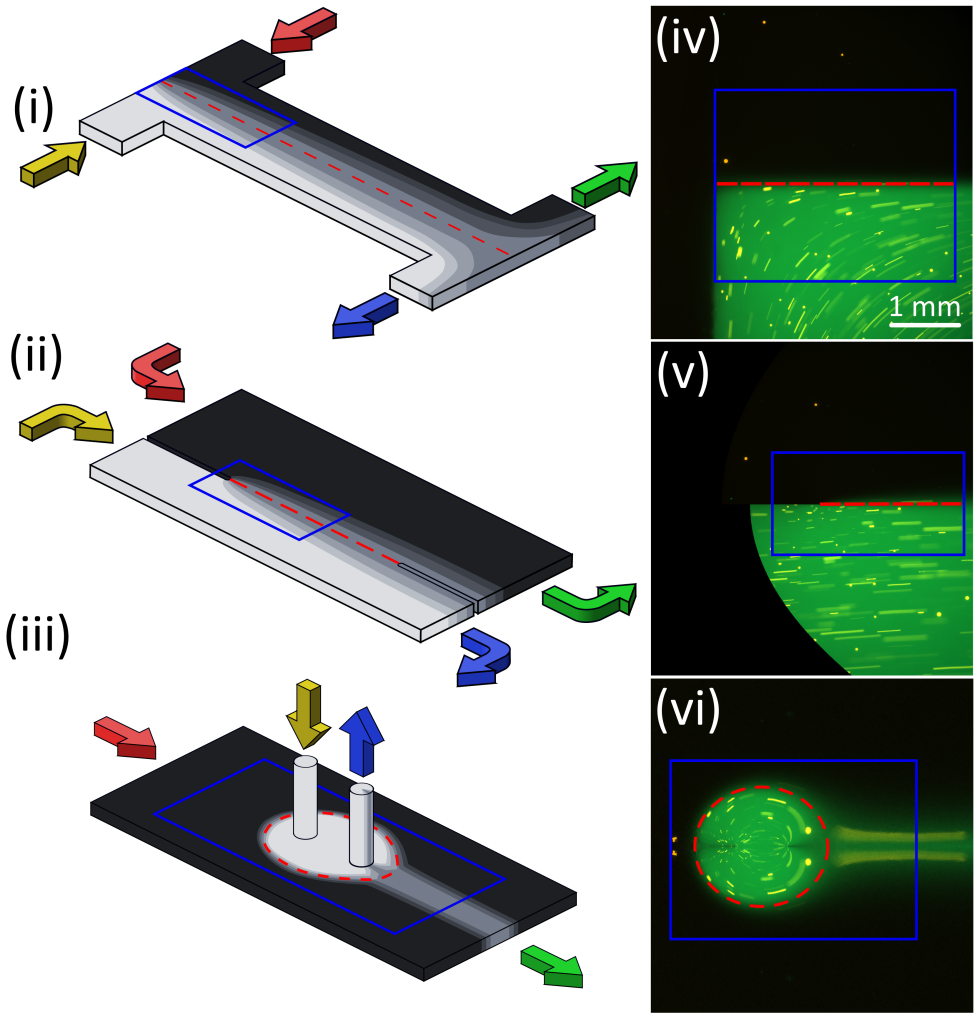

Figure 6.5 Analogy between microfluidic surface shield and H-Filter. Schematic illustration of flow and diffusion in an H-Filter (i), in the streamline coordinate problem for the microfluidic surface shield (ii), and in the microfluidic surface shield itself (iii). Experimental image of flow and diffusion in an H-Filter (iv) is transformed using conformal map to yield straight flow in the streamline domain (v) and flow in the microfluidic surface shield (vi), illustrating the analogy between the three domains.

6.10 Reabsorbtion for finite-sized patches

We have shown in section 6.8 how we can characterize the diffusive losses from the Rankine body in our experiments. In applications where the objective is to isolate a surface from an incoming flow, this diffusive exchange represents an "imperfection" to our shielding, which can be adjusted by modifying the Peclet number. We have also briefly discussed how this diffusive exchange could be exploited to generate open-space filtering systems.

In practical experiments where the objective is to isolate a reactive patch from an incoming flow, however, the actual exchange between the inside and the outside of the cloak can generally be completely negated. This is because our diffusion model considered the "worst-case" scenario where the entirety of the fluid injected by the point source is at a different concentration than the incoming flow. In a real experiment, the situation is likely to be very different.

In an experiment involving sensors or reactive surfaces, it is likely that both the incoming plane flow and the fluid injected by the point source will have zero concentration. The diffusive species will come not from the injecting point source but will diffuse from the the reactive surface to the flow. In the absence of a microfluidic surface shield, or when the system is turned "off", the flow will be a simple plane flow and the reactive patch will leave a tail of reagent that will be convected downstreams. The approximate shape of the tail can be estimated by using the known Green's function [154] [111]

$$G(x,y) = \frac{e^{\mathrm{Pe}x}}{2\pi} K_0\left(\mathrm{Pe}\sqrt{x^2+y^2}\right) \tag{6.3}$$

Where K_0 is an modified Bessel function of the second kind.

When the shielding system is turned on, the entirety of the tail can be reaspirated. In that case, it is sufficient to ensure that the entirety of the sensor or reactive surface is contained under the excluded volume, and that it doesn't overlap with the diffusion boundary layer.

In order to demonstrate this, we ran finite element simulations of the 2D convection-diffusion problem in a microfluidic surface shield system with a rectangular reactive patch located under the excluded volume. The reactive patch has no influence on the flow but is kept at a fixed concentration $c = 1$, while both the incoming and injected flow are at zero concentration. Using such simulations, we have shown that if the reactive patch is more than 2 or 3 caracteristic diffusion lengths from the boundary layer, the amount of reagent that "leaks out" of the shielding system is vanishingly small.

Examples of this situation are shown in figure 6.6.

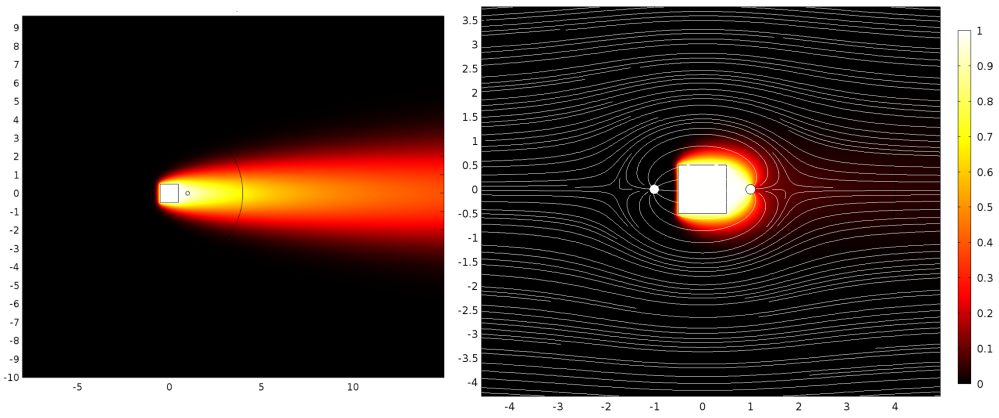

Figure 6.6 Microfluidic shielding of a finite-sized reactive patch. a) Concentration profile for a reactive patch in a plane flow for Pe = 10. b) The same reactive patch under a microfluidic surface shield, where the entirety of the wake is reaspirated (streamline overlaid in white for clarity)

In order to determine an analytical solution to this problem, we could find the image of the reactive patch in the streamline coordinate domain, then a Green's function would have to be convolved with a Kernel that has to be determined as part of the problem. This procedure is quite involved, however, in this case, it was sufficient to show that the exchange could be made exponentially small using simulations.

6.11 Transient aspects of the system

The proposed application for the microfluidic surface shield was protection of sensitive surfaces from an incoming flow (or conversely the isolation of a external flow from the wake generated by a reactive patch). Since the proposed experiments would involve turning the shield on and off, it was important to quantify the time scale associated with this switching, to determine how long it takes for the system to go from one state to another.

Because of the extremely low Reynolds numbers at play, (of the order of Re ≈ 0.001), we can approximate that the flow is established instantly as soon as the pump is turned on. The time scale for this establishment is approximately $t \approx \frac{\rho L^2}{\mu \mathrm{Re}} \approx 0.001s$. This very short timescale means that the establishment of the flow will be determined by the switching time of the syringe pumps, which is of the order of a second.

As for the establishment of the concentration profile, we find (theoretically and experimentally) that it was determined by the convection time $t_c \approx \frac{L}{U} \approx 15s$. This convective time scale is orders of magnitude smaller than the caracteristic diffusion time $t_d \approx \frac{L^2}{D} \approx 1.6h$.

The time scale which determines at what point the surface is isolated from the incoming flow is the time scale of establishment of the flow, which is about 1s determined by the switching time of the pump. Even though the concentration profile takes about 15s to reach steady-state, from the moment the flow is established we are ensured that the two regions are isolated from one another.

During experiments, while switching the system on and off, or while varying the ratio of injected fluid velocity to plane flow velocity, we saw that it was possible to use the system for generating chemical pulses that would then be carried downstream.

Another consequence of these different time scales is that when the microfluidic surface shield is turned off (or when the size of the shielded region is reduced by reducing the flow rate from the point source), the plane flow is established much faster than the concentration profile. In a situation where concentrated liquid was injected from the point source, this means that the footprint of the Rankine body remains there, and is then shed and convected downstreams. This behavior is illustrated in figure 6.7. This behavior could be used to generate regular trains of chemical pulses in a microfluidic channel, which could be useful in designing surface chemistry experiments involving frequency-dependent kinetics, or complex kinetics with time scales of the order of the second.

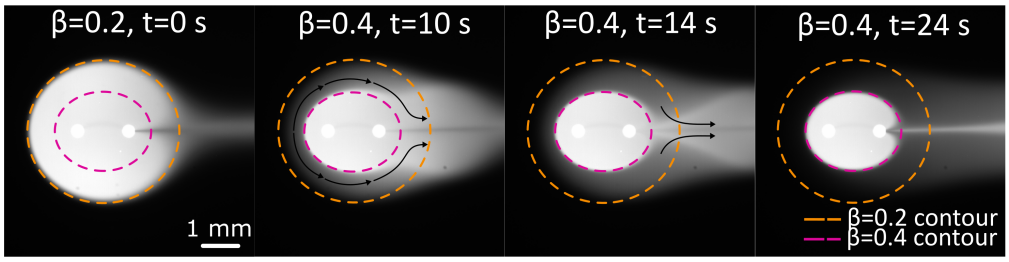

Figure 6.7 Generation of a chemical pulse with the microfluidic surface shield. At time $t = 0$, the system is in a steady-state, with a footprint highlighted in orange. The ratio of injected flow to plane flow is then instantly reduced. The new footprint, highlighted in purple, is much smaller, and all of the concentrated liquid that was in the area between these two regions is convected downstream, generating a single chemical pulse.

6.12 Discussion

The initial idea for the system presented in this section was to present it as a "microfluidic cloaking system", in analogy to cloaking systems in optics and other analogous domains. While presenting this work to reviewers, we ran into several critiques which eventually led to us changing the name of the system to better reflect its functionality. In this section we

briefly discuss these caveats as well as the implications for the technology itself.

One thing that was pointed out by reviewers is the fact that the surface shield we present is not omnidirectional, as opposed to many "cloaking" systems. This means that the system will only isolate the inner and outer region from one another if the flow is aligned with the source-sink doublet. In all other cases, there will be partial reabsorbtion, which will become greater as the system gets disaligned, as shown in figure 6.2. This critique makes sense if the system is to be viewed as an "invisibility cloak", but in the applications we propose, the systems are fabricated so as to ensure that this alignment is always respected. This is something that would have to be kept in mind in applications where the incoming flow is not something we control but something that could vary with time. In this case we could not just isolate a region from the outside flow without already having information about that flow.

Another critique was that our system wasn't actually shielding a rigid obstacle, but protecting a reactive patch that would be at the bottom of the channel. In "real" cloaking applications, the obstacle to be shielded would usually have an impact on the flow, while our reactive patch would still leave the plane flow undisturbed. A similar critique was connected to the fact that most cloaking systems involved some form of microstructured material with a variable parameter (for instance index of refraction), while our system did not have that. I believe these two are mostly semantic points, our original argument was that the flow serves as the "microstructured material" to cloak the concentration field, which in the absence of flow would be convected in the system. These critiques are mostly about whether or not our system can rightfully be called a "cloaking system", which in a sense is important, as branding it "cloaking" adds it to a pool of articles that can be cited by engineers in different fields who work on similar "cloaking" systems, but in another sense it is a point that is tangential to the real technological applications of the system, which we briefly covered in this section.

Another, more serious critique, was that the superposition of a dipole flow and a plane flow is something that has been known in fluid mechanics for a long time (and is presented in classic fluid mechanics textbooks such as Batchelor [20] or Lamb [44]). It was pointed out by reviewers that branding a flow profile that is well-known as a textbook example as a new invention and calling it "microfluidic cloaking" makes it appear as if there is more there than there actually is. I think there is some value to this critique, and it is important to be wary of the fine line between good branding and dishonest "salesmanship". I do believe, however, that there is significant technological value in the system that we presented.

In the first place, while superposition of dipole flow and plane flow is very simple on paper, the

technology we present allows for the generation of flow patterns that are perfectly described by potential flow formulation, and the arbitrary placement of flow singularities in this domain, which is something non-trivial and unheard of before, as far as I am aware. Moreover, beyond the simple generation of the flow pattern, we presented compelling cases for applications in surface chemistry, which themselves are not simple and require careful analysis. Finally, our analysis included in-depth discussion of diffusion in such a system, which is also something that is not trivial.

With all of that being said, a lot of published cloaking systems are of dubious value as technological objects. Very often, the value of these publications is either in showcasing thorough control of a phenomena through microstructured material, or making analogies between seemingly different areas of physics by making parallels between initially different systems of equations. This is in itself a valuable endeavor, but in this literature the fabrication of systems that solve a real technological problem sometimes is secondary to just reproducing results from classic optics papers.

This is not to say that the entire domain of cloaking is without value, but rather that our system has value beyond just being "true" cloaking or not. In the article, we presented a methodology for selective exposition of surfaces with applications in the domain of sensors, showed how to transfer filtering functionalities to 2D flow-field based systems, and showed a methodology for generating controlled chemical pulses down a microfluidic chamber. All of these functionalities were also achieved with systems that are relatively simple to fabricate and operate. At the end of the day, these applications all have the potential to have a significant impact in different domains of microfluidics, and would be worthwhile to investigate further, regardless of how the system is called.

CHAPTER 7 TECHNOLOGICAL APPLICATION - PIXELATED CHEMICAL DISPLAYS

7.1 Outline

The final technological application we present is Pixelated Chemical Displays (PCD). This system, initially fabricated and operated by Pierre-Alexandre Goyette, is in many ways the logical continuation of the work we introduced in our initial multipole article (as presented in section 3). The system consists in a periodic array of point-like apertures, injecting and aspirating fluid over a surface. The flow and concentration pattern generated by this system is a periodic array of polygonal cells, tiling the plane. The system thus acts as a sort of chemical analog to the pixel-based displays of computer screens, cellphones, etc.

This system is the largest integration and application of the principles of multipolar microfluidics. It could only happen at a point where the theory was extremely well understood, but more importantly at a moment when the principles of fabrications of such devices were mastered by my colleague Pierre-Alexandre.

The pixelated chemical display was published in Proceedings of the National Academy of Sciences (PNAS) in 2021 [19]. I refer the reader to the PNAS article, as well as Pierre-Alexandre Goyette's PhD dissertation [256] for a more complete discussion of the practical aspects of the device.

7.2 Contribution

The article related to this work [19] was written mostly by Pierre-Alexandre Goyette. I contributed the section on theoretical solution for the pixelated chemical display, parts of the supplementary material related to the theoretical analysis and handled communications with reviewers related to the theoretical aspects of the work. Pierre-Alexandre Goyette did the work of fabrication, took the experimental images, and handled the part related to analysis of the stability of pixelated displays (with help from Maude Tremblay who was doing an internship in the lab). My contribution to this work consists in the modeling of flow and diffusion in these systems, as well as the fact that the idea for the system grew out of our previous work with conformal transforms on multipolar flows.

7.3 Original Motivation

7.3.1 Multipole and Reconfigurable Microfluidics

Even before our initial work on microfluidic multipoles, there had been some work done around the idea of using arrays of point-like apertures to generate periodic concentration patterns over surfaces. In 2010, David Juncker's group at McGill used a 2 by 3 array of apertures to generate tunable concentration gradients over brain slices [207], the authors also showed how their system could be reconfigured to yield different concentration patterns. In 2016, IBM's research group showed how a linear array of source-sink pairs could be used to generate a comb-like pattern to stain breast cancer tissue slices [147]. Our 2019 Nature Communications article [15] showed how a rectangular array of apertures could be reconfigured to yield different concentration patterns at different times over a treated surface. All three systems are illustrated in figure 7.1.

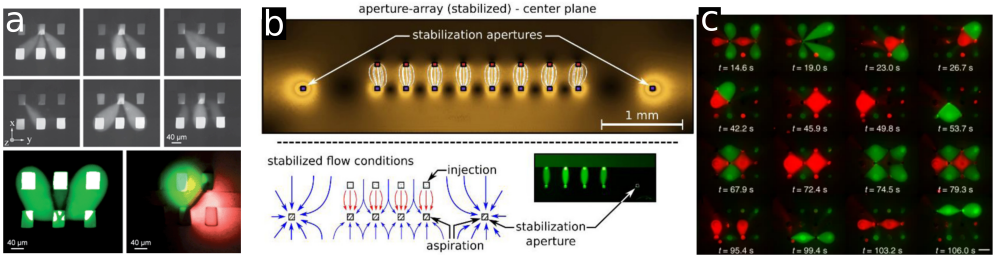

Figure 7.1 Precursors to the pixelated chemical display. a) Early reconfigurable probe-type system for the analysis of brain slices [207] b) Comb-type arrays for marking of breast cancer tissues [147] c) Our first published reconfigurable multipolar system [15]

Despite similarities in fabrication, we note that our system was one of the first to move away from the "scanning-probe" paradigm favored by other microfluidic-probe adjacent systems of the time. Up until that moment, The main idea behind all of these systems was to generate a chemical footprint that could then be scanned around a surface using a robotic arm. One of the main ideas introduced in our 2019 article, and explored further in this work on pixelated chemical displays, was that we could instead fabricate a system that is fixed in place, and modify the exposure of the surface not by scanning over it but by modifying the flow pattern the surface was exposed to. This idea of a reconfigurable chemical pattern over a surface formed the blueprint for what would become Pixelated Chemical Displays.

7.3.2 Polygonal Probes

The second puzzle-piece that opened up the way towards pixelated chemical displays was our discovery, early on, of the possibility of generating very stable polygon-shaped patterns. By applying simple power transforms of the form $f(z) = z^n$ on the concentration profile generated by a source-sink doublet, we found out that we could predict three types of radially symmetrical multipole shapes, illustrated in figure 7.2

These three "families" of radially symmetrical patterns could all be used to different ends. As we discussed in earlier sections, the flower-type (fig 7.2a) is the simplest type of multipolar geometry that can be used to simultaneously expose a surface to different chemical environments. Each "petal" can thus represent one condition in a multiplexed experiment. The "poppy" geometry (fig 7.2b) showcases complex mixing between the different injected reagents. It could thus be used to generate complex concentration gradients, or to study mixing between different diffusive substances, as was done in the so-called "microfluidic palette" [132]. The third type of radially symmetrical multipole we predicted in our initial article is the polygonal shape (fig 7.2c). We saw that by surrounding an injection aperture by a number of equally spaced aspiration apertures, the obtained concentration profile was a regular polygon, with the aspiration apertures at its vertices. This flow and concentration pattern has very sharp concentration gradients at its edges, and is a controllable, regular polygonal shape. We thus came up with the idea of using square-shaped polygonal "pixels" to tile the plane in a regular fashion.

In addition to suggesting its use as a unit to tile the plane, the polygonal multipole has the advantage of being much more stable to external perturbations than other multipolar shapes, as is described in section 7.10.

7.4 System Overview

The Pixelated Chemical Display (PCD) consists in a monolithic 3D printed block with a flat surface at the bottom of it. The flat surface is pierced by a regular array of apertures, themselves connected to holes in the side of the block by interior channels, which are then glued to plastic tubes and connected to syringe pumps (see figure 7.3). By correctly alternating injection and aspiration apertures, the system generates a flow pattern which is a tesselation of regular cells (or "pixels"), each of which is independent of the other and only interacts with it through a thin diffusion boundary layer.

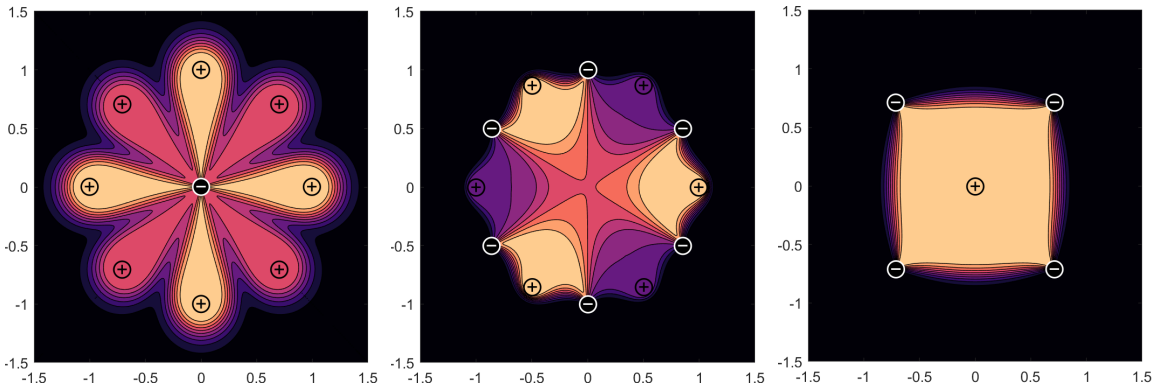

Figure 7.2 Families of radially symmetrical multipoles. a Flower-type, b “poppy” type and c Polygonal multipole

7.5 Fabrication and Operation

The system’s head was designed in CAD and 3D printed using a photolithography printer. Apertures were glued to plastic tubing which were then connected to manifolds that then connected to a smaller number of syringe pumps. In previous systems, each aperture was assigned to a single syringe pump but in Pixelated Chemical Displays it became necessary to have a single pump activate more than one aperture, due to the very large number of sources and sinks in the system. Space between the working surface and the PCD head was kept constant using spacers that were part of the 3D printed block (see figure 7.3a).

A schematic of the syringe pump and manifold setup is presented in figure 7.7, and we provide more discussion of the implications of multiplexing syringe pumps on the system’s operation in section 7.9.

CAD designs for previous multipole heads had been done by hand by Pierre-Alexandre Goyette, however this was not feasible for displays containing hundreds of apertures. He thus generated scripts that would automate the connection, within the PCD head, of each aperture to a side aperture that could then be glued to a tube. This allowed for flexible design of displays with varying geometries or number of apertures without requiring new immense design effort every time.

He did, however, glue every single tube by hand.

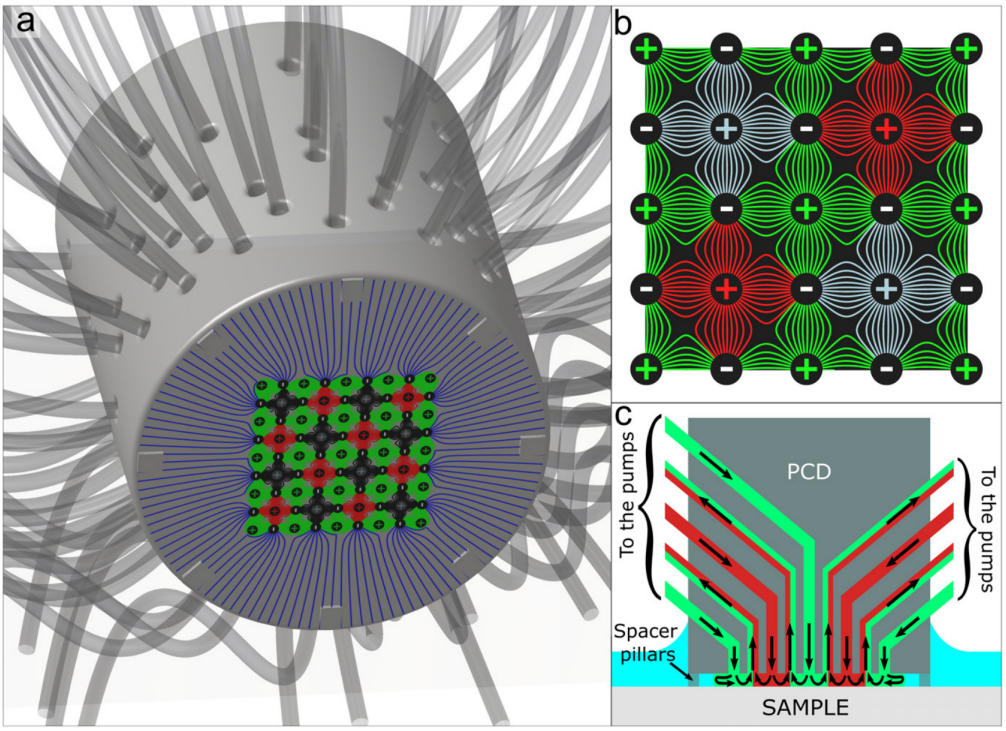

Figure 7.3 Pixelated chemical display system. a) Bottom view of the monolithic block b) Schematic of the aperture configuration, generating individual cells c) Cross-section of the system. Figure courtesy of Pierre-Alexandre Goyette, as published in [15]

7.6 Reagent Switching

Proof of concept experiments involving reagent switching were done with the Pixelated Chemical Displays. Selected apertures were grouped and connected to manifolds that were themselves connected to valves switching between two different syringe pumps, each with a different reagent. By correctly grouping pixels together, the system could be switched between 4 different chemical "images", with switching times of the order of the second. In this proof of concept experiment, the different configurations were hard coded in the system beforehand. True, complete, reconfigurability would require valves for each configurable apertures. The design of a complete, integrated system with valves and manifolds directly 3D printed within the PCD head was started and was supposed to be part of the project.

This design was to be part of a collaboration with Greg Nordin's group at BYU. This group has developed an expertise in 3D printers for integrated microfluidics [155]. The collaboration would have allowed the integration of large parts of the system in a single 3D printed head. Unfortunately, this part of the project had to be dropped because of the COVID pandemic of 2020-2021, which halted much of the in-person research being done at the time.

7.7 Analytic Solution for Diffusion in Pixelated Chemical Displays

In order to obtain an analytic solution for flow and diffusion in pixelated chemical display, we use a multi-step approach based on conformal maps to reduce the complex problem to a known one. The periodic domain is separated into square cells surrounded by symmetry boundary conditions, of which only a single one has to be solved to obtain the entire profile. A 4-vertices Schwarz-Christoffel map is used to "unwrap" one of these cells to a semi-infinite domain, where 4 apertures corresponding to the corners of the cell are distributed, with positions determined by the parameters of the map (see figure 7.4). The Schwarz-Christoffel map that links the square cell (z-domain) and the semi-infinite domain (w-domain) is given by the Jacobi Elliptic Sine

$$w = \mathrm{SN}\left(z|m\right) \tag{7.1}$$

Where the parameter m of the elliptic sine has to be determined using elliptic integrals (see [65]), and is given by $m \approx 0.02943$ for a square cell. Schematic illustration of the passage from the z-domain to the w-domain is given in figure 7.5.

The problem in the semi-infinite domain is very similar to other multipolar problems encountered previously, and the complex potential for it can be obtained as a superposition of point sources. If we identify the spacial coordinate of this semi-infinite domain as $w = u + iv$, the complex potential is given by

$$\Phi\left(w\right) = \log\left(w-1\right) + \log\left(w+1\right) + \log\left(w + m^{-\frac{1}{2}}\right) - \log\left(w - m^{-\frac{1}{2}}\right) \tag{7.2}$$

This complex potential can in turn be used to move to the streamline coordinate domain, where the solution for the concentration profile is the same as the one that was found in section 3

$$c = 0.5\left(1 \pm \mathrm{erf}\left(\mathrm{Im}\sqrt{\mathrm{Pe}\left(\Phi - \Phi_0\right)}\right)\right) \tag{7.3}$$

Where Φ_0 is the image of the stagnation point in the streamline coordinate domain.

7.8 Solution for Triangular and Hexagonal Pixels

Although maps from the semi-infinite plane to the interior of a square exist in terms of analytic (or semi-analytic) functions, no such map exists for triangles or hexagons. Such

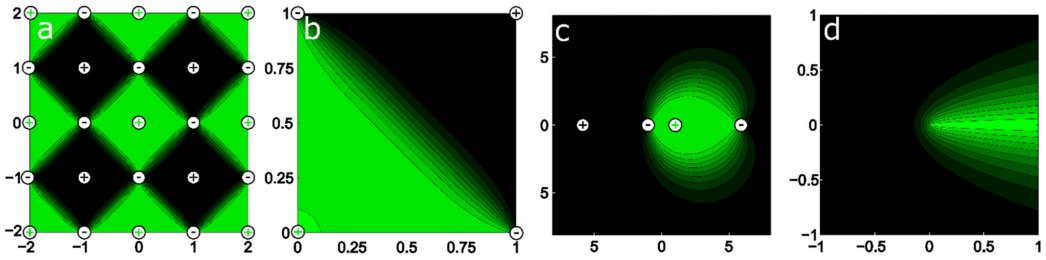

Figure 7.4 The different domains involved in the solution of the convection-diffusion problem for the pixelated chemical display. a) Periodic array of injection and aspiration apertures. b) A single square-cell taken from this same periodic array. c) "Unfolded" domain for a single cell. d) Streamline coordinate domain problem, equivalent to the one presented in section 3

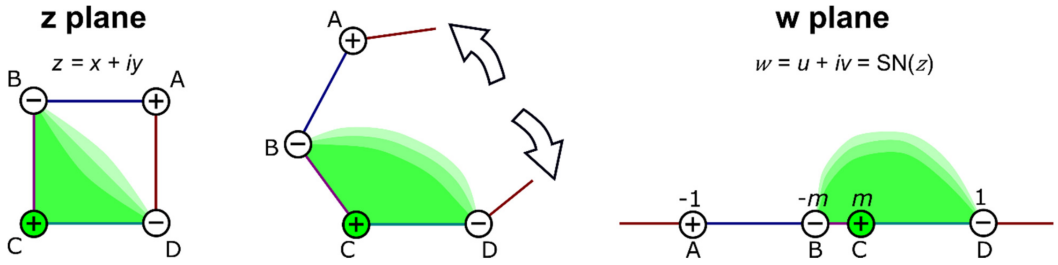

Figure 7.5 Schematic illustration showing how the 4-vertices Schwarz-Christoffel map allows us to pass from the closed square-shaped cell to a semi-infinite domain with 4 apertures

maps could be obtained by using numerical methods, such as those presented in [59] or [65], but the complexity of implementing these may prove to have diminishing returns when compared to simple direct numerical solution of the convection-diffusion problem. Otherwise, concentration profiles based on polygonal multipoles (such as the one shown in figure 7.2c) with an adjusted Peclet number may be a sufficient approximation for most cases.

7.9 Use of Manifolds

In the multipolar microfluidics systems we presented in previous sections, flow rates were fixed by assigning a single syringe pump to each injection or aspiration aperture. Because of this, small imperfections in the 3D printed head did not affect the flow, provided that the aperture did not become clogged or hydraulic resistance too high. However, in pixelated chemical displays, where there are dozens, if not hundreds of apertures, the feasability of assigning a single syringe pump to each aperture is greatly reduced. Instead, a system of manifolds is put in place, which enables the use of a single syringe pump to control several apertures at once. The downside of such an approach is that now, small differences in

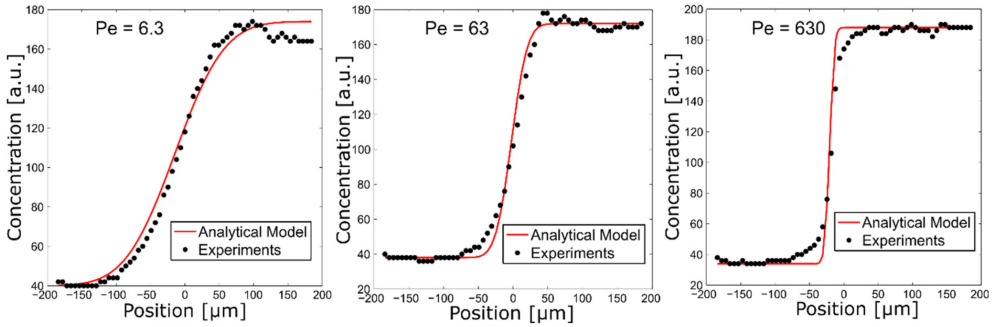

Figure 7.6 Comparison between analytic and experimental concentration profile for the diffusion boundary layer in pixelated chemical displays

hydraulic resistance between channels will lead to differences in flow rate in these apertures. The channels within the 3D printed head intrinsically have a lot of variability in their hydraulic resistance, due to the fact that we are working close to the 3D printer's resolution limit. This variability can be offset by adding a segment of plastic tubing of much higher resistance between the manifold and the 3D printed head (see figure 7.7). Doing so will ensure that the variability in resistance due to the 3D printer's resolution is small compared to the resistance of the tubing (which is much easier to control).

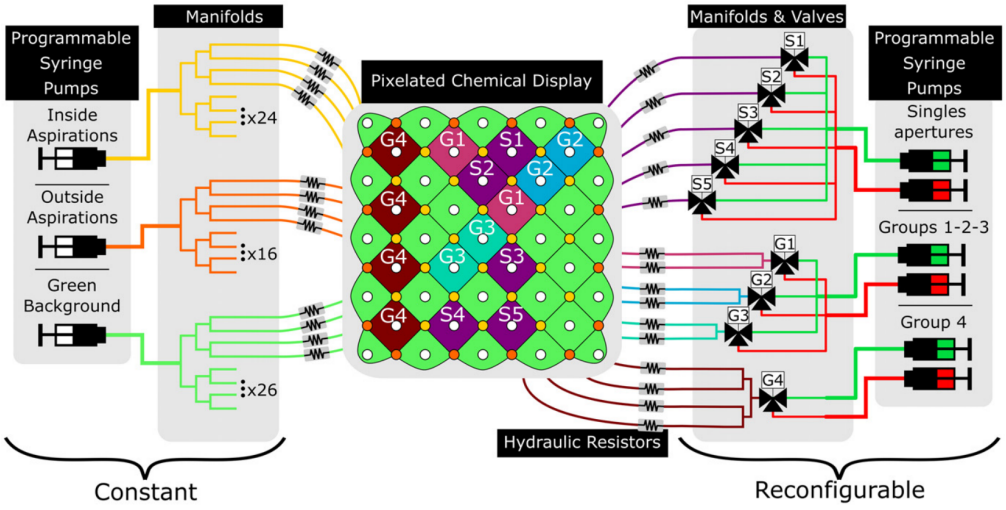

Figure 7.7 Schematic of the experimental setup for the pixelated chemical display. Individual syringe pumps are assigned to several apertures through a series of manifolds. Hydraulic resistances put between the manifolds and the 3D printed head ensure that the resistance of each channel is relatively constant and that the flow in each aperture is the same. Figure courtesy of Pierre-Alexandre Goyette, as published in [15]

Nonetheless, in these pixelated systems, the added variability in resistance makes it more

important to ensure that the flow pattern is relatively stable under small disturbances. Fortunately, the periodic arrangement of sources and sinks we present is indeed very stable under this type of disturbances.

7.10 Stability Analysis

Quantitative analysis of the stability of the Pixelated Chemical Display under variation of the flow rates was conducted by Maude Tremblay as part of her internship in the group. Finite element models for the 2D Laplace equation and associated convection-diffusion problem were constructed. Flow rates in each aperture was randomized by adding a bounded noise term to each, and a large number (around 1000 per condition) of simulations were run. The chemical footprint obtained in each simulation was compared to the expected footprint for the undisturbed system using morphological filters and segmentation algorithms. These simulations showed that the flow rate could be varied significantly within the PCD while keeping the error to a small area near the diffusion boundary layer (see fig. 7.8).

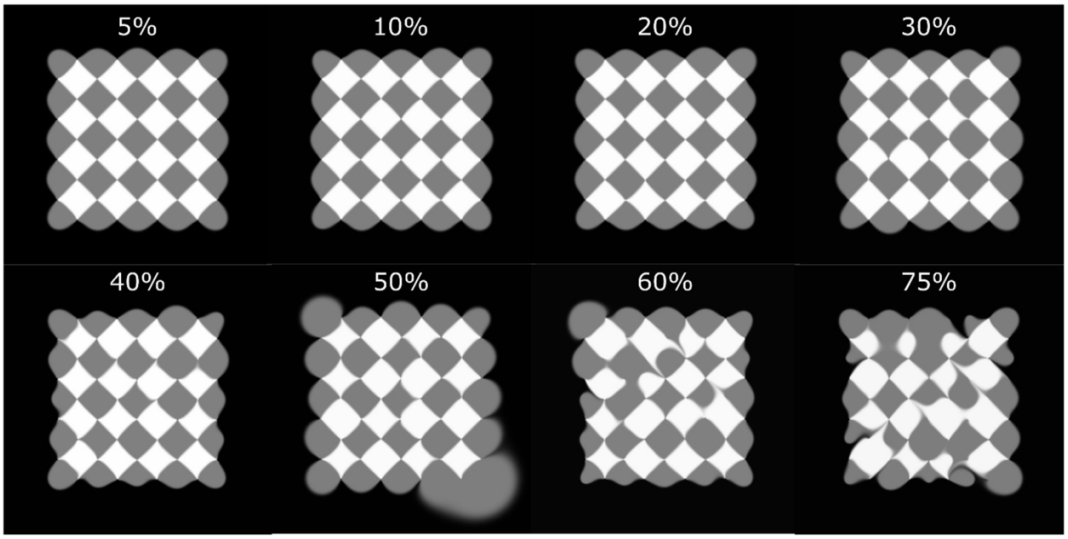

Figure 7.8 Effect of perturbation on flow rates in a Pixelated Chemical Display. Simulations were run for flow and diffusion in an 81-aperture PCD, with an error on the flow rate for each aperture. The figure shows one typical concentration profile for different error terms. Work done by Maude Tremblay under the supervision of Pierre-Alexandre Goyette

The simulations run for stability analysis used a noise term on the flow rate that was uniformly distributed through the system. Another "worst-case" scenario was investigated both experimentally and numerically by completely shutting off one injection and comparing the new profile to the undisturbed one, simulating the effect of clogging of a single aperture.

In this scenario, shown in figue 7.9, the disturbance was localized to the cell containing the clogged aperture, as well as a small disturbance in the boundaries of the surrounding cells, but left the rest of the flow and concentration profile largely unaffected.

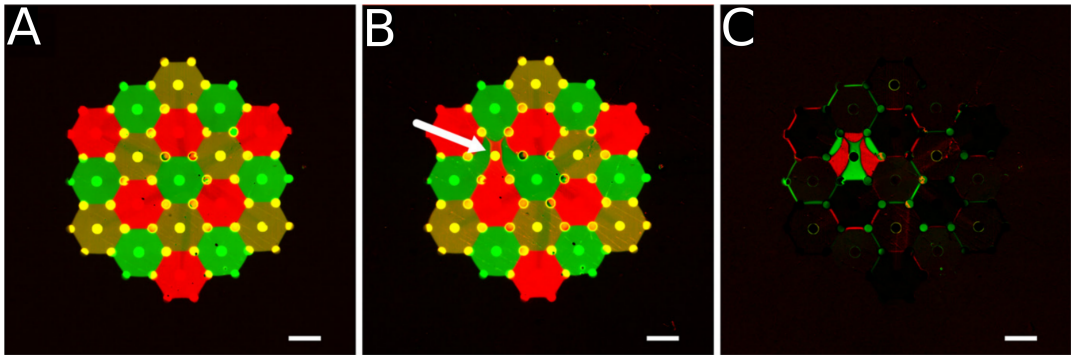

Figure 7.9 Experimental investigation of clogging of an injection aperture on a hexagonal PCD. A) Undisturbed concentration profile for a hexagonal array. B) The same array with an injection aperture turned off. C) Absolute difference between the two images. Figure courtesy of Pierre-Alexandre Goyette, as published in [15]

7.11 Hydrodynamic Flow Confinement

Another interesting characteristic of Pixelated Chemical Displays is the fact that they exhibit hydrodynamic flow confinement even in the absence of net inflow. For previous multipolar microfluidic systems (such as those presented in previous chapters), the only way to ensure that the system had a bounded footprint was to have a net aspiration that was bigger than the total injection rate in the system. This put a restriction on the experimental applications that could be explored, as the net inflow meant that the surface under analysis would have to be wet, to provide fluid to be aspirated. Pixelated Chemical Display are slightly different. Because of the periodic conditions on each cell, the only way for the system to be stable is if the net inflow of a single cell is exactly equal to the net outflow. If this isn't the case, the system loses its periodicity and the footprint collapses (see figure 7.10).

The only exception to this rule is the pixels on the contour of the device, which can operate with net inflow, net outflow, or equal inflow and outflow, yielding perturbation of the contour but leaving the inside of the system relatively undisturbed. Examples of systems operating with different net flow rates are shown in figure 7.11.

This means that the entire system can exhibit hydrodynamic flow confinement without requiring aspiration that is superior to injection, which in turn enables it to function over dry surfaces, or upside-down in a "fountain"-type mode of operation. Lifting up the requirement

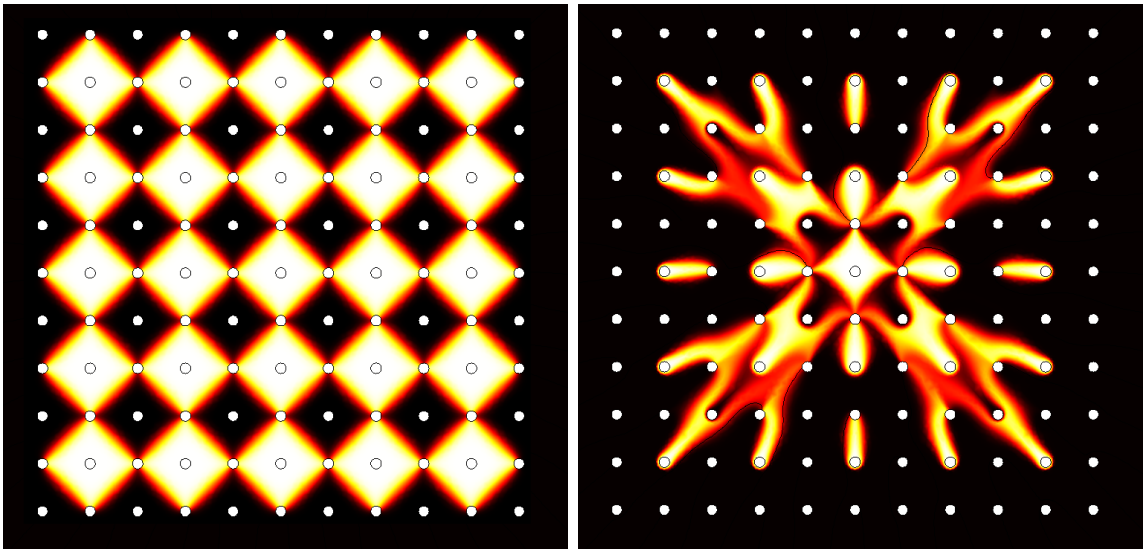

(a) (b)

Figure 7.10 Finite element simulations for the effect of net inflow on arrays of microfluidic pixels. a) Array in which injection and aspiration apertures are balanced, generating a periodic tesselation of cells. b) Array where aspiration is four times the injection rate, leading to the collapse of the pixels

for wet surfaces thus opens up the door to a wider range of applications for the system.

7.12 Transition to Pressure Pumps

For every multipolar system presented in this thesis, up to the Pixelated Chemical Display as it was published in 2021 in PNAS [19], syringe pumps were used to actuate the device. Syringe pumps have the advantage of precisely fixing the flow rate, and thus in smaller systems they allow us to work without having to match hydraulic resistances (provided there is no significant clogging). However, when designing larger integrated systems such as the PCD, syringe pumps have several downsides which become apparant.

Notable among these downsides is the imprecision of syringe pumps at very low flow rates, which puts a floor on the flow rates in these continuous streaming systems and thus leads to very high reagent usage (as well as barring us from exploring lower Peclet regimes).

The principal of these downsides, however, is the necessity for a large number of pumps, which makes the systems increasingly cumbersome and expensive as they are scaled up. This problem is partially solved by efficient use of manifolds, which allow us to use a single pump to activate several different apertures, but even in such a system, a different syringe pump

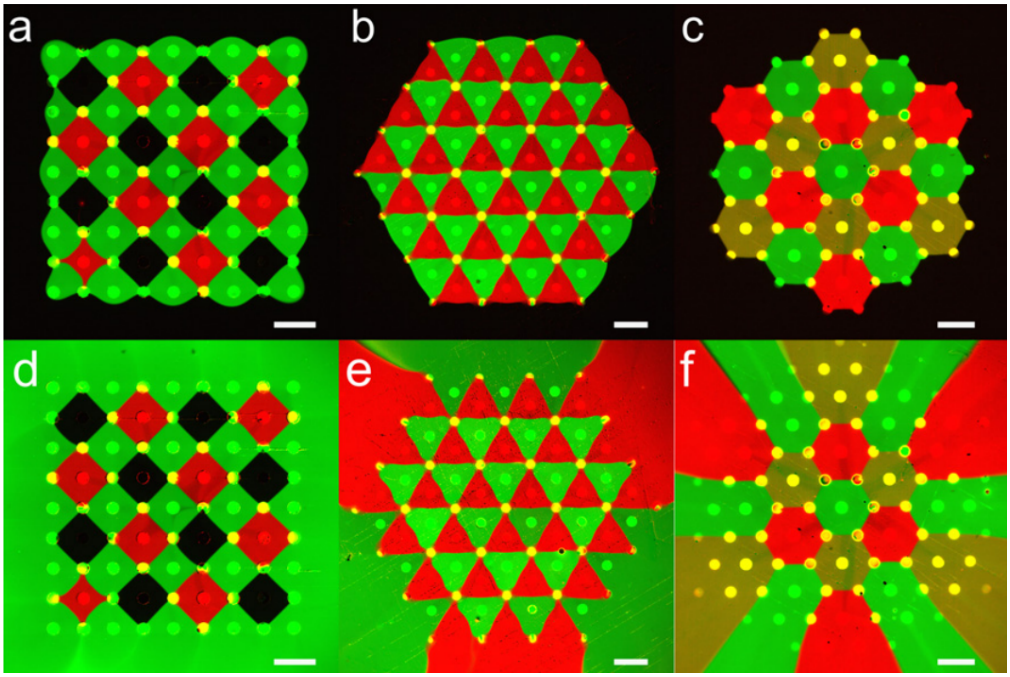

Figure 7.11 Pixelated chemical display operating in different regimes. a-c) PCDs operating with equal injection and aspiration d-f) The same systems but with superior injection on the contour. We can see that in both cases, the interior of the system remains undisturbed and the confinement of each pixel is preserved. Figure courtesy of Pierre-Alexandre Goyette, as published in [15]

has to be used for each different reagent. Transition to pressure pumps would enable, at least in theory, the activation of a system with an arbitrary number of apertures and reagents with only two pumps, one for injection and one for aspiration.

Transition from syringe pumps to pressure pumps is thus a necessary step towards the development of these systems for larger-scale applications. Some preliminary work has been done by Pierre-Alexandre Goyette and Dina Dorrigiv and can be found in the discussion of Pierre-Alexandre's dissertation [256], as well as more recent articles on applications of PCD [139].

7.13 Applications

The main area of application for pixelated chemical displays is in designing highly multiplexed experiments on surfaces. The system can expose a single surface to a large number of different environments in a single experimental step. Reconfigurability of the system also means that single areas of a surface can be sequentially exposed to different conditions.

A platform was developed by Dina Dorrigiv for the application of pixelated chemical displays to the treatment of 3D tumor models [139]. Spherical tumor tissues, called spheroids, were cultivated in arrays of wells. The array of wells is then exposed to different drug treatments via a pixelated chemical display. The same system was also used to sequentially expose spheroids to different dyes, as a proof-of concept demonstrating how the same spatial area under the pixelated chemical display can be reconfigured during the experiment. Such a multi-step experiment could eventually be used to study synergistic effects between different drugs, as a way of testing a large number of combinations in a single experiment. Results from Dina Dorrigiv's paper are shown in figure 7.12

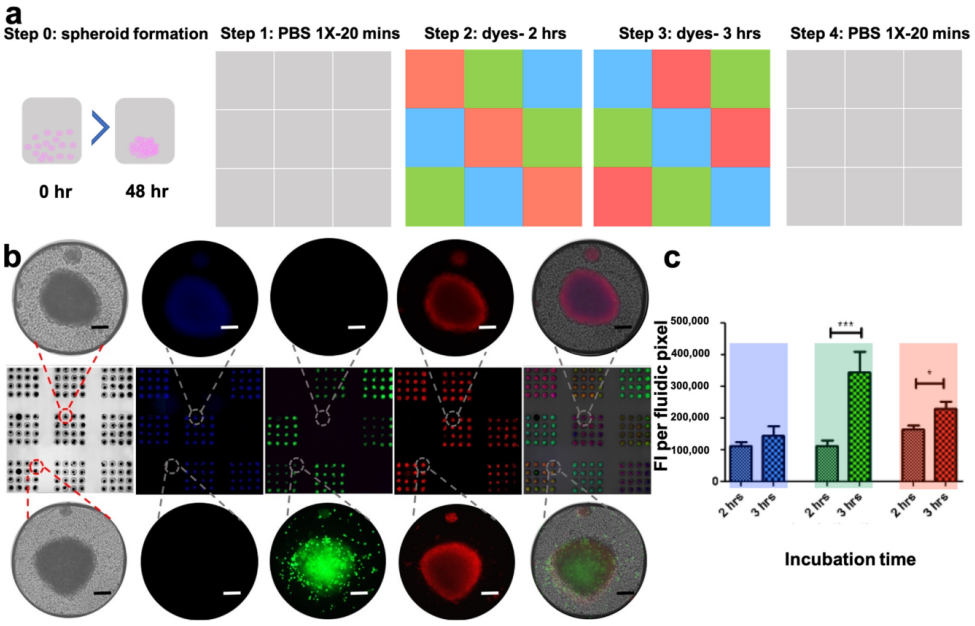

Figure 7.12 Multiplexed staining of spheroid tissues using pixelated chemical displays. a) Schematic of the multi-step experiment. b) Microscopy images of the stained spheroids c) Quantification of fluorescence intensity for each condition. Figure courtesy of Dina Dorrigiv, as published in [139]

7.14 Analogy with other existing systems

Pixelated chemical displays show really close functional analogies with other previously existing systems which we briefly mention here, namely blood flow in the choriocapillaris [165], as well as the "five-spot configuration" for oil extraction from porous soils [35]. Highighting these analogies serves two purposes. The first purpose is that this points the way to publications in other fields of science where similar problems have been solved, and which could be exploited to better understand the pixelated chemical display. Secondly, these analogies

open up the way for new applications to pixelated chemical displays, which could eventually be used as micromodels for either of these two systems.

7.14.1 Blood flow in the choriocapillaris

The Choriocapillaris is a semi-planar membrane that serves to irrigate the human retina. It is composed of a dense mesh of capillary vessels held together by rigid connective tissue. Irrigation in the choriocapillaris happens through regularly spaced apertures that inject and reaspirate blood in a regular pattern. The flow pattern thus obtained is exactly analogous to flow in the pixelated chemical display, with the exception that the apertures are arranged in a configuration resembling a uniform voronoi tiling rather than a square or hexagonal tiling. Illustration of blood flow in the choriocapillaris is shown in figure 7.13

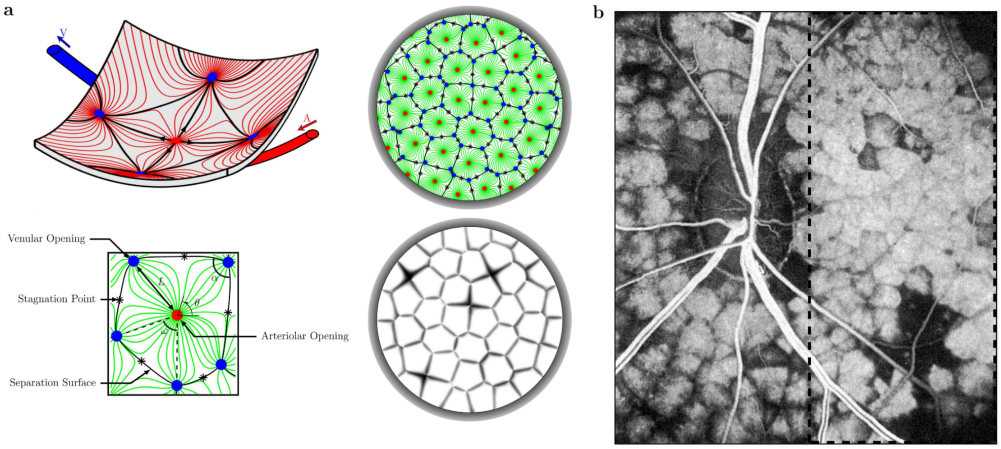

Figure 7.13 Blood flow in the choriocapillaris. a) Schematic representation of the flow pattern in the membrane. b) Fluorescence image of a human choriocapillaris. Taken from [165].

This configuration makes a lot of sense in light of what we have shown previously. We have seen in previous sections how clogging or irregularities in the flow rate of individual apertures only leads to very localised disturbance in the flow and concentration pattern in pixelated chemical displays. The same conclusion can be drawn in the choriocapillaris. Such a configuration for an irrigation system makes sense evolutionarily, as blocking of individual capillaries will potentially lead to problems that are localised, and have little risk of causing a failure of the entire retina.

Such analogies suggest the use of pixelated chemical displays, or similar systems, as micromodels for the choriocapillaris, which could eventually be used to study pathologies related to the retina, such as age-related macular degeneration (AMD).

7.14.2 Oil recovery with the five-spot configuration

We also briefly mention the so-called "five-spot configuration" used in oil recovery, for its very close analogy with the pixelated chemical display. In hydrocarbon recovery applications, arrays of wells are scattered over a planar region and water is injected through the soil, displacing the oil which is then reaspirated by aspiration wells. The configuration of injection and aspiration wells is exactly the same as the configuration of injection and aspiration apertures in the pixelated chemical display, albeit on the scale of the meter rather than hundreds of microns. Flow in such applications is complicated by the imiscibility of oil and water, which leads to viscous fingering instabilities. Eventually, viscous fingers "break through" the aspiration wells, and whatever oil was left in the cell is then unable to be recovered, which can make the method very inefficient, depending on the length and time scale of the instability. Illustration of the five-spot configuration, as well as experimental images from Hele-Shaw cell models, are shown in figure 7.14.

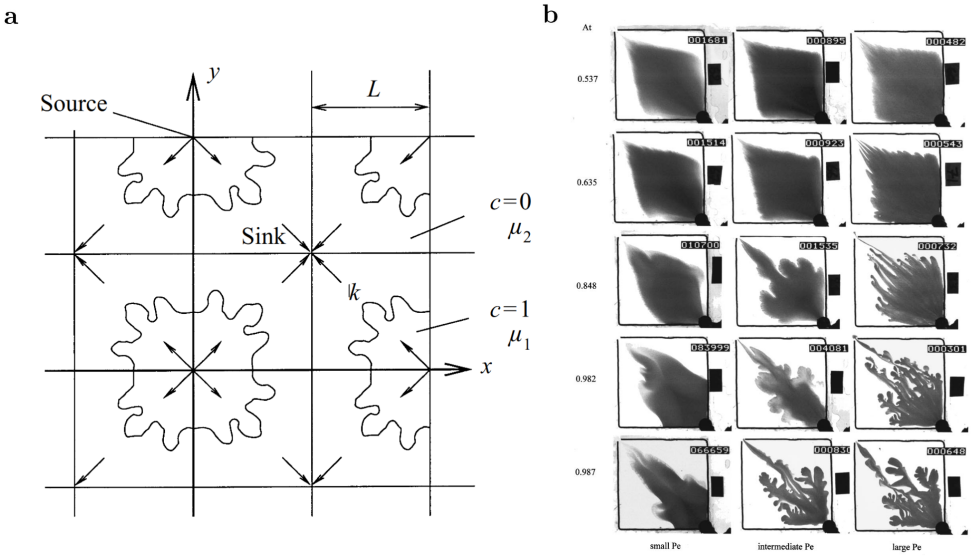

Figure 7.14 Oil recovery in the five-spot configuration. a) Schematic of the source-sink arrangement, from [35]. b) Experimental images of the water-oil pattern at breakthrough for different values of the important dimensionless numbers, from [257]

7.15 Limitations

We conclude this section with a brief discussion of the limitations of the pixelated chemical display technology. Pixelated chemical displays provide a stunning display of the control we have over planar microflow systems, both on a conceptual level and on a fabrication and

operation level. In this regard, they are somewhat analogous to Quake lab's microfluidic RAM [7], in that they serve more as a demonstration of our control than as a system that solves an immediate need.

Pixelated chemical displays open up the way for highly multiplexed experiments on surfaces, but they do so at the cost of systems with intricate 3D printed parts, expensive syringe pumps, etc. In addition, true reconfigurability in these experiments comes at a cost. Most of the proof-of-concept experiments we have realized did not have complete reconfigurability (in the way a regular LCD screen would), but rather had reconfigurability between different states that were "hard-coded" within the device. In this manner, completely reconfigurable systems have not been accomplished yet, and would require complex manifold and valve systems, while "semi-reconfigurable" systems come at the cost of additional design time for each individual experiment, which moves the system away from a "plug-and-play" simple solution.

In all of these cases, the question to be asked is not "does this system solve such or such problem", but it should always also include "can the problem be solved in a simpler way". A large number of problems can be solved by simple systems, such as lateral flow assays, and in cases where a lateral flow assay is sufficient, a lateral flow assay should probably be used.

In cases where multipolar chemical displays still offer advantages, such as the work on cell pathways done by previous member of the group Pierre Claperton [138] and current work by Maude Proulx in the group, it is also important to note that "flower"-type configurations are often much simpler and straightforward than 2D pixel arrays. Square pixels have the advantage of being more impressive to look at, and strike the imagination with their analogy to real LCD screens, but multiplexing between a small number of conditions or generation of controllable gradients may still be better done with simpler multipolar configurations, such as those shown in sections 3 and 4.

CHAPTER 8 GENERAL DISCUSSION

I conclude this dissertation with a short discussion on the possibilities and limitations inherent in the presented work. Several of these discussion points have been mentioned in previous sections, or in the associated publications, but I felt it was still relevant to compile the more general points in one section.

I begin with discussion regarding the analytical models themselves, then move on to discussion of the field-based microfluidic technologies directly connected to the presented models, then end up on a very brief discussion on the field of microfluidics at large.

Some of the points I mention in this discussion may seem to go in a different direction than what I have argued in the rest of this document, or in previous articles or publications. My point here is not to undermine the work that was done, but rather highlight tensions that exists within this work and within technological research in general. I hope that by providing opposing arguments and letting them exist side-by-side, I can present a more complete view of what I believe are really interesting and complex questions, in a way that we can rarely do in normal scientific publications.

8.1 Relevance of analytical models

8.1.1 Why do analytical modeling?

The first thing I want to discuss is the relevance of using analytical models. Why should we get interested in "analytical solutions" in the first place, especially in an era where numerical solutions can be implemented readily and run in a matter of seconds (especially for elliptic problems like the ones we are dealing with)? In previous sections, as well as in the articles published throughout my PhD, I have made several relatively straightforward arguments for this. These justifications in favor of analytical models have included direct access to the scaling behavior of the solution in terms of its physical parameters, extensibility to other geometries, as well as the highly multiscale aspect of the problems at hand, which warrants special treatment and runs the risk of making simulations very expensive if not treated properly. In this discussion section, I want to make a more nuanced point, since I believe that the question is more complex than it might seem at first.

I believe that, while analytical solutions do have their share of utilitarian advantages, these advantages are often not the only reason why we pursue them. A part of the interest, I believe, is also aesthetic in nature. Having a closed-form solution to a problem, especially

one that can be written concisely, feels good, and gives one the impression that we have mastery over that problem. It is, in many ways, more pleasing and "neat" than pages and pages of numerical data, as it presumably says a lot with very little.

As far as utilitarian problem-solving goes, the analytical approach may not always be the most straightforward one, or even necessarily the most useful one, and if our aim is just to solve a specific engineering problem for a concrete application, numerical methods may end up being more useful. Of course, we are not just doing this sort of work to obtain quantitative results, but are also driven by scientific curiosity.

It is still important to keep track of what we are solving for and why we are doing it, lest we end up solving very complicated problems that have very little relevance.

8.1.2 What counts as "analytical" solutions?

The question of the use of analytical models is further complicated by the fact that some problems blur the line between what counts as "analytical" and what doesn't. An example of such a problem could include complex obstacle problems where the solution has to be expressed in terms of Fourier series, with coefficients determined through iterative processes [45] (see figure 8.1). Other examples of problems that blur the line between numerical and analytical could include Green's function problems where the solution is obtained through numerical convolution of a known kernel [111], Wiener-Hopf methods where the solution is expressed as the inverse Fourier transform of a known analytical expression [108], or problems involving conformal maps where the map doesn't have a closed-form solution and has to be obtained using iterative methods [59].

In all of these cases, the search for a solution to the problem can still have scientific interest, and be worthy of being pursued, but a lot of the rhetoric that we use for selling analytical work as "cleaner" or "more useful" becomes blurred, especially in the case of elliptic problems where the solution through 2D finite difference methods or 2D finite elements methods may be more straightforward.

It is also worth noting that we have, somewhat arbitrarily, decided that 2D depth-averaged flow and concentration maps are what counts as a "complete analytical solution" to the transport problem at hand. 2D flow and concentration maps have the advantage of being readily comparable to microPIV and fluorescence microscopy images directly, which adds to the interest. However, we have neglected much of what happens in the z dimension, where a lot of the physics that is relevant to the problem happens (see section 5.11). In this way, what can be called a "complete analytical model" is somewhat loose, and can include, depending on

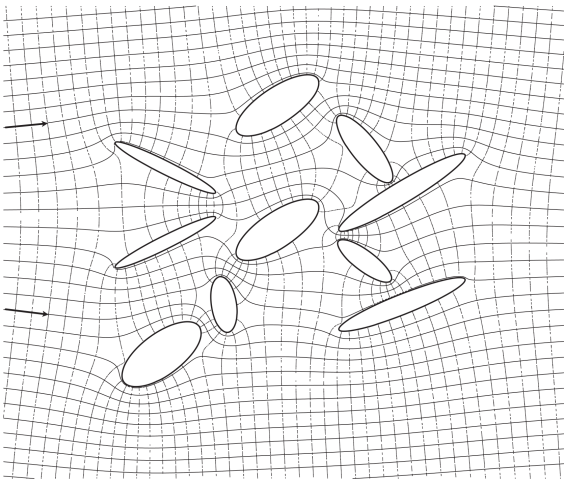

Figure 8.1 Flow field around obstacles in a 2D aquifer, such a flow-field is obtained using series solutions where the coefficients have to be determined using iterative methods. Taken from [45]

the situation, a range of very different tools, including 1D scaling behavior, 2D maps averaged along one direction for simplified geometries, full 3D solutions that may or may not involve symmetries, etc. In the case of the current work, various iterations of "complete theoretical descriptions" of the systems at hand have been presented over the years [124] [133] [15] [16], which itself is a bit strange (how strong is a claim to a "complete analytical model" if every subsequent publication showcases an "even more complete model"?). There also remains somewhat of a gap between the practical problems that are being solved and the answers that this "complete theory" is providing.

8.1.3 How is this applied in the present work?

The main advantage of our models has been in helping us imagine and predict new systems quickly. Once we had a model for diffusion in microfluidic probes, and the means to transform the solution using simple maps, it became pretty straightforward to then play with a number of different possible maps and thus predict new systems to be fabricated. In this way, the quantitative aspects of the theoretical model were of less importance than the use of them as ways to imagine new systems.

Thinking in terms of arrays of apertures and ways to transform them led us, very early on, to the idea of the pixelated chemical display. However, the solution for convection-diffusion in a rectangular array of apertures requires the evaluation of complex elliptic integrals, which are evaluated using iterative methods that are quite slow. The analytical solution presented in 7.7

also only takes into account cases where all of the apertures are perfectly mass-balanced, and doesn't allow us to model what happens at the edge of the PCD, or what happens when there are imperfections in the flow rate. For most of this analysis, 2D finite element simulations were used instead. Solving the convection-diffusion equation using 2D finite element methods for most of the systems presented in this work only takes a couple of second and remains a useful tool for geometries that don't possess obvious symmetries.

Moreover, the systems we have been working with operate in extremely high Peclet regimes, where the "pure convection" solution is usually sufficient. In the case of the work presented here, in almost all cases we had to make an effort to lower the Peclet number experimentally, in order to get concentration profiles that we could actually compare with the theory (otherwise we would get gradients that too sharp when compared to the spatial resolution of the fluorescence images). In applications involving staining or reagent multiplexing, the gradient at the boundary layer is usually excluded from the relevant domain anyways, and we are working within the "constant concentration" area. In all of these applications, knowledge of the pure convection solution combined with the fact that the boundary layer scales as $\sqrt{\mathrm{Pe}}$ is probably sufficient for most practical purpose. There have been examples of applications of multipolar microfluidic systems where the concentration gradient is important (for example studies of chemotaxis using microfluidic quadrupoles [143]), but even in these cases, 1D knowledge of how the gradient scales with Pe was sufficient.

In realistic cases, even running the syringe pumps at the lowest possible flow rates, the concentration gradients in the 2D plane are extremely sharp and can usually be neglected. This may change in future applications involving pressure pumps, which could get to much lower flow rates. Working at these lower flow rates would also mitigate the problem of high reagent consumption, at the cost of increasing the size of the boundary layer somewhat. There might thus be some optimisation warranted here, which models can help guide.

Applications similar to the microfluidic palette [132], where a system is used to generate complex, multi-substance gradients, may still benefit from complete description of the 2D concentration profile, in a way where simple scaling may not be sufficient. The "poppy" geometry, which we have presented a couple of times throughout the work (see for example figure 7.2b), may be useful for this sort of application. However, there hasn't been a lot of work in this direction as of yet.

8.1.4 The true advantages of theoretical modeling

All of that being said, I do believe that analytical modeling has a place in a design pipeline, even beyond pure scientific curiosity. The main advantage that this sort of analysis gives

us, I think, is the ability to make analogies between different fields of science. The initial impetus for the project was in finding out the analogy between flow fields in 2D Hele-Shaw cells and 2D electric fields. This discovery opened up the way to using a host of tools that had already been developped for classical electrostatics, and apply them to the domain of microfluidics. Further down the line, I investigated the analogy between 2D Hele-Shaw flow and 2D Darcy flows, which had been highlighted early on in the work but hadn't been completely explicited yet. This analogy enabled the creation of links between the current work and various domains of groundwater research, which I have highlighted throughout this document. In both cases, the advantage of rigorously highlighting similarities between different domains is twofold. First, it allows us to directly use a wealth of known results from other fields, saving a lot of time and possibly making us think of things we wouldn't have in previous ways of thinking. Second, it opens up the way to new applications of the technologies we are fabricating, as I have highlighted in sections 6.7 and 7.14. This sort of analogy-making between different seemingly unrelated fields of science is probably the biggest advantage of strong theoretical models, more so than the determination of precise quantitative data (which numerical methods can often do just as well).

Simple but far-reaching theoretical models also determine the landscape of what sort of systems can be imagined. Thinking in terms of arrangements of sources and sinks in 2D, and in terms of transforming space, has enabled the design of new systems that couldn't even be conceived of in the old "networks of microchannels" paradigm. In this way, theory determines the field of "what can be thought of", and new tools open up new ways of thinking, which is another advantage that goes beyond the simple determination of quantitative data.

A final advantage of theoretical modelling is that, if done properly, it can make us more aware of the range of validity of our models. In order to reach the solutions that we have been working with, we have been making a number of approximations, namely

- The system is in a steady state
- Inertial effect are negligible everywhere in the domain
- The thickness of the Hele-Shaw cell is much smaller than the other relevant length scales in the problem
- The Hele-Shaw cell has uniform depth throughout
- Apertures are point-like, and the interesting parts of the flow are not underneath the apertures

- Solutions are dilute, such that concentration doesn't affect flow properties and diffusivity is constant
- Concentration is uniform along the depth axis
- The effect of any wall within the domain can be neglected, so that we can use potential flow description
- Knowledge of the 2D flow and concentration profile is sufficient to give us meaningful knowledge of what happens in surface reaction applications (more on that in section 8.2.1)

Working from first principles hopefully gives us a better understanding of all of the approximations that we are making, and thus of the range of applicability of the results we obtain. This is to be contrasted to some of the very "plug-and-play" CFD packages that exist nowadays, where one can draw the geometry, add a physics modules picked from a library, press "play" and obtain numerical results. In these cases, a similar number of important decisions and approximations are being made, but they are sometimes hidden from the user for the sake of usability, and this can sometimes lead to questionable results if the user isn't being careful. Likewise, understanding the approximations and limitations of the systems we are working with enable us to then use numerical tools more efficiently, for example in allowing us to show that an equivalent 2D problem yields the same information as the bulkier, full 3D multiscale problem.

At the end of the day, experimental, numerical, and analytical tool all contribute to a larger toolbox and should work hand in hand to tackle concrete problems.

8.2 Extension to problems involving other phenomena

Discussion of the approximations we have been making in developing our flow and concentration maps brings us to another point which has been raised several times about the current work, namely its applicability to problems involving different physics (multiphase flow, complex reaction, transient aspects, microstructured chambers, variable gaps, etc). In a sense, the problems we have been analyzing are maybe some of the most elaborate ones in which it is possible to obtain a simple closed-form solution valid over the entire domain. We are solving for convection-diffusion in a 2D domain with very complex flow patterns and obtain an expression for the entire concentration field, which in itself is quite impressive. Obtaining this simple closed-form expression hinges on being able to use conformal maps, which itself requires all of the approximations listed in section 8.1.4 to hold. Most of the time, extension

to problems with different physics will mean that the closed-form solution breaks down and the problem has to be studied from the start. These extensions may also mean that we need to rethink what we are looking for as an "analytical solution", since complete flow and diffusion profiles may no longer be obtainable.

We discussed some other physical problems that come into play in 2D flow field applications in chapter 5, particularly subsection 5.11. We briefly list some extensions to problem with different physics here.

8.2.1 Interaction with surfaces

Most of the applications that have been proposed for multipolar microfluidic systems, as well as pixelated chemical displays, involve interaction with either a reactive surface, or some sort of porous reactive slab. In most of these cases, the "depth-average" approximation breaks down and it is important to consider what happens in the third dimension. The most complete solutions for such problems are often 1 or 2-dimensional solutions along the other axis, where flow is unidirectional and the depth direction is one of the independent variables. Examples of such solutions include the analysis of transport from a reactive patch [107], or of the interface between Stokes flow and porous flow [238]. These two problems, and related solutions, are illustrated in figure 8.2.

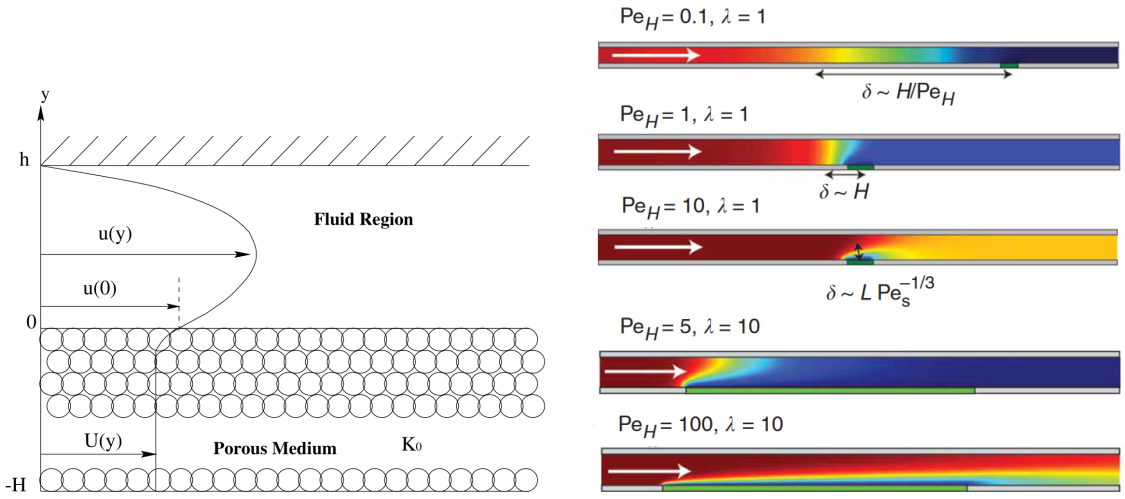

(a) (b)

Figure 8.2 2D solutions to transport problems along the vertical direction. a Boundary condition between Stokes flow and Darcy flow in a channel, taken from [239], b Multi-parameter analysis of the wake behind a reactive patch, taken from [113]

In many cases, while we are not in possession of a "complete solution", knowledge of the 2D convection-diffusion solution without surface reaction can be combined with knowledge of the unidirectional surface reaction problem to give us a good idea of how a system will behave. The same can probably be done for interfaces with porous medium. In cases where the porosity of the medium is very low (which is the case for many tumor samples), the problem can be decoupled between a 2D convection-diffusion problem in the Hele-Shaw chamber and a pure diffusion problem in the tissue.

8.2.2 Multiphase flow

A natural extension of the work presented in the dissertation seems to be problems of multiphase flow in Hele-Shaw cells. The solution procedure we have presented for flow and diffusion, with its use of conformal maps, is actually applicable to a small subset of multiphase flow problems where the interface is relatively controlled. Potential flow formulations have been made to approximate flow in and around droplet ensembles [126], and a combination of potential flow formulation and conformal maps have been used to model flow in self-coalescence modules [38], with analogies to viscous fingering.

However, in most applications involving multiphase flow in Hele-Shaw cells, the interfaces are unstable, and fingering instabilities appear [31]. Theoretical analysis of such unstable interfaces requires a machinery that is different from the one we exposed in this thesis, but the problem has been studied at length elsewhere [32] [39] [33].

8.2.3 Uneven channel cross-section

The solutions we have presented require that the depth be constant over the entire Hele-Shaw cell. Extension of these results to problems with varying depth could be possible. We list two avenues for further work here.

First, solutions to flow in large chambers segmented in different areas of constant depth are probably obtainable. Similar solutions exist in [45] for Darcy flow segmented in regions of different permeability. Such a solution procedure is probably transferable directly and would allow for the theoretical determination of flow in complex structured chambers. Since the flow determined this way is still a potential flow, the entire procedure for solving the associated convection-diffusion problem would still be applicable. An illustration of a flow profile obtained this way is shown in figure 8.3.

A second way in which problems may exhibit non-constant depth could be in problems involving surface rugosity. In these cases, if the surface rugosity is high enough that it has

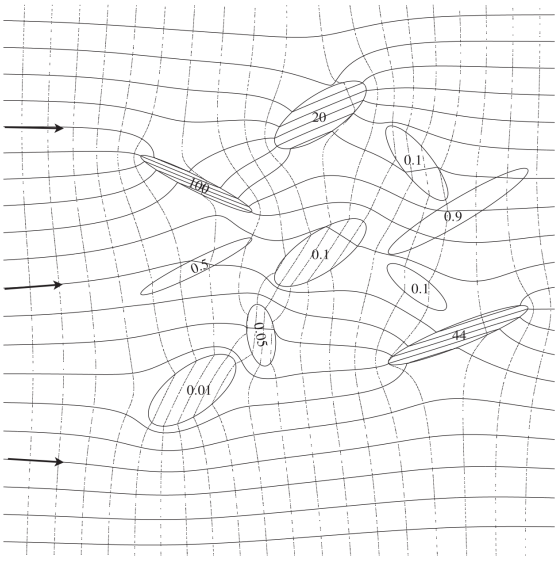

Figure 8.3 Flow field in an aquifer with inhomogeneous flow conductivity, a similar procedure could be used to model Hele-Shaw cells with varying depth. Taken from [45]

to be considered, solutions could be obtained using domain perturbation methods, such as those explicited in [23]. However, the resulting problem would likely involve highly nonlinear equations, and its solution may not be straightforward.

8.2.4 Transient problems

A final aspect that might be interesting to look at is the extension of the results to transient problems. The solution procedure we have been presenting presupposes that the problem is in a steady-state. This is a reasonable assumption in most cases, as the response time for the Stokes flow is virtually instantaneous, and the time it takes for the diffusion profile to reach steady-state is governed by the convection time scale, which is also very low. This means that in many cases, we can obtain solutions for transient problems as sequences of steady-state solutions.

In section 6.11 we have discussed the generation of chemical pulses from microfluidic surface shields, which are inherently transient phenomena. In this case, the problem could be reduced to a problem of convection-diffusion of a set chemical patch in a straight flow, which can be solved by convolution of a simple Green's function.

Another application in which transient aspects would be interesting to study is in chaotic mixing. 2D chaotic micromixers have been studied in the early 2000s [127] [258]. These micromixers consisted of plane domains in which point-like apertures are sequentially activated,

leading to a folding action similar to that observed in channel-based mixers [259]. Such a system is illustrated in figure 8.4. Such transient behavior could be an avenue for further study in the field of multipolar flows.

Figure 8.4 2D chaotic micromixer with 3 point-like apertures. Sequentially activating each aperture leads to a folding of the concentration pattern onto itself. Taken from [127]

8.3 The future of multipolar microfluidics

I will now make some remarks on the future applications of "multipolar microfluidic" technologies, as well as pixelated chemical displays. I believe these technologies are very impressive, and showcase an immense control over both theory and the fabrication. However, they have been faced with some hurdles when it comes to applications. I think it is important to be aware of the limitations of such systems in order to properly plan future areas of research in the field.

8.3.1 The race for more apertures

The microfluidic probe [8] was undoubtedly an innovative system that opened up the way to thinking of microfluidics in different terms than what had been done previously. One direct consequence of it in the academic field is that, in the following years, there was a sort of race from the 3 or 4 research groups associated with early probe research where groups tried to publish every imaginable combination of apertures. We note for example different combinations of four-aperture probes [124] [145], linear arrays of probes [147], as well as our own work on microfluidic multipoles [15]. There are of course diminishing returns, as far as novelty goes, to adding more and more apertures to the same system. Another problem of adding apertures is the prohibitive barrier of entry that multipolar microfluidics, which stands in the way of widespread adaptability.

8.3.2 Barrier of entry

One of the big problems of multipolar systems is their somewhat large barrier of entry. Much of the work of IBM research group in Zurich on microfluidic probes involved systems that were microfabricated on silicon in a clean room, and operated using mechanized robotic arms. This sort of setup makes for very high quality results in the context of an industrial research group, but is prohibitively expensive and stands in the way of widespread adoption.

Work from our group and others [142] focused instead on 3D printed systems. These 3D printed systems lose to silicon microfabrication when it comes to large scale production, but are much cheaper as far as prototyping goes. They also open up the way to the fabrication of monolithic systems with interior 3D channel architecture (such as the pixelated chemical display) which would be require some rethinking to be fabricated using traditional silicon etching. Our group has also been focusing on "reconfigurability" as a selling point for multipolar systems, where we no longer need a robotic arm, but instead modify the flow from a single static device throughout the experiment. These two changes make for a protocol that is cheaper than the previous one, but the operation of open-space systems may still be quite expensive when compared to other standard microfluidic setups such as lateral flow assays or paper-based systems.

One big hurdle, as was discussed in section 7, is the necessity for large numbers of syringe pumps, which can get expensive really fast. More recent work has been done on transitioning to pressure pumps with systems of valves and manifolds, in order to alleviate this cost. However, while these reduce the number of pumps required, the system itself becomes more complex, requiring manifolds and systems of valves. This is probably the way to go for large scale integration of 2D microfluidic systems, but for many applications this may still lose to simple lateral flow assays as far as costs go.

An additional "hidden" cost for these systems, which is one that is mentioned by Albert Folch in 2016 [260], is that it requires a trained PhD student to fabricate and operate. It took Pierre-Alexandre 4 years of very hard work to get the expertise to fabricate and operate his pixelated chemical displays, and by the end the fabrication process still took him about half a day for assembling the entire system. In an academic setting, PhD students come cheap, but one should not underestimate the real cost associated with this expertise when trying to translate these technologies to any sort of real-world application. This is, again, to be compared with simple microchannel systems, which undergraduate students can be trained to fabricate and operate in a matter of a couple of hours.

This much higher complexity and barrier to entry that multipolar systems and pixelated

chemical displays have means that any application they are used for should be one that cannot be realized using simpler means. It is not constructive to use a very complex system to solve a simple problem.

8.3.3 Reagent consumption

One application that multipolar systems have been proposed for is treatment of reactive surfaces, be they cancer tissues, patterned antibodies for immunoassays, or sensors. This makes sense as large surfaces are not directly processable through tight microchannels, and thus surface treatment seems to present itself as a logical application for these probe-type systems. However, application of multipolar systems to the treatment of surfaces runs into two major hurdles.

The first hurdle is the problem of reagent consumption. Microfluidic probes, multipoles, or pixelated chemical displays are systems that operate in a constant streaming fashion, which significantly increases the amount of reagent that is used. Aspiration apertures almost always reaspirate reagent from more than one injection, so that in the best case what is aspirated is a diluted version of what was injected, and in the worst case what is reaspirated is a mix of the different reagents that were injected. This means that there is no straightforward way to reuse the reaspirated reagent, and it is usually counted as a loss.

This problem is compounded by the fact that, in the case of a reactive surface, the surface will interact with reagent in a thin boundary layer above it (see figure 8.5). Concretely, this means that most of the injected reagent will not even come in contact with the reactive surface, and will just directly go to the aspiration aperture, where it is wasted. In order to increase reagent intake of the surface, we have to increase the Peclet number (which is done by increasing flow rates). While this increases reagent intake to the surface, it also makes this boundary layer thinner and thinner. In this way, the amount of reagent wasted increases quicker than the amount of reagent that is consumed by the reactive surface, exacerbating the problem even more.

These systems thus lose one of the main advantages of microfluidics, which is the use of minute amounts of fluids (especially expensive ones). Switching to pressure pumps will allow for access to much smaller flow rates, enabling smaller reagent consumption. However lower flow rate does mean lower Pe, and thus less sharp interfaces when multiplexing, as well as smaller net absorbtion by the surface.

Figure 8.5 Cross-section of a channel with a reactive surface at the bottom, the surface generates a thin boundary layer above it, and a significant portion of the injected reagent does not interact with it. Taken from [113]

8.3.4 Problem of diffusion

Another problem that comes up when treating surfaces is the problem of diffusion within porous surface. A main selling point of pixelated chemical displays, and multipolar systems in general, is their ability to spatially multiplex different reagents. At high Peclet numbers, pixelated chemical displays can generate very sharply distinct patterns of reagents over a surface. However, the entire analysis has been done while only considering what happens within the liquid phase of the Hele-Shaw cell, and not what happens within the surface.

Experiments when treating porous surfaces, such as hydrogels (or eventually cancer tissues) tell a different story. Indeed, biologically relevant surfaces usually have a very low porosity, so that not much of the injected fluid actually penetrates within the surface. The reagent is thus left to penetrate the tissue through diffusive processes, which are very slow. The main disadvantage of these purely diffusive processes is that they completely blur the sharp interfaces that were present in the concentration pattern from the liquid phase (see figure 8.6). This inability to preserve the sharp spatial multiplexing when treating biological surfaces becomes a big hurdle to a large number of potential applications of pixelated chemical displays, and somewhat defeats the interest of using the multipolar system in the first place.

This effect may be mitigated when treating very thin biological surfaces. In this case, experiment times could be kept small enough that diffusion within the tissue is negligible, and allow us to preserve the sharp multiplexing we are looking for.

8.3.5 Search for applications

All of these points considered, I believe that we haven't yet found an application for the more complex multipolar systems that has a strong technological or commercial potential. In many ways, I believe we have been working backwards somewhat. We have developed a very interesting technology that couldn't be thought of before. However, when it comes time to actually put it to use we don't have much. Several applications have been discussed so

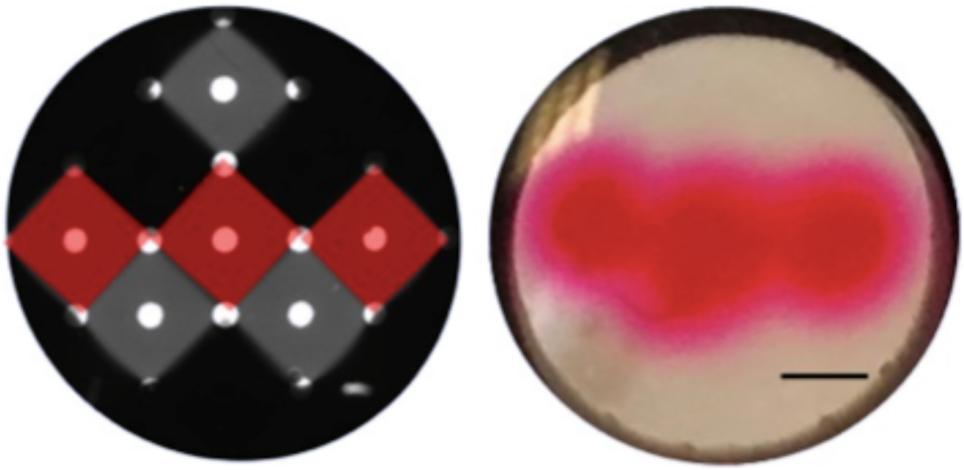

Figure 8.6 Failed tissue staining experiment. A pixelated chemical display was left over a porous agarose slab with similar properties as tumor slices. On the left is the concentration pattern as observed within the liquid phase. On the right is the resulting staining pattern within the agarose slab. After a couple of hours, diffusive processes had completely erased the sharp reagent multiplexing. Image provided by Dina Dorrigiv

far, and some may yield promising results, but most of them either hit the problems that I have listed above, or they solve a problem for which there already exists a much simpler solution. This sort of backwards process, where we have a hammer and are looking for nails, makes some sense in a research environment. We have at our disposal tools that cost a lot of time and money to develop and we want to extract as much value from them as possible. In a sense, it would be counterproductive to always look for new solutions to problems and not try to exploit what we already have at hand. I do believe, however, that it is a tendency we have to be aware of, so that we can orient research in productive directions. This approach of "starting with the solution" and looking for a problem is something that I believe exists not just in this work but in the wider area of research in engineering, and is worth pointing out.

In a sense, "open-space microfluidics" might be a domain that has come and gone, without ever truly finding its footing. The unfortunate closure of IBM research group in Zurich removed one of the big players in this field, and the other groups that were working on these technologies (our group and Mohammad Qasaimeh's group in Abu Dhabi) seem to be moving away from it. In almost 20 years of development, a lot of systems have been published but little has been done in terms of convincing practical applications. This is a bit disappointing, as I do believe that the systems we developed are very interesting and allow us to explore an area of fluid mechanics that is difficult to play with otherwise, and which has its own unique

qualitative features not found anywhere else. These technologies might still find applications one day, maybe in more fundamental areas of research in fluid mechanics, but it might be under new branding, and in directions that are different from the ones we envisioned when we were first working on them.

8.4 Where does this work go next?

I want to conclude with a number of possible directions where this work could be headed next. The development of a theoretical framework for 2D microfluidics, combined with the techniques for rapid fabrication of multipolar microfluidic systems that Pierre-Alexandre developed, have opened up a whole new space of investigation, of which we have only explored the surface.

8.4.1 Multipolar technologies

The systems we have been presenting open up possibilities for highly multiplexed chemistry, as well as precise treatment of surfaces. Moreover, we have presented a complete framework for the rapid generation of complex 2D flow patterns and concentration gradients in large microfluidic chambers, or in 2D "open-space" domains. The systems we have been presenting can be fabricated using simple 3D printing tools and pump systems that are easily accessible to research groups with a start-up fund, enabling researchers to experimentally explore these flor and concentration fields in a rapid manner.

Beyond multiplexed surface treatment, the systems we present can be used as physical micro-models for more complex flow phenomena described by the same sets of equations. Examples we have mentioned throughout this work includes flow in 2D aquifers [45], complex growth phenomena [261], turbulent transport [191], vortex structures in some regimes of the Navier-Stokes equation [106], etc.

8.4.2 Transport phenomena in 2 dimensions

Beyond microfluidics, there is a wealth of phenomena that are described by the 2D convection-diffusion equation, or equations analogous to it. Add to this the range of growth phenomena that have strong ties with the mathematics we have been studying, such as diffusion-limited aggregation [262], dendritic growth [263], viscous fingering processes [29], etc. The models we presented could serve as a starting point to study more complex transport phenomena at a range of scale, a number of examples of which we show in figure 8.7.

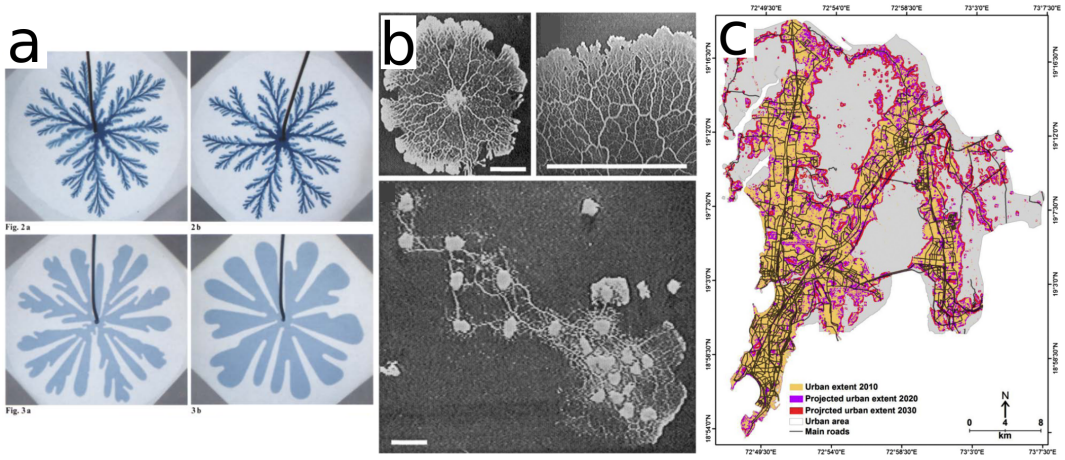

Figure 8.7 Growth processes with analogies to the current work. a) Viscous fingering in Hele-Shaw cells [264]. b) Growth of slime mold organisms [265]. c) Urban sprawl for large cities [266]

There also exists a good volume of work on using conformal transformations to analyze percolation clusters and other critical phenomena [267] [268]. This could be an avenue to push the current work in a more theoretical direction, analyzing the symmetries of various systems. Making links with percolation would also open up analogies with a range of new physics, including gellation [269] [270], 2D turbulence [271], forest fire propagation [272] [273], epidemiology [274], water infiltration in soils [34], etc.

CHAPTER 9 CONCLUSION

9.1 Summary of work

We have presented a unified framework for modeling flow and diffusion in field-based microfluidic systems. We first demonstrated how the tools of conformal transforms and potential flow can be used to analyze transport in microfluidic probes, then extended these same tools to a vast range of microfluidic technologies, from channel junctions to flow in large chambers, making links with multiphase flow, micromodels for porous flow and even some biological systems. We ended by presenting how this toolbox could allow us to think about the design of microfluidic systems differently, enabling us to design new unseen technologies like microfluidic surface shields and pixelated chemical displays.

9.2 Impact

The work presented has the potential to have a significant impact on the microfluidic community, especially through my last review article, which strives to make these results accessible and easy to use for graduate students in the field. While microfluidic probes and microfluidic probe adjacent systems don't see as much interest in the field as they did 10 years ago, the general framework of 2D convection-diffusion applies to an immense range of systems, and is not going to get obsolete overnight. Moreover, I believe this project is a good demonstration of how far theory-assisted design can be pushed. We started with a simple problem, extracted the most general features we could from it, and used the idea to think about design differently. I believe this sort of approach could form the template for future research, perhaps starting from different theoretical assumptions. I could imagine similar frameworks being build to analyze different transport phenomena, be they growth processes, multiphase flows, reactive flows, and maybe unlocking new ideas for technologies that couldn't be thought of before. I also believe that there is value in the many links that were made in this work between microfluidics and other fields like groundwater mechanics, turbulent transport, etc. Many of the problems we face in microfluidics have already been solved in other places, and having these bridges in place to readily access these other fields is maybe more invaluable than any reformulation I could make in my papers. Likewise, these bridges might open up ideas for applications of microfluidic systems to problems beyond the usual ones in life sciences.

9.3 Limitations

Of course, the use of conformal transforms to study 2D flows relies on a number of assumptions: they can only model problems in steady-state, in the absence of reaction term, the gap has to be uniform, etc. Many of these limitations have been mentioned in the discussion section already. However when studying more complex problems I think these solutions could still provide reasonable first approximations or "0-order" solutions for flows with additional physics.

I think the main value of this work lies less in being a "one size fits all" solution for every imaginable microfluidic system, and more in being a powerful tool added to the arsenal of engineers and scientists, side by side with other methods.

9.4 Future Research

Research on applying the technologies developed in this PhD, namely pixelated chemical displays and flower-type multipoles, is already well underway in the group, so I won't give more recommendations for these. I think some of this work is very promising and is being done by very talented engineers, and I have no doubts that it will lead to good research.

I want to end by recommending general directions for the theoretical part of the group's research. When I entered the group, a lot of the research projects were very entrenched in physics, fluid mechanics, modelling, and fabrication. As the years went by, new collaborations were formed with the CHUM, and the research projects slowly moved from theory to application. Today, the group includes a healthy number of students working on biological applications of technologies that we developped in these early years. In this way, we get projects that are very solid and integrated, starting from first principles and going all the way down to biologically relevant results.

I do believe, however, that it would be worthy, at this point, to renew the modeling section of the group. This can only be done if new projects are found, and these projects should stem from new questions related to fundamental fluid mechanics or transport phenomena. I look forward to seeing new students work on interesting transport problems, and seeing how the tools they develop inform the design of new microfluidics we can't even think of today.

REFERENCES

[1] K. E. Petersen, "Silicon as a mechanical material," *Proceedings of the IEEE*, vol. 70, no. 5, pp. 420–457, 1982.

[2] G. M. Whitesides, "The origins and the future of microfluidics," *nature*, vol. 442, no. 7101, pp. 368–373, 2006.

[3] R. K. Shah and A. L. London, *Laminar flow forced convection in ducts: a source book for compact heat exchanger analytical data*. Academic press, 2014.

[4] A. E. Kamholz and P. Yager, "Theoretical analysis of molecular diffusion in pressure-driven laminar flow in microfluidic channels," *Biophysical journal*, vol. 80, no. 1, pp. 155–160, 2001.

[5] H. Bruus, *Theoretical microfluidics*. Oxford university press, 2007, vol. 18.

[6] F. K. Balagaddé, H. Song, J. Ozaki, C. H. Collins, M. Barnet, F. H. Arnold, S. R. Quake, and L. You, "A synthetic escherichia coli predator–prey ecosystem," *Molecular systems biology*, vol. 4, no. 1, p. 187, 2008.

[7] T. Thorsen, S. J. Maerkl, and S. R. Quake, "Microfluidic large-scale integration," *Science*, vol. 298, no. 5593, pp. 580–584, 2002.

[8] D. Juncker, H. Schmid, and E. Delamarche, "Multipurpose microfluidic probe," *Nature materials*, vol. 4, no. 8, pp. 622–628, 2005.

[9] T. Kim, M. Pinelis, and M. M. Maharbiz, "Generating steep, shear-free gradients of small molecules for cell culture," *Biomedical microdevices*, vol. 11, no. 1, pp. 65–73, 2009.

[10] T. Beatus, R. H. Bar-Ziv, and T. Tlusty, "The physics of 2d microfluidic droplet ensembles," *Physics reports*, vol. 516, no. 3, pp. 103–145, 2012.

[11] D. Di Carlo, L. Y. Wu, and L. P. Lee, "Dynamic single cell culture array," *Lab on a Chip*, vol. 6, no. 11, pp. 1445–1449, 2006.

[12] T. Thorsen, R. W. Roberts, F. H. Arnold, and S. R. Quake, "Dynamic pattern formation in a vesicle-generating microfluidic device," *Physical review letters*, vol. 86, no. 18, p. 4163, 2001.

[13] A. Shenoy, C. V. Rao, and C. M. Schroeder, "Stokes trap for multiplexed particle manipulation and assembly using fluidics," *Proceedings of the National Academy of Sciences*, vol. 113, no. 15, pp. 3976–3981, 2016.

[14] K. V. Christ and K. T. Turner, "Design of hydrodynamically confined microfluidics: controlling flow envelope and pressure," *Lab on a chip*, vol. 11, no. 8, pp. 1491–1501, 2011.

[15] P.-A. Goyette, É. Boulais, F. Normandeau, G. Laberge, D. Juncker, and T. Gervais, "Microfluidic multipoles theory and applications," *Nature communications*, vol. 10, no. 1, pp. 1–10, 2019.

[16] E. Boulais and T. Gervais, "Two-dimensional convection–diffusion in multipolar flows with applications in microfluidics and groundwater flow," *Physics of Fluids*, vol. 32, no. 12, p. 122001, 2020.

[17] ——, "The 2d microfluidics cookbook," *Lab on a Chip*, 2023.

[18] O. Boyadjian, E. Boulais, and T. Gervais, "Microfluidic surface shields: Control of flow and diffusion over sensitive surfaces," *Physical Review Applied*, vol. 17, no. 1, p. 014012, 2022.

[19] P.-A. Goyette, É. Boulais, M. Tremblay, and T. Gervais, "Pixel-based open-space microfluidics for versatile surface processing," *Proceedings of the National Academy of Sciences*, vol. 118, no. 2, 2021.

[20] G. Batchelor, *An introduction to fluid dynamics*. Cambridge university press, 2000.

[21] T. M. Squires and T. G. Mason, "Fluid mechanics of microrheology," *Annual review of fluid mechanics*, vol. 42, pp. 413–438, 2010.

[22] E. M. Purcell, "Life at low reynolds number," *American journal of physics*, vol. 45, no. 1, pp. 3–11, 1977.

[23] L. G. Leal, *Advanced transport phenomena: fluid mechanics and convective transport processes*. Cambridge University Press, 2007, vol. 7.

[24] J. L. M. Poiseuille, *Recherches expérimentales sur le mouvement des liquides de nature différente dans les tubes de très petits diamètres*, 1847.

[25] M. Z. Bazant, "Exact solutions and physical analogies for unidirectional flows," *Physical Review Fluids*, vol. 1, no. 2, p. 024001, 2016.

[26] E. Bassous, H. Taub, and L. Kuhn, "Ink jet printing nozzle arrays etched in silicon," *Applied physics letters*, vol. 31, no. 2, pp. 135–137, 1977.

[27] S. C. Terry, J. H. Jerman, and J. B. Angell, "A gas chromatographic air analyzer fabricated on a silicon wafer," *IEEE transactions on electron devices*, vol. 26, no. 12, pp. 1880–1886, 1979.

[28] H. S. Hele-Shaw, "Flow of water," *Nature*, vol. 58, no. 1509, pp. 520–520, 1898.

[29] P. G. Saffman and G. I. Taylor, "The penetration of a fluid into a porous medium or hele-shaw cell containing a more viscous liquid," *Proceedings of the Royal Society of London. Series A. Mathematical and Physical Sciences*, vol. 245, no. 1242, pp. 312–329, 1958.

[30] P. Saffman, "Viscous fingering in hele-shaw cells," *Journal of Fluid Mechanics*, vol. 173, pp. 73–94, 1986.

[31] L. Paterson, "Radial fingering in a hele shaw cell," *Journal of Fluid Mechanics*, vol. 113, pp. 513–529, 1981.

[32] D. Bensimon, L. P. Kadanoff, S. Liang, B. I. Shraiman, and C. Tang, "Viscous flows in two dimensions," *Reviews of Modern Physics*, vol. 58, no. 4, p. 977, 1986.

[33] D. A. Kessler, J. Koplik, and H. Levine, "Pattern selection in fingered growth phenomena," *Advances in physics*, vol. 37, no. 3, pp. 255–339, 1988.

[34] M. Sahimi, "Flow phenomena in rocks: from continuum models to fractals, percolation, cellular automata, and simulated annealing," *Reviews of modern physics*, vol. 65, no. 4, p. 1393, 1993.

[35] C.-Y. Chen and E. Meiburg, "Miscible porous media displacements in the quarter five-spot configuration. part 1. the homogeneous case," *Journal of Fluid Mechanics*, vol. 371, pp. 233–268, 1998.

[36] S.-Y. Teh, R. Lin, L.-H. Hung, and A. P. Lee, "Droplet microfluidics," *Lab on a Chip*, vol. 8, no. 2, pp. 198–220, 2008.

[37] A. Ferrari, J. Jimenez-Martinez, T. L. Borgne, Y. Méheust, and I. Lunati, "Challenges in modeling unstable two-phase flow experiments in porous micromodels," *Water Resources Research*, vol. 51, no. 3, pp. 1381–1400, 2015.

[38] O. Gökçe, S. Castonguay, Y. Temiz, T. Gervais, and E. Delamarche, "Self-coalescing flows in microfluidics for pulse-shaped delivery of reagents," *Nature*, vol. 574, no. 7777, pp. 228–232, 2019.

[39] G. M. Homsy, "Viscous fingering in porous media," *Annual review of fluid mechanics*, vol. 19, no. 1, pp. 271–311, 1987.

[40] H. Darcy, *Les fontaines publiques de la ville de Dijon: exposition et application des principes à suivre et des formules à employer dans les questions de distribution d'eau.* Victor dalmont, 1856, vol. 1.

[41] J. Bear, *Hydraulics of groundwater.* Courier Corporation, 2012.

[42] A. W. Martinez, S. T. Phillips, M. J. Butte, and G. M. Whitesides, "Patterned paper as a platform for inexpensive, low-volume, portable bioassays," *Angewandte Chemie*, vol. 119, no. 8, pp. 1340–1342, 2007.

[43] D. T. Eddington and D. J. Beebe, "Flow control with hydrogels," *Advanced drug delivery reviews*, vol. 56, no. 2, pp. 199–210, 2004.

[44] H. Lamb, *Hydrodynamics.* University Press, 1924.

[45] O. D. Strack, *Groundwater mechanics.* prentice hall, 1989.

[46] P. Saffman and J. Sheffield, "Flow over a wing with an attached free vortex," *Studies in Applied Mathematics*, vol. 57, no. 2, pp. 107–117, 1977.

[47] P. G. Saffman, *Vortex dynamics.* Cambridge university press, 1995.

[48] J. Watts, J. Rankine, F. Barnes, and J. Napier, "Shipbuilding, theoretical and practical," *RSA Journal*, vol. 12, p. 731, 1863.

[49] J. Hunt and P. Mulhearn, "Turbulent dispersion from sources near two-dimensional obstacles," *Journal of Fluid Mechanics*, vol. 61, no. 2, pp. 245–274, 1973.

[50] A. C. Gringarten and J. Sauty, "A theoretical study of heat extraction from aquifers with uniform regional flow," *Journal of geophysical research*, vol. 80, no. 35, pp. 4956–4962, 1975.

[51] E. Milnes and P. Perrochet, "Assessing the impact of thermal feedback and recycling in open-loop groundwater heat pump (gwhp) systems: a complementary design tool," *Hydrogeology journal*, vol. 21, no. 2, pp. 505–514, 2013.

[52] O. Strack, "Some cases of interface flow towards drains," *Journal of Engineering Mathematics*, vol. 6, no. 2, pp. 175–191, 1972.

[53] J. Koplik, S. Redner, and E. Hinch, "Tracer dispersion in planar multipole flows," *Physical Review E*, vol. 50, no. 6, p. 4650, 1994.

[54] G. Dagan, "Spacing of drains by an approximate method," *Journal of the Irrigation and Drainage Division*, vol. 90, no. 1, pp. 41–66, 1964.

[55] D. Grove and W. Beetem, "Porosity and dispersion constant calculations for a fractured carbonate aquifer using the two well tracer method," *Water Resources Research*, vol. 7, no. 1, pp. 128–134, 1971.

[56] P. L. McCarty, M. N. Goltz, G. D. Hopkins, M. E. Dolan, J. P. Allan, B. T. Kawakami, and T. Carrothers, "Full-scale evaluation of in situ cometabolic degradation of trichloroethylene in groundwater through toluene injection," *Environmental Science & Technology*, vol. 32, no. 1, pp. 88–100, 1998.

[57] G. Dagan and J. Bear, "Solving the problem of local interface upconing in a coastal aquifer by the method of small perturbations," *Journal of hydraulic research*, vol. 6, no. 1, pp. 15–44, 1968.

[58] J. W. Brown and R. V. Churchill, *Complex variables and applications*. McGraw-Hill,, 2009.

[59] R. Schinzinger and P. A. Laura, *Conformal mapping: methods and applications*. Courier Corporation, 2012.

[60] W. B. Smythe, "Static and dynamic electricity," 1988.

[61] U. Leonhardt, "Optical conformal mapping," *science*, vol. 312, no. 5781, pp. 1777–1780, 2006.

[62] M. Balcerzak and S. Raynor, "Steady state temperature distribution and heat flow in prismatic bars with isothermal boundary conditions," *International Journal of Heat and Mass Transfer*, vol. 3, no. 2, pp. 113–125, 1961.

[63] B. Shraiman and D. Bensimon, "Singularities in nonlocal interface dynamics," in *Dynamics of Curved Fronts*. Elsevier, 1988, pp. 197–199.

[64] A. E. Green and W. Zerna, *Theoretical elasticity*. Courier Corporation, 1992.

[65] T. A. Driscoll and L. N. Trefethen, *Schwarz-christoffel mapping*. Cambridge University Press, 2002, vol. 8.

[66] L. N. Trefethen, "Analysis and design of polygonal resistors by conformal mapping," *Zeitschrift für angewandte Mathematik und Physik ZAMP*, vol. 35, no. 5, pp. 692–704, 1984.

[67] P. Cattaneo, "Capacitance calculation in a microstrip detector and its applications to signal processing," *Nuclear Instruments and Methods in Physics Research Section A: Accelerators, Spectrometers, Detectors and Associated Equipment*, vol. 295, no. 1-2, pp. 207–218, 1990.

[68] P. A. Laura and E. A. Susemihl, "Determination of heat flow shape factors for hollow, regular polygonal prisms," *Nuclear Engineering and Design*, vol. 25, no. 3, pp. 409–412, 1973.

[69] H. H. Meinke, K. Lange, and J. Ruger, "Te-and tm-waves in waveguides of very general cross section," *Proceedings of the IEEE*, vol. 51, no. 11, pp. 1436–1443, 1963.

[70] H. Tada, P. C. Paris, and G. R. Irwin, "The stress analysis of cracks," *Handbook, Del Research Corporation*, vol. 34, no. 1973, 1973.

[71] D. Crowdy and J. Marshall, "Conformal mappings between canonical multiply connected domains," *Computational Methods and Function Theory*, vol. 6, pp. 59–76, 2006.

[72] D. Crowdy, *Solving problems in multiply connected domains*. SIAM, 2020.

[73] W. M. Deen, *Analysis of transport phenomena*. Oxford university press New York, 1998, vol. 2.

[74] T. L. Carus, *Lucretius on the Nature of Things*. G. Bell and sons, 1882.

[75] J. Ingenhousz, *Nouvelles expériences et observations sur divers objets de physique*. Chez T. Barrois le jeune, 1785, vol. 1.

[76] J. W. S. B. Rayleigh, *The theory of sound*. Macmillan, 1896, vol. 2.

[77] J. Perrin, *Les atomes*. Cnrs, 1914.

[78] J. B. J. Fourier, *Théorie analytique de la chaleur*. Gauthier-Villars et fils, 1888.

[79] A. Fick, "On liquid diffusion," *The London, Edinburgh, and Dublin Philosophical Magazine and Journal of Science*, vol. 10, no. 63, pp. 30–39, 1855.

[80] L. Bachelier, "Théorie de la spéculation," in *Annales scientifiques de l'École normale supérieure*, vol. 17, 1900, pp. 21–86.

[81] K. Pearson, "The problem of the random walk," *Nature*, vol. 72, no. 1865, pp. 294–294, 1905.

[82] A. Einstein *et al.*, "On the motion of small particles suspended in liquids at rest required by the molecular-kinetic theory of heat," *Annalen der physik*, vol. 17, no. 549-560, p. 208, 1905.

[83] J. Perrin, "Mouvement brownien et réalité moléculaire," in *Annales de Chimie et de Physique*, vol. 18, 1909, pp. 1–114.

[84] P. Saffman, "A theory of dispersion in a porous medium," *Journal of Fluid Mechanics*, vol. 6, no. 3, pp. 321–349, 1959.

[85] G. De Josselin de Jong, "Longitudinal and transverse diffusion in granular deposits," *Eos, Transactions American Geophysical Union*, vol. 39, no. 1, pp. 67–74, 1958.

[86] S. Havlin and D. Ben-Avraham, "Diffusion in disordered media," *Advances in physics*, vol. 36, no. 6, pp. 695–798, 1987.

[87] Y. Gefen, A. Aharony, and S. Alexander, "Anomalous diffusion on percolating clusters," *Physical Review Letters*, vol. 50, no. 1, p. 77, 1983.

[88] J.-P. Bouchaud and A. Georges, "Anomalous diffusion in disordered media: statistical mechanisms, models and physical applications," *Physics reports*, vol. 195, no. 4-5, pp. 127–293, 1990.

[89] M. C. Gonzalez, C. A. Hidalgo, and A.-L. Barabasi, "Understanding individual human mobility patterns," *nature*, vol. 453, no. 7196, pp. 779–782, 2008.

[90] F. Höfling and T. Franosch, "Anomalous transport in the crowded world of biological cells," *Reports on Progress in Physics*, vol. 76, no. 4, p. 046602, 2013.

[91] K. W. Morton, *RNumerical solution of convection-diffusion problems*. CRC Press, 1996.

[92] M. Stynes, "Steady-state convection-diffusion problems," *Acta Numerica*, vol. 14, pp. 445–508, 2005.

[93] B. Fornberg, "Steady incompressible flow past a row of circular cylinders," *Journal of Fluid Mechanics*, vol. 225, pp. 655–671, 1991.

[94] R. Natarajan and A. Acrivos, "The instability of the steady flow past spheres and disks," *Journal of Fluid Mechanics*, vol. 254, pp. 323–344, 1993.

[95] T. J. M. Boyd and J. J. Sanderson, "Plasma dynamics," *Plasma dynamics*, 1969.

[96] W. Van Roosbroeck, "Theory of the flow of electrons and holes in germanium and other semiconductors," *The Bell System Technical Journal*, vol. 29, no. 4, pp. 560–607, 1950.

[97] F. Black and M. Scholes, "The pricing of options and corporate liabilities," *Journal of political economy*, vol. 81, no. 3, pp. 637–654, 1973.

[98] G. I. Taylor, "Dispersion of soluble matter in solvent flowing slowly through a tube," *Proceedings of the Royal Society of London. Series A. Mathematical and Physical Sciences*, vol. 219, no. 1137, pp. 186–203, 1953.

[99] R. Aris, "On the dispersion of a solute in a fluid flowing through a tube," *Proceedings of the Royal Society of London. Series A. Mathematical and Physical Sciences*, vol. 235, no. 1200, pp. 67–77, 1956.

[100] M. Z. Bazant, "Conformal mapping of some non-harmonic functions in transport theory," *Proceedings of the Royal Society of London. Series A: Mathematical, Physical and Engineering Sciences*, vol. 460, no. 2045, pp. 1433–1452, 2004.

[101] J. Boussinesq, "Sur le pouvoir refroidissant d'un courant liquide ou gazeux," *J. Phys. Theor. Appl.*, vol. 1, no. 1, pp. 71–75, 1902.

[102] A. D. Polyanin and V. F. Zaitsev, *Handbook of ordinary differential equations: exact solutions, methods, and problems*. Chapman and Hall/CRC, 2017.

[103] I. Eames and J. Bush, "Longitudinal dispersion by bodies fixed in a potential flow," *Proceedings of the Royal Society of London. Series A: Mathematical, Physical and Engineering Sciences*, vol. 455, no. 1990, pp. 3665–3686, 1999.

[104] J. Hunt and I. Eames, "The disappearance of laminar and turbulent wakes in complex flows," *Journal of Fluid Mechanics*, vol. 457, pp. 111–132, 2002.

[105] L. M. Cummings, Y. E. Hohlov, S. D. Howison, and K. Kornev, "Two-dimensional solidification and melting in potential flows," *Journal of Fluid Mechanics*, vol. 378, pp. 1–18, 1999.

[106] M. Z. Bazant and H. Moffatt, "Exact solutions of the navier–stokes equations having steady vortex structures," *Journal of Fluid Mechanics*, vol. 541, pp. 55–64, 2005.

[107] A. Lévêque, "Les lois de la transmission de chaleur par convection..." Ph.D. dissertation, 1928.

[108] S. Springer and T. J. Pedley, "The solution of heat transfer problems by the wiener-hopf technique. i. leading edge of a hot film," *Proceedings of the Royal Society of London. A. Mathematical and Physical Sciences*, vol. 333, no. 1594, pp. 347–362, 1973.

[109] S. G. Springer, "The solution of heat-transfer problems by the wiener—hopf technique ii. trailing edge of a hot film," *Proceedings of the Royal Society of London. A. Mathematical and Physical Sciences*, vol. 337, no. 1610, pp. 395–412, 1974.

[110] C. E. Pearson, "On the finite strip problem," *Quarterly of Applied Mathematics*, vol. 15, no. 2, pp. 203–208, 1957.

[111] J. Choi, D. Margetis, T. M. Squires, and M. Z. Bazant, "Steady advection–diffusion around finite absorbers in two-dimensional potential flows," *Journal of Fluid Mechanics*, vol. 536, pp. 155–184, 2005.

[112] A. Acrivos and T. D. Taylor, "Heat and mass transfer from single spheres in stokes flow," *The Physics of Fluids*, vol. 5, no. 4, pp. 387–394, 1962.

[113] T. M. Squires, R. J. Messinger, and S. R. Manalis, "Making it stick: convection, reaction and diffusion in surface-based biosensors," *Nature biotechnology*, vol. 26, no. 4, pp. 417–426, 2008.

[114] M. C. Cross and P. C. Hohenberg, "Pattern formation outside of equilibrium," *Reviews of modern physics*, vol. 65, no. 3, p. 851, 1993.

[115] V. Petrov, V. Gaspar, J. Masere, and K. Showalter, "Controlling chaos in the belousov—zhabotinsky reaction," *Nature*, vol. 361, no. 6409, pp. 240–243, 1993.

[116] A. M. Turing, "The chemical basis of morphogenesis," *Bulletin of mathematical biology*, vol. 52, pp. 153–197, 1990.

[117] J. Vilar, R. Solé, and J. Rubı, "On the origin of plankton patchiness," *Physica A: Statistical Mechanics and its Applications*, vol. 317, no. 1-2, pp. 239–246, 2003.

[118] S. A. Levin, . H. C. Muller-Landau, . R. Nathan, and . J. Chave, "The ecology and evolution of seed dispersal: a theoretical perspective," *Annual Review of Ecology, Evolution, and Systematics*, vol. 34, no. 1, pp. 575–604, 2003.

[119] S. Kondo and T. Miura, "Reaction-diffusion model as a framework for understanding biological pattern formation," *science*, vol. 329, no. 5999, pp. 1616–1620, 2010.

[120] S. Kondo, M. Watanabe, and S. Miyazawa, "Studies of turing pattern formation in zebrafish skin," *Philosophical Transactions of the Royal Society A*, vol. 379, no. 2213, p. 20200274, 2021.

[121] M. P. Hassell, H. N. Comins, and R. M. Mayt, "Spatial structure and chaos in insect population dynamics," *Nature*, vol. 353, no. 6341, pp. 255–258, 1991.

[122] L. A. Segel and J. L. Jackson, "Dissipative structure: an explanation and an ecological example," *Journal of theoretical biology*, vol. 37, no. 3, pp. 545–559, 1972.

[123] A. Witkin and M. Kass, "Reaction-diffusion textures," in *Proceedings of the 18th annual conference on computer graphics and interactive techniques*, 1991, pp. 299–308.

[124] M. A. Qasaimeh, T. Gervais, and D. Juncker, "Microfluidic quadrupole and floating concentration gradient," *Nature communications*, vol. 2, no. 1, pp. 1–8, 2011.

[125] M. Tanyeri, E. M. Johnson-Chavarria, and C. M. Schroeder, "Hydrodynamic trap for single particles and cells," *Applied physics letters*, vol. 96, no. 22, 2010.

[126] T. Beatus, T. Tlusty, and R. Bar-Ziv, "Phonons in a one-dimensional microfluidic crystal," *Nature Physics*, vol. 2, no. 11, pp. 743–748, 2006.

[127] P. L. Boyland, H. Aref, and M. A. Stremler, "Topological fluid mechanics of stirring," *Journal of Fluid Mechanics*, vol. 403, pp. 277–304, 2000.

[128] A. E. Kamholz, B. H. Weigl, B. A. Finlayson, and P. Yager, "Quantitative analysis of molecular interaction in a microfluidic channel: the t-sensor," *Analytical chemistry*, vol. 71, no. 23, pp. 5340–5347, 1999.

[129] N. L. Jeon, S. K. Dertinger, D. T. Chiu, I. S. Choi, A. D. Stroock, and G. M. Whitesides, "Generation of solution and surface gradients using microfluidic systems," *Langmuir*, vol. 16, no. 22, pp. 8311–8316, 2000.

[130] D. Irimia, D. A. Geba, and M. Toner, "Universal microfluidic gradient generator," *Analytical chemistry*, vol. 78, no. 10, pp. 3472–3477, 2006.

[131] C.-Y. Lee, C.-L. Chang, Y.-N. Wang, and L.-M. Fu, "Microfluidic mixing: a review," *International journal of molecular sciences*, vol. 12, no. 5, pp. 3263–3287, 2011.

[132] J. Atencia, J. Morrow, and L. E. Locascio, "The microfluidic palette: a diffusive gradient generator with spatio-temporal control," *Lab on a Chip*, vol. 9, no. 18, pp. 2707–2714, 2009.

[133] M. Safavieh, M. A. Qasaimeh, A. Vakil, D. Juncker, and T. Gervais, "Two-aperture microfluidic probes as flow dipoles: Theory and applications," *Scientific reports*, vol. 5, no. 1, pp. 1–16, 2015.

[134] A. Sarkar, S. Kolitz, D. A. Lauffenburger, and J. Han, "Microfluidic probe for single-cell analysis in adherent tissue culture," *Nature communications*, vol. 5, no. 1, pp. 1–8, 2014.

[135] G. C. Randall and P. S. Doyle, "Permeation-driven flow in poly (dimethylsiloxane) microfluidic devices," *Proceedings of the National Academy of Sciences*, vol. 102, no. 31, pp. 10 813–10 818, 2005.

[136] B. Davidovitch, H. E. Hentschel, Z. Olami, I. Procaccia, L. M. Sander, and E. Somfai, "Diffusion limited aggregation and iterated conformal maps," *Physical Review E*, vol. 59, no. 2, p. 1368, 1999.

[137] M. Hastings, "Fractal to nonfractal phase transition in the dielectric breakdown model," *Physical Review Letters*, vol. 87, no. 17, p. 175502, 2001.

[138] P. Clapperton Richard, "Afficheurs microfluidiques comme outil d'étude des voies de signalisation cellulaires en biologie des systèmes," Ph.D. dissertation, Polytechnique Montréal, 2022.

[139] D. Dorrigiv, P.-A. Goyette, A. St-Georges-Robillard, A.-M. Mes-Masson, and T. Gervais, "Pixelated microfluidics for drug screening on tumour spheroids and ex vivo microdissected tumour explants," *Cancers*, vol. 15, no. 4, p. 1060, 2023.

[140] G. V. Kaigala, R. D. Lovchik, and E. Delamarche, "Microfluidics in the "open space" for performing localized chemistry on biological interfaces," *Angewandte Chemie International Edition*, vol. 51, no. 45, pp. 11 224–11 240, 2012.

[141] R. D. Lovchik, G. V. Kaigala, M. Georgiadis, and E. Delamarche, "Micro-immunohistochemistry using a microfluidic probe," *Lab on a Chip*, vol. 12, no. 6, pp. 1040–1043, 2012.

[142] A. Brimmo, P.-A. Goyette, R. Alnemari, T. Gervais, and M. A. Qasaimeh, "3d printed microfluidic probes," *Scientific reports*, vol. 8, no. 1, pp. 1–8, 2018.

[143] M. A. Qasaimeh, M. Pyzik, M. Astolfi, S. M. Vidal, and D. Juncker, "Neutrophil chemotaxis in moving gradients," *Advanced Biosystems*, vol. 2, no. 7, p. 1700243, 2018.

[144] G. Kaigala, R. Lovchik, U. Drechsler, and E. Delamarche, "A vertical microfluidic probe," *Langmuir*, vol. 27, no. 9, pp. 5686–5693, 2011.

[145] J. Autebert, A. Kashyap, R. D. Lovchik, E. Delamarche, and G. V. Kaigala, "Hierarchical hydrodynamic flow confinement: efficient use and retrieval of chemicals for microscale chemistry on surfaces," *Langmuir*, vol. 30, no. 12, pp. 3640–3645, 2014.

[146] J. F. Cors, A. Stucki, and G. V. Kaigala, "Hydrodynamic thermal confinement: creating thermo-chemical microenvironments on surfaces," *Chemical Communications*, vol. 52, no. 88, pp. 13 035–13 038, 2016.

[147] D. P. Taylor, I. Zeaf, R. D. Lovchik, and G. V. Kaigala, "Centimeter-scale surface interactions using hydrodynamic flow confinements," *Langmuir*, vol. 32, no. 41, pp. 10 537–10 544, 2016.

[148] D. Chen, W. Du, Y. Liu, W. Liu, A. Kuznetsov, F. E. Mendez, L. H. Philipson, and R. F. Ismagilov, "The chemistrode: a droplet-based microfluidic device for stimulation and recording with high temporal, spatial, and chemical resolution," *Proceedings of the National Academy of Sciences*, vol. 105, no. 44, pp. 16 843–16 848, 2008.

[149] A. Meister, M. Gabi, P. Behr, P. Studer, J. Voros, P. Niedermann, J. Bitterli, J. Polesel-Maris, M. Liley, H. Heinzelmann *et al.*, "Fluidfm: combining atomic force microscopy and nanofluidics in a universal liquid delivery system for single cell applications and beyond," *Nano letters*, vol. 9, no. 6, pp. 2501–2507, 2009.

[150] A. Ainla, G. D. Jeffries, R. Brune, O. Orwar, and A. Jesorka, "A multifunctional pipette," *Lab on a Chip*, vol. 12, no. 7, pp. 1255–1261, 2012.

[151] H. Tavana, A. Jovic, B. Mosadegh, Q. Lee, X. Liu, K. Luker, G. Luker, S. Weiss, and S. Takayama, "Nanolitre liquid patterning in aqueous environments for spatially defined reagent delivery to mammalian cells," *Nature materials*, vol. 8, no. 9, pp. 736–741, 2009.

[152] É. Boulais and T. Gervais, "Hele-shaw flow theory in the context of open microfluidics: From dipoles to quadrupoles," *Open-Space Microfluidics: Concepts, Implementations, Applications*, 2018.

[153] E. Delamarche and G. V. Kaigala, *Open-space microfluidics: concepts, implementations, applications*. John Wiley & Sons, 2018.

[154] A. D. Polyanin, *Handbook of linear partial differential equations for engineers and scientists*. Chapman and hall/crc, 2001.

[155] H. Gong, B. P. Bickham, A. T. Woolley, and G. P. Nordin, "Custom 3d printer and resin for 18 μm$\times$ 20 μm microfluidic flow channels," *Lab on a Chip*, vol. 17, no. 17, pp. 2899–2909, 2017.

[156] J. B. Knight, A. Vishwanath, J. P. Brody, and R. H. Austin, "Hydrodynamic focusing on a silicon chip: mixing nanoliters in microseconds," *Physical review letters*, vol. 80, no. 17, p. 3863, 1998.

[157] B. H. Weigl and P. Yager, "Microfluidic diffusion-based separation and detection," *Science*, vol. 283, no. 5400, pp. 346–347, 1999.

[158] B. Webb and C.-F. Ma, "Single-phase liquid jet impingement heat transfer," in *Advances in heat transfer*. Elsevier, 1995, vol. 26, pp. 105–217.

[159] D. Spalding, "Theory of mixing and chemical reaction in the opposed-jet diffusion flame," *ARS Journal*, vol. 31, no. 6, pp. 763–771, 1961.

[160] P. Kurowski, I. Ippolito, J. Hulin, J. Koplik, and E. Hinch, "Anomalous dispersion in a dipole flow geometry," *Physics of Fluids*, vol. 6, no. 1, pp. 108–117, 1994.

[161] J. Luo and P. K. Kitanidis, "Fluid residence times within a recirculation zone created by an extraction–injection well pair," *Journal of Hydrology*, vol. 295, no. 1-4, pp. 149–162, 2004.

[162] J. Luo, M. Dentz, O. A. Cirpka, and P. K. Kitanidis, "Breakthrough curve tailing in a dipole flow field," *Water Resources Research*, vol. 43, no. 9, 2007.

[163] G. De Josselin de Jong, "Singularity distributions for the analysis of multiple-fluid flow through porous media," *Journal of Geophysical Research*, vol. 65, no. 11, pp. 3739–3758, 1960.

[164] B. Cui, H. Diamant, B. Lin, and S. A. Rice, "Anomalous hydrodynamic interaction in a quasi-two-dimensional suspension," *Physical review letters*, vol. 92, no. 25, p. 258301, 2004.

[165] M. Zouache, I. Eames, C. Klettner, and P. Luthert, "Form, shape and function: segmented blood flow in the choriocapillaris," *Scientific reports*, vol. 6, no. 1, pp. 1–13, 2016.

[166] J. Jackson and G. Symmons, "The pressure distribution in a hydrostatic thrust bearing," *International Journal of Mechanical Sciences*, vol. 7, no. 4, pp. 239–242, 1965.

[167] H. W. Woolard, "A theoretical analysis of the viscous flow in a narrowly spaced radial diffuser," 1957.

[168] M. Kamal and S. Kenig, "The injection molding of thermoplastics part i: Theoretical model," *Polymer Engineering & Science*, vol. 12, no. 4, pp. 294–301, 1972.

[169] G. I. Taylor, "The formation of emulsions in definable fields of flow," *Proceedings of the Royal Society of London. Series A, containing papers of a mathematical and physical character*, vol. 146, no. 858, pp. 501–523, 1934.

[170] J. M. Burgers, "A mathematical model illustrating the theory of turbulence," *Advances in applied mechanics*, vol. 1, pp. 171–199, 1948.

[171] A. Nakajima, M. Ishida, T. Fujimori, Y. Wakamoto, and S. Sawai, "The microfluidic lighthouse: An omnidirectional gradient generator," *Lab on a Chip*, vol. 16, no. 22, pp. 4382–4394, 2016.

[172] J. S. Lee, R. Dylla-Spears, N. P. Teclemariam, and S. J. Muller, "Microfluidic four-roll mill for all flow types," *Applied physics letters*, vol. 90, no. 7, p. 074103, 2007.

[173] D. P. Taylor and G. V. Kaigala, "Reconfigurable microfluidics: Real-time shaping of virtual channels through hydrodynamic forces," *Lab on a Chip*, vol. 20, no. 10, pp. 1720–1728, 2020.

[174] M. Zouache, I. Eames, C. Klettner, and P. Luthert, "Flow and passive transport in planar multipolar flows," *Journal of Fluid Mechanics*, vol. 858, pp. 184–227, 2019.

[175] J. Da Costa and R. Bennett, "The pattern of flow in the vicinity of a recharging and discharging pair of wells in an aquifer having areal parallel flow: Helsinki," *UGGI/AIHS, Publ*, no. 52, 1960.

[176] D. Grove, W. Beetem, and F. Sower, "Fluid travel time between a recharging and discharging well pair in an aquifer having a uniform regional flow field," *Water resources research*, vol. 6, no. 5, pp. 1404–1410, 1970.

[177] R. F. Ismagilov, A. D. Stroock, P. J. Kenis, G. Whitesides, and H. A. Stone, "Experimental and theoretical scaling laws for transverse diffusive broadening in two-phase laminar flows in microchannels," *Applied Physics Letters*, vol. 76, no. 17, pp. 2376–2378, 2000.

[178] J. L. Osborn, B. Lutz, E. Fu, P. Kauffman, D. Y. Stevens, and P. Yager, "Microfluidics without pumps: reinventing the t-sensor and h-filter in paper networks," *Lab on a Chip*, vol. 10, no. 20, pp. 2659–2665, 2010.

[179] G. Bodvarsson, "Thermal problems in the siting of reinjection wells," *Geothermics*, vol. 1, no. 2, pp. 63–66, 1972.

[180] J. Bear and G. Dagan, "Some exact solutions of interface problems by means of the hodograph method," *Journal of Geophysical Research*, vol. 69, no. 8, pp. 1563–1572, 1964.

[181] G. De Josselin de Jong, "A many-valued hodograph in an interface problem," *Water Resources Research*, vol. 1, no. 4, pp. 543–555, 1965.

[182] J. Carlson and A. Heins, "The reflection of an electromagnetic plane wave by an infinite set of plates. i," *Quarterly of Applied Mathematics*, vol. 4, no. 4, pp. 313–329, 1947.

[183] L. V. King, "Xii. on the convection of heat from small cylinders in a stream of fluid: Determination of the convection constants of small platinum wires with applications to hot-wire anemometry," *Philosophical transactions of the royal society of London. series A, containing papers of a mathematical or physical character*, vol. 214, no. 509-522, pp. 373–432, 1914.

[184] J. P. Brody and P. Yager, "Diffusion-based extraction in a microfabricated device," *Sensors and Actuators A: Physical*, vol. 58, no. 1, pp. 13–18, 1997.

[185] O. Gökçe, S. Castonguay, Y. Temiz, T. Gervais, and E. Delamarche, "Self-coalescing flows in microfluidics for pulse-shaped delivery of reagents," *Nature*, vol. 574, no. 7777, pp. 228–232, 2019.

[186] P. Gravesen, J. Branebjerg, and O. S. Jensen, "Microfluidics-a review," *Journal of micromechanics and microengineering*, vol. 3, no. 4, p. 168, 1993.

[187] C. D. Chin, V. Linder, and S. K. Sia, "Lab-on-a-chip devices for global health: Past studies and future opportunities," *Lab on a Chip*, vol. 7, no. 1, pp. 41–57, 2007.

[188] S. Hudson, F. Phelan Jr, M. Handler, J. Cabral, K. Migler, and E. Amis, "Microfluidic analog of the four-roll mill," *Applied Physics Letters*, vol. 85, no. 2, pp. 335–337, 2004.

[189] C. J. Pipe and G. H. McKinley, "Microfluidic rheometry," *Mechanics research communications*, vol. 36, no. 1, pp. 110–120, 2009.

[190] M. Tanyeri, M. Ranka, N. Sittipolkul, and C. M. Schroeder, "A microfluidic-based hydrodynamic trap: design and implementation," *Lab on a Chip*, vol. 11, no. 10, pp. 1786–1794, 2011.

[191] J. Puttock and J. Hunt, "Turbulent diffusion from sources near obstacles with separated wakes—part i. an eddy diffusivity model," *Atmospheric Environment (1967)*, vol. 13, no. 1, pp. 1–13, 1979.

[192] A. Haji-Sheikh and E. M. Sparrow, "The floating random walk and its application to monte carlo solutions of heat equations," *SIAM Journal on Applied Mathematics*, vol. 14, no. 2, pp. 370–389, 1966.

[193] M. Zimmermann, H. Schmid, P. Hunziker, and E. Delamarche, "Capillary pumps for autonomous capillary systems," *Lab on a Chip*, vol. 7, no. 1, pp. 119–125, 2007.

[194] J. Gauteplass, K. Chaudhary, A. R. Kovscek, and M. A. Fernø, "Pore-level foam generation and flow for mobility control in fractured systems," *Colloids and Surfaces A: Physicochemical and Engineering Aspects*, vol. 468, pp. 184–192, 2015.

[195] N. Karadimitriou, M. Musterd, P. Kleingeld, M. Kreutzer, S. Hassanizadeh, and V. Joekar-Niasar, "On the fabrication of pdms micromodels by rapid prototyping, and their use in two-phase flow studies," *Water Resources Research*, vol. 49, no. 4, pp. 2056–2067, 2013.

[196] S. L. Anna, N. Bontoux, and H. A. Stone, "Formation of dispersions using "flow focusing" in microchannels," *Applied physics letters*, vol. 82, no. 3, pp. 364–366, 2003.

[197] P. Garstecki, M. J. Fuerstman, H. A. Stone, and G. M. Whitesides, "Formation of droplets and bubbles in a microfluidic t-junction—scaling and mechanism of break-up," *Lab on a Chip*, vol. 6, no. 3, pp. 437–446, 2006.

[198] F. S. Fritzsch, C. Dusny, O. Frick, and A. Schmid, "Single-cell analysis in biotechnology, systems biology, and biocatalysis," *Annual review of chemical and biomolecular engineering*, vol. 3, pp. 129–155, 2012.

[199] C. M. Schroeder, "Single polymer dynamics for molecular rheology," *Journal of Rheology*, vol. 62, no. 1, pp. 371–403, 2018.

[200] A. T. Brimmo and M. A. Qasaimeh, "Stagnation point flows in analytical chemistry and life sciences," *RSC advances*, vol. 7, no. 81, pp. 51 206–51 232, 2017.

[201] N. Li Jeon, H. Baskaran, S. K. Dertinger, G. M. Whitesides, L. Van De Water, and M. Toner, "Neutrophil chemotaxis in linear and complex gradients of interleukin-8 formed in a microfabricated device," *Nature biotechnology*, vol. 20, no. 8, pp. 826–830, 2002.

[202] S. Boyden, "The chemotactic effect of mixtures of antibody and antigen on polymorphonuclear leucocytes," *The Journal of experimental medicine*, vol. 115, no. 3, pp. 453–466, 1962.

[203] D. Zicha, G. A. Dunn, and A. F. Brown, "A new direct-viewing chemotaxis chamber," *Journal of cell science*, vol. 99, no. 4, pp. 769–775, 1991.

[204] J. Olofsson, J. Pihl, J. Sinclair, E. Sahlin, M. Karlsson, and O. Orwar, "A microfluidics approach to the problem of creating separate solution environments accessible from macroscopic volumes," *Analytical chemistry*, vol. 76, no. 17, pp. 4968–4976, 2004.

[205] A. Ainla, G. Jeffries, and A. Jesorka, "Hydrodynamic flow confinement technology in microfluidic perfusion devices," *Micromachines*, vol. 3, no. 2, pp. 442–461, 2012.

[206] J. W. Cheng, T. C. Chang, N. Bhattacharjee, and A. Folch, "An open-chamber flow-focusing device for focal stimulation of micropatterned cells," *Biomicrofluidics*, vol. 10, no. 2, p. 024122, 2016.

[207] A. Queval, N. R. Ghattamaneni, C. M. Perrault, R. Gill, M. Mirzaei, R. A. McKinney, and D. Juncker, "Chamber and microfluidic probe for microperfusion of organotypic brain slices," *Lab on a Chip*, vol. 10, no. 3, pp. 326–334, 2010.

[208] A. G. Toh, Z. Wang, C. Yang, and N.-T. Nguyen, "Engineering microfluidic concentration gradient generators for biological applications," *Microfluidics and Nanofluidics*, vol. 16, no. 1, pp. 1–18, 2014.

[209] J. R. Rettig and A. Folch, "Large-scale single-cell trapping and imaging using microwell arrays," *Analytical chemistry*, vol. 77, no. 17, pp. 5628–5634, 2005.

[210] C. Lipp, K. Uning, J. Cottet, D. Migliozzi, A. Bertsch, and P. Renaud, "Planar hydrodynamic traps and buried channels for bead and cell trapping and releasing," *Lab on a Chip*, vol. 21, no. 19, pp. 3686–3694, 2021.

[211] H. Song, D. L. Chen, and R. F. Ismagilov, "Reactions in droplets in microfluidic channels," *Angewandte chemie international edition*, vol. 45, no. 44, pp. 7336–7356, 2006.

[212] D. Juncker, H. Schmid, U. Drechsler, H. Wolf, M. Wolf, B. Michel, N. de Rooij, and E. Delamarche, "Autonomous microfluidic capillary system," *Analytical chemistry*, vol. 74, no. 24, pp. 6139–6144, 2002.

[213] O. Gökçe, C. Mercandetti, and E. Delamarche, "High-content optical codes for protecting rapid diagnostic tests from counterfeiting," *Analytical chemistry*, vol. 90, no. 12, pp. 7383–7390, 2018.

[214] S. Haward, "Microfluidic extensional rheometry using stagnation point flow," *Biomicrofluidics*, vol. 10, no. 4, p. 043401, 2016.

[215] A. Anbari, H.-T. Chien, S. S. Datta, W. Deng, D. A. Weitz, and J. Fan, "Microfluidic model porous media: Fabrication and applications," *Small*, vol. 14, no. 18, p. 1703575, 2018.

[216] C. E. Stanley, G. Grossmann, X. C. i Solvas, and A. J. deMello, "Soil-on-a-chip: microfluidic platforms for environmental organismal studies," *Lab on a Chip*, vol. 16, no. 2, pp. 228–241, 2016.

[217] K. Vafai, *Porous media*. CRC, 2010.

[218] B. Gustafsson and A. Vasil'ev, *Conformal and potential analysis in Hele-Shaw cells*. Springer Science & Business Media, 2006.

[219] S. K. Murthy, A. Sin, R. G. Tompkins, and M. Toner, "Effect of flow and surface conditions on human lymphocyte isolation using microfluidic chambers," *Langmuir*, vol. 20, no. 26, pp. 11 649–11 655, 2004.

[220] A. Sin, S. K. Murthy, A. Revzin, R. G. Tompkins, and M. Toner, "Enrichment using antibody-coated microfluidic chambers in shear flow: Model mixtures of human lymphocytes," *Biotechnology and bioengineering*, vol. 91, no. 7, pp. 816–826, 2005.

[221] K. V. Christ, C. Park, K. S. Masters, and K. T. Turner, "Design and characterization of a hydrodynamically confined microflow device for applying controlled loads to investigate single-cell mechanics," *Microfluidics and Nanofluidics*, vol. 23, no. 4, pp. 1–14, 2019.

[222] D. Zwillinger and V. Dobrushkin, *Handbook of differential equations*. Chapman and Hall/CRC, 1998.

[223] M. Abramowitz and I. A. Stegun, *Handbook of mathematical functions with formulas, graphs, and mathematical tables*. US Government printing office, 1964, vol. 55.

[224] E. W. Washburn, "The dynamics of capillary flow," *Physical review*, vol. 17, no. 3, p. 273, 1921.

[225] M. Z. Bazant and D. Crowdy, "Conformal mapping methods for interfacial dynamics," in *Handbook of materials modeling*. Springer, 2005, pp. 1417–1451.

[226] C. N. Baroud, F. Gallaire, and R. Dangla, "Dynamics of microfluidic droplets," *Lab on a Chip*, vol. 10, no. 16, pp. 2032–2045, 2010.

[227] P. Moller, "A radial diffuser using incompressible flow between narrowly spaced disks," 1966.

[228] A. Chatterjee and D. White, "Radial entry flow of a newtonian fluid," *Journal of Physics D: Applied Physics*, vol. 22, no. 7, p. 915, 1989.

[229] A. Chatterjee and L. Deviprasath, "Heat transfer in confined laminar axisymmetric impinging jets at small nozzle-plate distances: the role of upstream vorticity diffusion," *Numerical Heat Transfer: Part A: Applications*, vol. 39, no. 8, pp. 777–800, 2001.

[230] T. Gervais and K. F. Jensen, "Mass transport and surface reactions in microfluidic systems," *Chemical engineering science*, vol. 61, no. 4, pp. 1102–1121, 2006.

[231] E. P. Kartalov, J. F. Zhong, A. Scherer, S. R. Quake, C. R. Taylor, and W. French Anderson, "High-throughput multi-antigen microfluidic fluorescence immunoassays," *BioTechniques*, vol. 40, no. 1, pp. 85–90, 2006.

[232] E. Delamarche, A. Bernard, H. Schmid, B. Michel, and H. Biebuyck, "Patterned delivery of immunoglobulins to surfaces using microfluidic networks," *Science*, vol. 276, no. 5313, pp. 779–781, 1997.

[233] E. Delamarche, D. Juncker, and H. Schmid, "Microfluidics for processing surfaces and miniaturizing biological assays," *Advanced Materials*, vol. 17, no. 24, pp. 2911–2933, 2005.

[234] K. V. Christ and K. T. Turner, "Methods to measure the strength of cell adhesion to substrates," *Journal of Adhesion Science and Technology*, vol. 24, no. 13-14, pp. 2027–2058, 2010.

[235] M. S. Kim, T. Kim, S.-Y. Kong, S. Kwon, C. Y. Bae, J. Choi, C. H. Kim, E. S. Lee, and J.-K. Park, "Breast cancer diagnosis using a microfluidic multiplexed immunohistochemistry platform," *PloS one*, vol. 5, no. 5, p. e10441, 2010.

[236] A. Mahadevan, A. Orpe, A. Kudrolli, and L. Mahadevan, "Flow-induced channelization in a porous medium," *EPL (Europhysics Letters)*, vol. 98, no. 5, p. 58003, 2012.

[237] G. S. Beavers and D. D. Joseph, "Boundary conditions at a naturally permeable wall," *Journal of fluid mechanics*, vol. 30, no. 1, pp. 197–207, 1967.

[238] P. G. Saffman, "On the boundary condition at the surface of a porous medium," *Studies in applied mathematics*, vol. 50, no. 2, pp. 93–101, 1971.

[239] B. Goyeau, D. Lhuillier, D. Gobin, and M. Velarde, "Momentum transport at a fluid–porous interface," *International Journal of Heat and Mass Transfer*, vol. 46, no. 21, pp. 4071–4081, 2003.

[240] M. Chandesris and D. Jamet, "Boundary conditions at a planar fluid–porous interface for a poiseuille flow," *International Journal of Heat and Mass Transfer*, vol. 49, no. 13-14, pp. 2137–2150, 2006.

[241] A. Goharzadeh, A. Khalili, and B. B. Jørgensen, "Transition layer thickness at a fluid-porous interface," *Physics of Fluids*, vol. 17, no. 5, p. 057102, 2005.

[242] J. B. Pendry, D. Schurig, and D. R. Smith, "Controlling electromagnetic fields," *science*, vol. 312, no. 5781, pp. 1780–1782, 2006.

[243] S. A. Cummer and D. Schurig, "One path to acoustic cloaking," *New journal of physics*, vol. 9, no. 3, p. 45, 2007.

[244] M. Farhat, S. Guenneau, and S. Enoch, "Ultrabroadband elastic cloaking in thin plates," *Physical review letters*, vol. 103, no. 2, p. 024301, 2009.

[245] S. Brûlé, E. Javelaud, S. Enoch, and S. Guenneau, "Experiments on seismic metamaterials: molding surface waves," *Physical review letters*, vol. 112, no. 13, p. 133901, 2014.

[246] M. Farhat, S. Enoch, S. Guenneau, and A. Movchan, "Broadband cylindrical acoustic cloak for linear surface waves in a fluid," *Physical review letters*, vol. 101, no. 13, p. 134501, 2008.

[247] S. Zhang, D. A. Genov, C. Sun, and X. Zhang, "Cloaking of matter waves," *Physical Review Letters*, vol. 100, no. 12, p. 123002, 2008.

[248] R. Schittny, M. Kadic, S. Guenneau, and M. Wegener, "Experiments on transformation thermodynamics: molding the flow of heat," *Physical review letters*, vol. 110, no. 19, p. 195901, 2013.

[249] F. Avanzini, G. Falasco, and M. Esposito, "Chemical cloaking," *Physical Review E*, vol. 101, no. 6, p. 060102, 2020.

[250] Y. A. Urzhumov and D. R. Smith, "Fluid flow control with transformation media," *Physical review letters*, vol. 107, no. 7, p. 074501, 2011.

[251] J. Homola and M. Piliarik, *Surface plasmon resonance (SPR) sensors*. Springer, 2006.

[252] M. R. Foreman, J. D. Swaim, and F. Vollmer, "Whispering gallery mode sensors," *Advances in optics and photonics*, vol. 7, no. 2, pp. 168–240, 2015.

[253] J. Auge, P. Hauptmann, F. Eichelbaum, and S. Rösler, "Quartz crystal microbalance sensor in liquids," *Sensors and Actuators B: Chemical*, vol. 19, no. 1-3, pp. 518–522, 1994.

[254] J. El-Ali, P. K. Sorger, and K. F. Jensen, "Cells on chips," *Nature*, vol. 442, no. 7101, pp. 403–411, 2006.

[255] A. Bernard, B. Michel, and E. Delamarche, "Micromosaic immunoassays," *Analytical chemistry*, vol. 73, no. 1, pp. 8–12, 2001.

[256] P.-A. F. Goyette, "Highly multiplexable open-space microfluidics," Ph.D. dissertation, Polytechnique Montréal, 2021.

[257] P. Petitjeans, C.-Y. Chen, E. Meiburg, and T. Maxworthy, "Miscible quarter five-spot displacements in a hele-shaw cell and the role of flow-induced dispersion," *Physics of Fluids*, vol. 11, no. 7, pp. 1705–1716, 1999.

[258] M. A. Stremler, F. R. Haselton, and H. Aref, "Designing for chaos: applications of chaotic advection at the microscale," *Philosophical Transactions of the Royal Society of London. Series A: Mathematical, Physical and Engineering Sciences*, vol. 362, no. 1818, pp. 1019–1036, 2004.

[259] A. D. Stroock, S. K. Dertinger, A. Ajdari, I. Mezic, H. A. Stone, and G. M. Whitesides, "Chaotic mixer for microchannels," *Science*, vol. 295, no. 5555, pp. 647–651, 2002.

[260] A. Folch, *Introduction to bioMEMS*. CRC Press, 2016.

[261] M. Z. Bazant, J. Choi, and B. Davidovitch, "Advection-diffusion-limited aggregation," *Chaos: An Interdisciplinary Journal of Nonlinear Science*, vol. 14, no. 4, pp. S7–S7, 2004.

[262] T. A. Witten Jr and L. M. Sander, "Diffusion-limited aggregation, a kinetic critical phenomenon," *Physical review letters*, vol. 47, no. 19, p. 1400, 1981.

[263] J. S. Langer, "Instabilities and pattern formation in crystal growth," *Reviews of modern physics*, vol. 52, no. 1, p. 1, 1980.

[264] J.-D. Chen, "Radial viscous fingering patterns in hele-shaw cells," *Experiments in fluids*, vol. 5, no. 6, pp. 363–371, 1987.

[265] T. Nakagaki, "Smart behavior of true slime mold in a labyrinth," *Research in Microbiology*, vol. 152, no. 9, pp. 767–770, 2001.

[266] H. S. Moghadam and M. Helbich, "Spatiotemporal urbanization processes in the megacity of mumbai, india: A markov chains-cellular automata urban growth model," *Applied Geography*, vol. 40, pp. 140–149, 2013.

[267] R. Langlands, P. Pouliot, and Y. Saint-Aubin, "Conformal invariance in two-dimensional percolation," *Bulletin of the American Mathematical Society*, vol. 30, no. 1, pp. 1–61, 1994.

[268] S. Smirnov, "Critical percolation in the plane: conformal invariance, cardy's formula, scaling limits," *Comptes Rendus de l'Académie des Sciences-Series I-Mathematics*, vol. 333, no. 3, pp. 239–244, 2001.

[269] P. J. Flory, "Thermodynamics of high polymer solutions," *The Journal of chemical physics*, vol. 9, no. 8, pp. 660–660, 1941.

[270] H. J. Herrmann, "Geometrical cluster growth models and kinetic gelation," *Physics Reports*, vol. 136, no. 3, pp. 153–224, 1986.

[271] D. Bernard, G. Boffetta, A. Celani, and G. Falkovich, "Conformal invariance in two-dimensional turbulence," *Nature Physics*, vol. 2, no. 2, pp. 124–128, 2006.

[272] P. Grassberger and H. Kantz, "On a forest fire model with supposed self-organized criticality," *Journal of Statistical Physics*, vol. 63, pp. 685–700, 1991.

[273] G. MacKay and N. Jan, "Forest fires as critical phenomena," *Journal of Physics A: Mathematical and General*, vol. 17, no. 14, p. L757, 1984.

[274] J. L. Cardy and P. Grassberger, "Epidemic models and percolation," *Journal of Physics A: Mathematical and General*, vol. 18, no. 6, p. L267, 1985.